2011

Profiling ArabidopsisArogenate Dehydratases: Dimerization and Subcellular Localization Patterns

Danielle Marie Styranko

Profiling *Arabidopsis* Arogenate Dehydratases: Dimerization and Subcellular Localization Patterns

(Spine title: Profiling of ADT Dimers)

(Thesis format: Monograph)

by

Danielle Marie Styranko

Graduate Program in Biology

A thesis submitted in partial fulfillment
of the requirements for the degree of
Master of Science

School of Graduate and Postdoctoral Studies
The University of Western Ontario
London, Ontario Canada

THE UNIVERSITY OF WESTERN ONTARIO

SCHOOL OF GRADUATE AND POSTDOCTORAL STUDIES

CERTIFICATE OF EXAMINATION

Supervisor

Dr. Susanne Kohalmi

Advisory Committee

Dr. Denis Maxwell

Dr. Sash Damjanovski

Examining Board

Dr. Mark Gijzen

Dr. Shiva Singh

Dr. Greg Thorn

The thesis by

Danielle Marie Styranko

entitled:

Profiling *Arabidopsis* Arogenate Dehydratases: Dimerization and Subcellular Localization Patterns

is accepted in partial fulfillment of the requirements for the degree of Master of Science

Date: 22 July 2011

Dr. Graham Thompson

Chair of the Examining Board

ABSTRACT

In *Arabidopsis*, a family of six arogenate dehydratases (ADTs) has been identified which catalyze the terminal step of phenylalanine biosynthesis. ADTs share considerable sequence similarity to bacterial prephenate dehydratases, which form homodimers. The protein-protein interaction profiles of *Arabidopsis* ADTs were characterized using Yeast-2-Hybrid and Bi-molecular Fluorescence Complementation approaches. Results show that ADT1, but not ADT2, is able to form homo- and heterodimers with all other ADTs in yeast. In contrast, all six ADTs form all possible homo- and heterodimer combinations *in planta*, where they display two different subcellular localization patterns. Most ADT dimers localize to the chloroplast in a stromule-like pattern, but ADT5 dimers also localize in a nuclear-like pattern. Large scale cDNA library screens also identified a number of other putative interactors, suggesting that ADTs may be part of a larger protein complex. This study is the first to characterize the protein-protein interaction profiles of plant ADTs.

Keywords: Arogenate Dehydratase; Chloroplast Localization; Complex Formation; Heterodimer; Homodimer; Nuclear Localization; Phenylalanine Biosynthesis; Stromule.

ACKNOWLEDGMENTS

There are many people, both professionally and personally, whom I would like to thank for making this thesis possible. First of all, I would like to thank my supervisor, Dr. Susanne Kohalmi, for giving me the opportunity to take on this project, and for all of her guidance and support, both technical and emotional, over the years. Second, I would like to thank my advisory committee, Drs. Denis Maxwell and Sash Damjanovski, for their helpful advice. I would also like to thank my colleagues, especially Crystal Bross, for sharing in all of the joy and frustration graduate school. A special thank you goes to Dr. Yuhai Cui, Gang (Gary) Tian, and everyone at Agriculture and Agri-food Canada, for making the large scale cDNA library screens and confocal microscope work possible. I would also like to thank Katlynn for taking my late night phone calls, and for always being willing to listen. Finally, a heartfelt thank you goes to my parents, Kathy and Sheldon, for their constant, albeit long distance, support, and for always believing that I could accomplish anything I put my mind to. I would not be where I am today without their unwavering love and support.

TABLE OF CONTENTS

LIST OF TABLES

LIST OF FIGURES

LIST OF APPENDICES

LIST OF ABBREVIATIONS

Note: SI units are not listed.

%	percent
3AT	3-amino-1,2,4-triazole
Abbr.	abbreviation
ACS	1-aminocyclo-propane-1-carboxylate synthase
ACT	aspartokinase-chorismate mutase-TyrA
ADH	arogenate dehydrogenase
ADT	arogenate dehydratase
amp ^{r}	ampicillin resistance
AO	aldehyde oxidase
AT	aminotransferase
att	attenuation site
BAR	Basta resistance
BiFC	bi-molecular fluorescence complementation
bp	base pairs
ccdB	bacterial negative selectable marker
CDT	cyclohexadienyl dehydratase
CM	chorismate mutase
Cm ^{r}	chloramphenicol resistance
co-IP	co-immunoprecipitation
CRA1	CRUCIFERINA
DB	DNA-binding domain
DHAP	3-deoxy-7-phosphoheptulonate
DMF	dimethyl formamide
DMSO	dimethyl sulfoxide
EDTA	ethylenediaminetetraacedic acid
FHY1	FAR-RED ELONGATED HYPOCOTYL 1
FL	full length
GFP	green fluorescent protein
GGH	γ-glutamyl hydrolase

I	intermediate length
kan ^{r}	kanamycin resistance
kb	kilo base
LB	Luria-Bertani
MAT a	mating type a
MAT α	mating type α
MES	2-(*N*-morpholino)-ethanesulfonic acid
NLS	nuclear localization signal
OD	optical density
PAI	phosphoribosylanthranilate isomerase
PCR	polymerase chain reaction
PDH	prephenate dehydrogenase
PDT	prephenate dehydratase
PEG	polyethylene glycol
Phe	phenylalanine
S	short length
SA	self-activation
SD	synthetic dextrose
SDS	sodium dodecyl sulfate
TA	transcription activation domain
TAIR	The *Arabidopsis* Information Resource
TBE	Tris-borate-EDTA
TE	Tris-EDTA
TIC	translocon of the inner membrane of the chloroplast
TP	transit peptide
TOC	translocon of the outer membrane of the chloroplast
UAS	upstream activating sequence
v/v	volume/volume
w/v	weight/volume
x-α-gal	5-bromo-4-chloro-3-indolyl-α-D-galactopyranoside
x-β-gal	5-bromo-4-chloro-3-indolyl-β-D-galactopyranoside
Y2H	yeast-2-hybrid

YC	C-terminal half of YFP
YEB	yeast extract and beef
YFP	yellow fluorescent protein
YN	N-terminal half of YFP
YPDA	yeast-peptone-dextrose-adenine

1 INTRODUCTION

1.1 Aromatic Amino Acid Biosynthesis

Plants are sessile organisms that have a number of unique characteristics compared to other eukaryotes. One of these unique characteristics is the presence of specialized organelles called chloroplasts, which are best known as the site of photosynthesis. However, in plants chloroplasts are also the site of many other processes, including the biosynthesis of some amino acids. The branched chain amino acids leucine, isoleucine, and valine (Binder, 2010), the sulfur-containing amino acids cysteine and methionine (Jander and Joshi, 2010; Hell *et al.*, 2002), and the aromatic amino acids tryptophan, tyrosine, and phenylalanine (Phe; Tzin and Galili, 2010a and 2010b) are all synthesized in the chloroplasts.

In plants and microorganisms the aromatic amino acids are all synthesized from chorismate, the end-product of shikimate pathway (Figure 1; Tzin and Galili, 2010a; Herrmann and Weaver, 1999). The conversion of chorismate to anthranilate, catalyzed by an anthranilate synthase, is the first committed step towards tryptophan biosynthesis, while conversion to prephenate, performed by a chorismate mutase (CM), is the first committed step towards both tyrosine and Phe (Tzin and Galili, 2010a). The tyrosine and Phe biosynthesis pathways are closely linked and require similar enzymatic steps to convert prephenate to the respective end products. In most microorganims, prephenate is converted to phenylpyruvate by a prephenate dehydratase (PDT) in a dehydration/decarboxylation reaction, after which phenylpyruvate is transaminated by an aminotransferase (AT). Similarly, prephenate can be converted into p-hydroxyphenylpyruvate by a prephenate dehydrogenase (PDH), which is then converted to tyrosine by an AT. In plants, however, these enzymatic steps are predominantly performed in reverse (Figure 1; Maeda *et al.*, 2010; Tzin and Galili, 2010a; Cho *et al.*, 2007; Jung *et al.*, 1986). Prephenate is first transaminated to arogenate by a prephenate AT, after which arogenate can be converted to tyrosine by an arogenate dehydrogenase (ADH), or to phenylalanine by an arogenate dehydratase (ADT). This study focuses on Phe biosynthesis.

Figure 1. The Terminal Steps of Aromatic Amino Acid Biosynthesis Following the Synthesis of Chorismate in the Shikimate Pathway. Following the synthesis of chorismate, the first committed step in tryptophan biosynthesis is directed by an anthranilate synthase. Chorismate can also be converted to prephenate by a chorismate mutase, which is the first committed step in phenylalanine and tyrosine biosynthesis. Prephenate can be converted tyrosine via either a hydroxyphenylpyruvate (in microorganisms) or arogenate (in plants) intermediate in a series of transamination and decarboxylation reactions. Prephenate can also be converted to phenylalanine via two intermediates. In the Prephenate Pathway (shown in blue), prephenate can be dehydrated/decarboxylated by a prephenate dehydratase to produce phenylpyruvate, and subsequently transaminated to arogenate. In the Arogenate Pathway (shown in green) prephenate is first transaminated to arogenate and then dehydrated/decarboxylated by an arogenate dehydrogenase. For steps at which there are multiple isozymes in *Arabidopsis* the number of isozymes is indicated below the enzyme. Dashed lines indicate multiple enzymatic steps. Modified from Tzin and Galili, 2010a.

ADH: arogenate dehydrogenase; ADT: arogenate dehydratase; AS: anthranilate synthase; AT: aminotransferase; CM: chorismate mutase; DAHP: 3-deoxy-7-phosphoheptulonate synthase; PAI: phosphoribosylanthranilate isomerase; PDH: prephenate dehydrogenase; PDT: prephenate dehydratase.

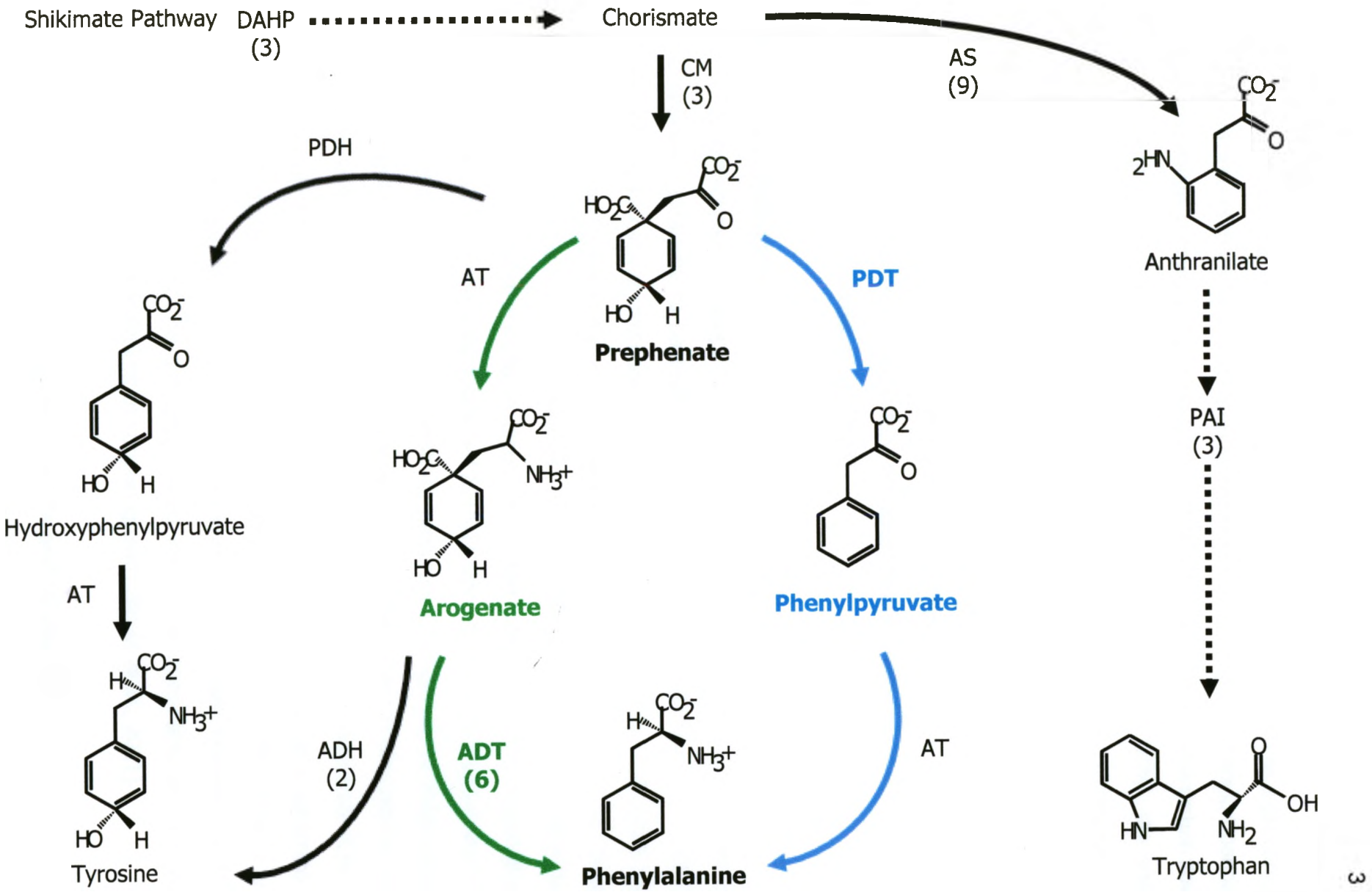
Shikimate Pathway
DAHP
(3)
Chorismate
CM
(3)
AS
(9)
PDH
AT
PDT
Prephenate
Anthranilate
Hydroxyphenylpyruvate
Arogenate
Phenylpyruvate
PAI
(3)
AT
ADH
(2)
ADT
(6)
AT
Tyrosine
Phenylalanine
Tryptophan

1.2 The Importance of Phenylalanine

In the plant cell, Phe is required both for protein synthesis and as a precursor for the synthesis of many aromatic compounds, including those of the phenylpropanoid and glucosinolate pathways (Tzin and Galili, 2010a). More than 30% of the carbon flow in plants enters the phenylpropanoid pathway alone (Razal *et al.* 1996), the end-products of which are required for structure (such as lignins), and pigmentation and UV protection (such as anthocyanins). Many glucosinolates are potent pathogen defense compounds (Kliebenstein *et al.*, 2001). It is therefore important for plants to regulate and maintain an adequate pool of Phe. Furthermore, Phe is important for human health, as it is an essential dietary requirement for mammals (Fürst and Stehle, 2004), and as many plant-derived aromatic secondary metabolites are antioxidants which aid in disease prevention (Ververdis *et al.*, 2007).

1.3 *Arabidopsis* ADTs

In *Arabidopsis thaliana*, a family of six ADTs has been identified based on amino acid sequence similarity to bacterial PDTs (Cho *et al.*, 2007; Ehlting *et al.*, 2005). *Arabidopsis* ADTs catalyze the conversion of arogenate to Phe (Maeda *et al.*, 2010; Cho *et al.*, 2007), and form three different phylogenetic subfamilies (Figure 2). These subfamilies seem to be highly conserved as other plant ADTs, such that those identified in rice (a monocot) and petunia (a dicot) follow the same subfamily organization (Figure 2). ADTs were originally annotated as PDTs since ADT and PDT sequences are so similar that one cannot predict substrate preference (arogenate or prephenate) based on sequence alone. However, they were re-classified when *in vitro* biochemical analyses showed that all six ADTs preferentially use arogenate as a substrate (Cho *et al.*, 2007). Only ADT1, ADT2, and ADT6 are able to use prephenate as a substrate *in vitro*, and with much lower efficiency (Cho *et al.*, 2007). The PDT activity of ADT1 and ADT2 was confirmed *in vivo* using a PDT knockout strain of yeast, however the PDT activity of ADT6 could not be detected *in vivo*, and it was speculated that the PDT activity of ADT6 was not sufficient to support growth (Bross *et al.*, 2011).

1.3.1 Domain Structure of Bacterial PDTs and *Arabidopsis* ADTs

Like bacterial PDTs, *Arabidopsis* ADTs have a highly conserved catalytic domain

Figure 2. Rooted Phylogenetic Tree of Select Plant ADTs. Plant ADTs typically fall into three subfamilies, which include both monocots and dicots. Subfamily I is shown in green, subfamily II in orange, and subfamily III in blue. The CDT sequence from *Pseudomonas aeruginosa*, which catalyzes an ADT/PDT-like reaction but is not closely related to ADTs and PDTs (Zhao *et al.*, 1992), was included to root the tree. The rooted tree was generated with DNAMAN (Lynnon BioSoft, version 6.0) using full length ADT protein sequences and a bootstrap of 1000. The numbers at the branch points indicate the bootstrap values, and the horizontal scale indicates the sequence divergence. Modified from Maeda *et al*, 2010; Yamada *et al.*, 2008; Cho *et al.*, 2007.

ADT: arogenate dehydratase; CDT: cyclohexadienyl dehydratase. *At: Arabidopsis thaliana*; *Os*: *Oryza sativa*; *Pa: Pseudomonas aeruginosa; Ph*: *Petunia x hybrida*.

Accessions: *At*ADT1: At1g11790; *At*ADT2: At3g07630; *At*ADT3: At2g27820; *At*ADT4: At3g44720; *At*ADT5: At5g22630, *At*ADT6: At1g08250; *Os*ADT1: Os03g17730; *Os*ADT2: Os04g33390; *Os*ADT3: Os07g49390; *Os*ADT4: Os09g39230; *Pa*CDT: AAC08596; *Ph*ADT1: FJ790412; *Ph*ADT2: FJ790413; *Ph*ADT3: FJ790414.

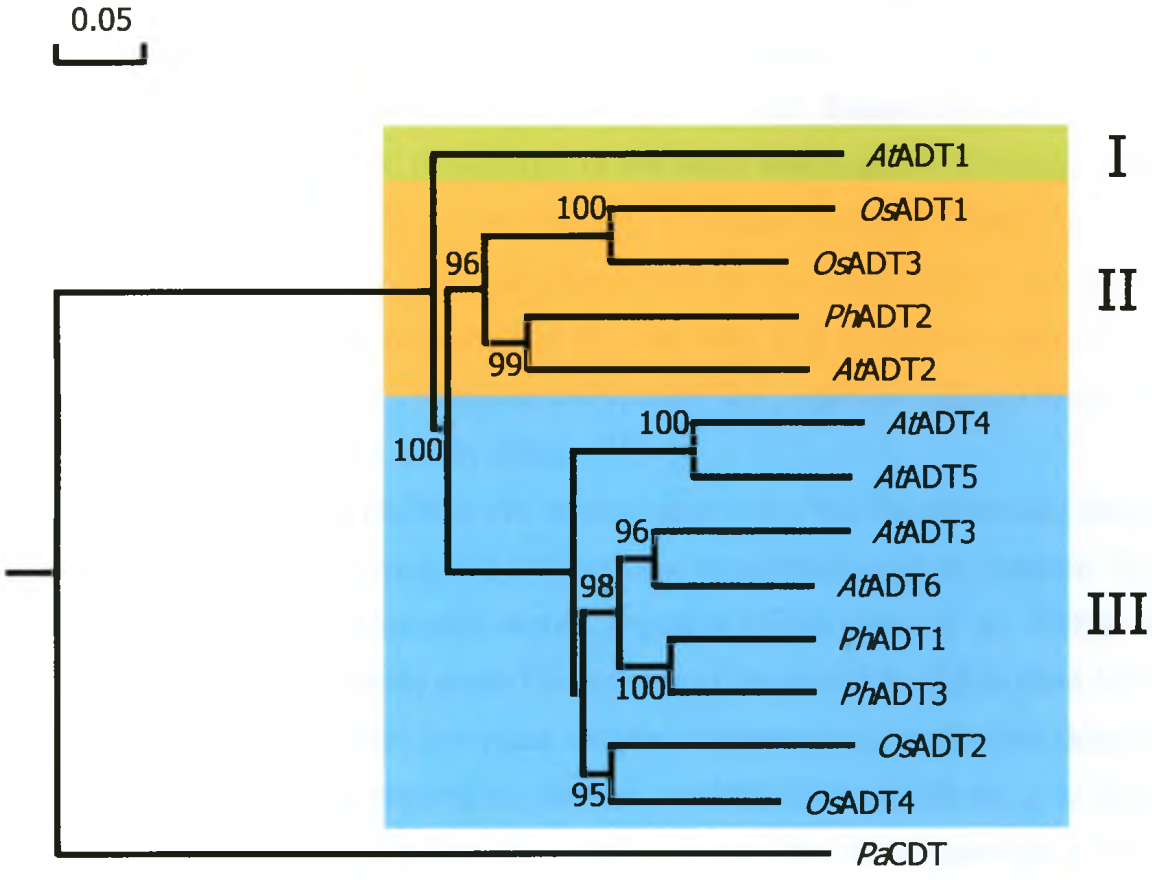
0.05
AtADT1
OsADT1
OsADT3
PhADT2
AtADT2
AtADT4
AtADT5
AtADT3
AtADT6
PhADT1
PhADT3
OsADT2
OsADT4
PaCDT
100
96
99
100
98
100
95
I
II
III

followed by a C-terminal ACT regulatory domain, which is required for allosteric regulation of the enzyme (Figure 3; Tan *et al.*, 2008; Vivan *et al.*, 2008). Plant ADTs also have a highly variable N-terminal transit peptide which directs these enzymes to the chloroplast (Maeda *et al.* 2010; Rippert *et al.*, 2009; Bross and Kohalmi, unpublished). Although transit peptides vary in length and they do not often share a high degree of sequence similarity, they do share some common structural properties, including a high proportion of basic amino acids (Theg and Scott, 1993). In the cytosol, targeting of transit peptide-containing preproteins requires the assistance of chaperone proteins, which loosely fold and phosphorylate the preproteins to assist their transport to the outer envelope of the chloroplast (Li and Chiu, 2010; Bédard and Jarvis, 2005). Receptor proteins in the TOC (translocon of the outer membrane of the chloroplast) complex recognize the preprotein and facilitate its active transport through the TOC channel, where it activates the TIC (translocon of the inner membrane of the chloroplast) complex. Dual activation of the TIC and TOC complexes leads to the formation of a supercomplex that allows transport of the preprotein into the stroma (Li and Chiu, 2010; Bédard and Jarvis, 2005).

Most known transit peptides are cleaved upon entry into the chloroplast stroma to release a functional enzyme, but at least four chloroplast-localized proteins have been identified with non-cleavable transit peptides (Armbruster *et al.*, 2009). No experimental evidence currently exists for cleavage of the transit peptide in plant ADTs, and both biochemical analyses and yeast complementation data indicate that cleavage of the transit peptide is not required to produce a functional enzyme (Bross *et al.* 2011; Cho *et al.*, 2007). As a result, the boundary between the transit peptide and the catalytic domain in plant ADTs continues to be defined based on alignment to bacterial PDTs. However, there is a small region immediately upstream of the bacterially-defined catalytic domain that is more highly conserved than the rest of the transit peptide sequence (Figure 3). As such, it is unclear whether this sequence, termed the intermediate region, is part of the transit peptide, or whether it is actually part of the catalytic domain in plants.

Figure 3. Amino Acid Sequence Alignment of *Arabidopsis* ADTs. Protein sequences were translated from full length coding sequences and show a high degree of similarity between the six ADTs. White circles above the sequence mark amino acids which are predicted to be involved in dimerization based on comparison to bacterial PDTs (Tan *et al.*, 2008). Colored bars above the sequence alignment represent the different domains: Green: transit peptide; Dark blue: catalytic domain; Light blue: ACT regulatory domain; Yellow: Intermediate region of unknown identity. The numbers on the right-hand side are in reference to the N-terminal end of each ADT, and the red box marks a cryptic GAL4-type activation domain (see section 4.1.1). Shading within the sequences indicates amino acid conservation: Black = 100%, Medium Grey = 75%, Light Grey = 50%, White <50%. Modified from Bross *et al.,* 2011.

Accessions: ADT1: At1g11790; ADT2: At3g07630; ADT3: At2g27820; ADT4: At3g44720; ADT5: At5g22630, ADT6: At1g08250.

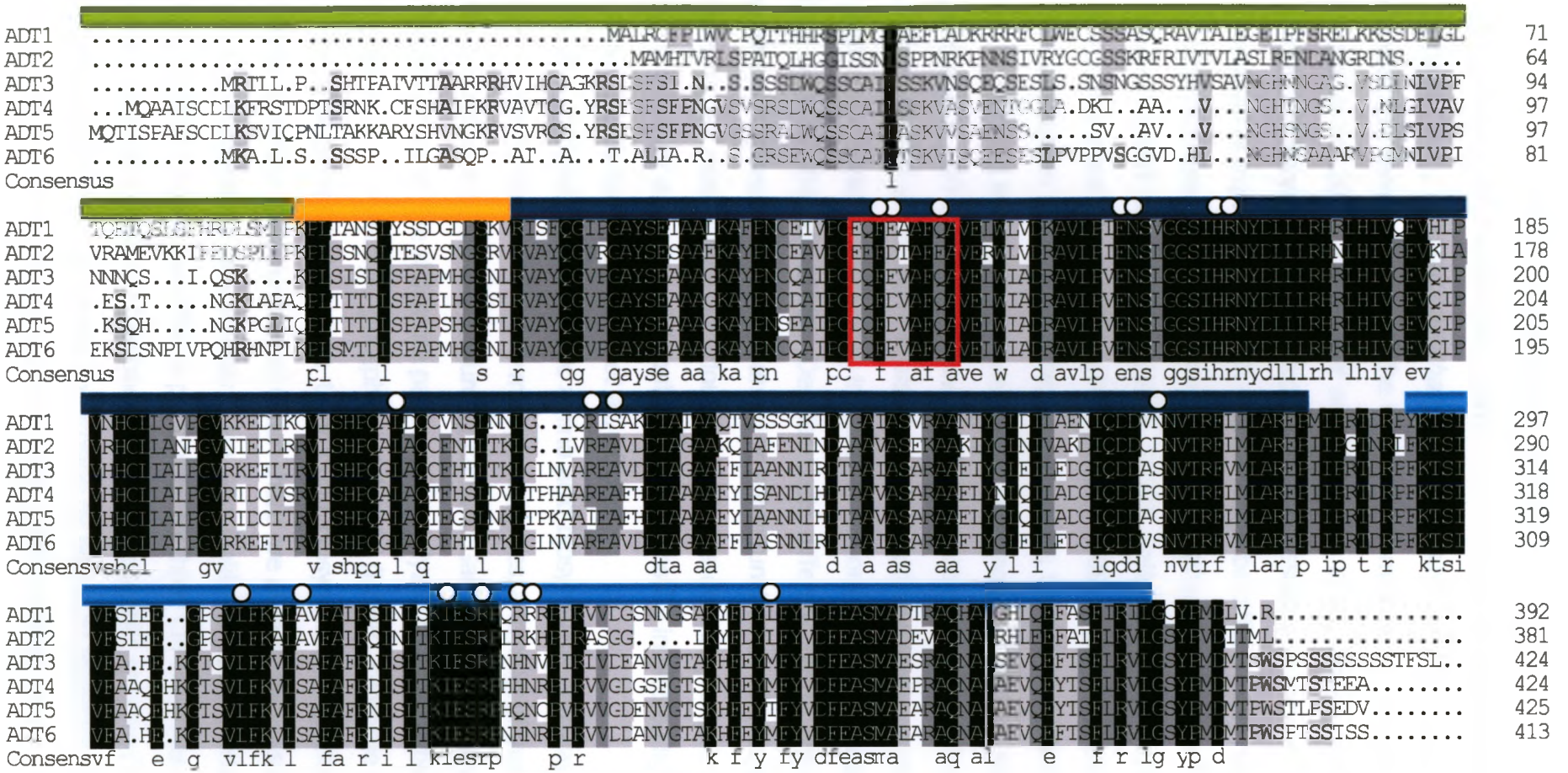
ADT1
ADT2
ADT3
ADT4
ADT5
ADT6
Consensus

1.3.2 ADTs: Catalyzing an Important Regulatory Step?

The presence of multiple ADT isoforms in *Arabidopsis* (six), rice (four), petunia (three), poplar (five), *Nicotiana benthamiana* (two), soybean (two) and maize (three) suggests that this terminal step of Phe biosynthesis may be an important regulatory step (Maeda *et al.*, 2010; Yamada *et al.*, 2008; Cho *et al.*, 2007; Hamberger *et al.*, 2006). All six *Arabidopsis* ADTs are expressed in all tissues and conditions tested thus far, but the level of expression of each ADT seems to be differentially regulated. While ADT2 is highly expressed in all tissues, ADT3 is only highly expressed in flowers, seeds, and siliques (Rippert *et al.*, 2009; Hood, 2008). Both ADT4 and ADT5 are highly expressed in the stem (Hood, 2008; Ehlting *et al.*, 2005), which is in accordance with their proposed role in lignification (Corea *et al.*, 2010; Laskar *et al.*, 2010). ADT3 has also been implicated in the UV light response (referred to as PD1 in Warpeha *et al.*, 2008), and ADT3, ADT4, and ADT5 have been shown to respond to cold stress (Hood, 2008). Expression of all six ADTs is also increased during recovery from heat stress, when protein synthesis is proposed to increase in response to the degradation of heat-damaged proteins (Hood, 2008). Despite their different tissue distributions and environmental responses, there appears to be some functional redundancy among the ADT isoforms, as most single and double knockouts do not produce a discernable phenotype, however an *adt4-adt5* double knockout results in altered lignification and plants whose stems collapse (Corea *et al.*, 2010).

In the shikimate and aromatic amino acid biosynthesis pathways, only a few enzymatic reactions are performed by multiple isozymes, and most of these correspond to a branch-point in the pathway (Figure 1; Tzin and Galili, 2010a). In *Arabidopsis*, the first committed step of the shikimate pathway is catalyzed by at least two isoforms (a third is putative) of 3-deoxy-7-phosphoheptulonate (DAHP) synthase (Keith *et al.*, 1991). The first committed step to tryptophan biosynthesis is performed by the anthranlilate synthase holoenzyme, of which there are at least two α subunits and at least three β subunits in *Arabidopsis* (Tzin and Galili, 2010b). Similarly, the first committed step to tyrosine and Phe is performed by three CM isozymes, two of which are plastidic, while the other is a feedback-insensitive cytosolic enzyme (Tzin and Galili, 2010a). Arogenate can be converted to tyrosine by two ADH isozymes (Rippert *et al.*, 2009) or to Phe by six ADT isozymes (Cho *et al.*, 2007; Ehlting *et al.*, 2005). Multiple

enzymes have also been described in tomato for DAHP synthase (Görlach *et al.*, 1993a) and chorismate synthase (Görlach *et al.*, 1993b), while sorghum, potato, and *Nicotiana sylvestris* all have at least two CM enzymes (Schmid and Amrhein, 1995). The presence of multiple, differentially expressed or regulated isozymes at any given step in the biosynthetic pathway creates an opportunity for greater flexibility in regulating not just that biosynthetic step, but also the pathway as a whole.

1.4 Dimerization of Bacterial PDTs

Recent crystallization data suggest that bacterial PDTs exhibit complex tertiary and quaternary structures. PDT monomers from *Staphylococcus aureus* and *Chlorobium tepidum* (Tan *et al.*, 2008), as well as *Mycobacterium tuberculosis* (Vivan *et al.*, 2008) have been shown to form symmetric dimers, in which the dimerization interface extends through both the catalytic and ACT domains (Figure 4B and 4C). It has been suggested that these dimers may be the active unit of the enzyme, and that these dimers may themselves dimerize to form tetramers (Tan *et al.*, 2008). Like other ACT domain-containing enzymes (Curien *et al.*, 2008; Mas-Droux *et al.*, 2006), allosteric regulation of the PDT enzyme involves conformational changes in the active site of the dimer which are directed by conformational changes in the ACT portion of the dimer (Tan *et al.*, 2008). In the absence of Phe, the dimer remains in an open conformation which allows access to the PDT active site. However, binding of two Phe at the ACT dimer interface induces a conformational change which reduces access to the PDT active site, referred to as the closed conformation (Tan *et al.*, 2008; Zhang *et al.*, 1998). Based on 3D structure, a number of amino acids have been predicted to mediate the interactions between the two bacterial monomers (Tan *et al.*, 2008), however these predictions have not been experimentally confirmed.

1.4.1 Homology Modeling of *Arabidopsis* ADTs

Being that *Arabidopsis* ADTs share considerable sequence similarity to bacterial PDTs, it is not surprising that *in silico* homology modeling of all six *Arabidopsis* ADTs (without the transit peptide sequence) predicts that they will form 3D structures which are very similar to the crystalized bacterial PDTs (Figure 4A and 4B; Laskar *et al.*, 2010; Kohalmi, unpublished). Nine of the 18 amino acids that correspond to those predicted

Figure 4. 3D Structures of Select ADTs and PDTs. A. Ribbon drawing of *Arabidopsis* ADT2 based on homology modeling. Modified from Laskar *et al.*, 2010. **B.** Ribbon drawing of the crystalized *S. aureus* PDT. **C.** Ribbon drawing of the symmetric *S. aureus* PDT dimer. The dimerization interface (dashed line) extends across both the catalytic and ACT regulatory domains. The catalytic and regulatory domains are indicated to the left (A, B) or right (C), and the catalytic cleft is marked by an arrow. Note that (C) is rotated 90° counterclockwise from (B). Modified from Tan *et al.*, 2008 (B and C).

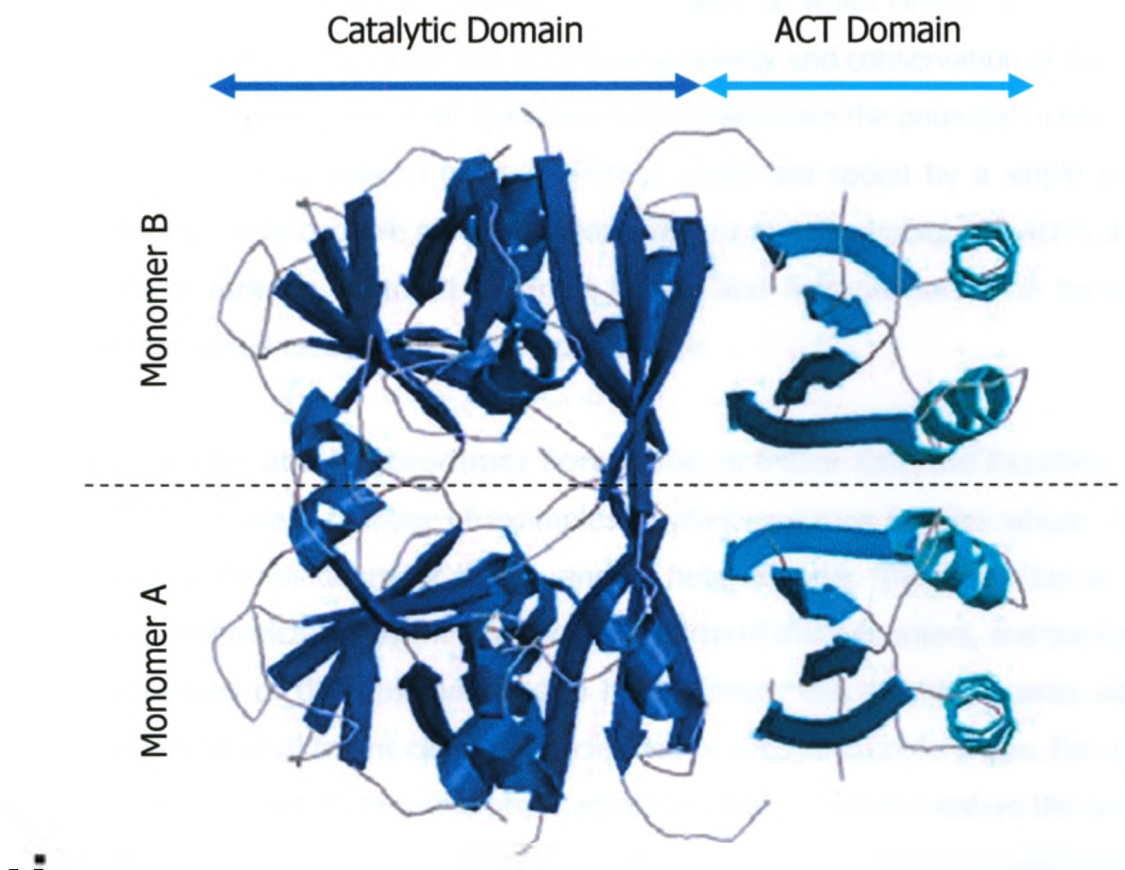
Catalytic Domain
ACT Domain
Monomer B
Monomer A

C.

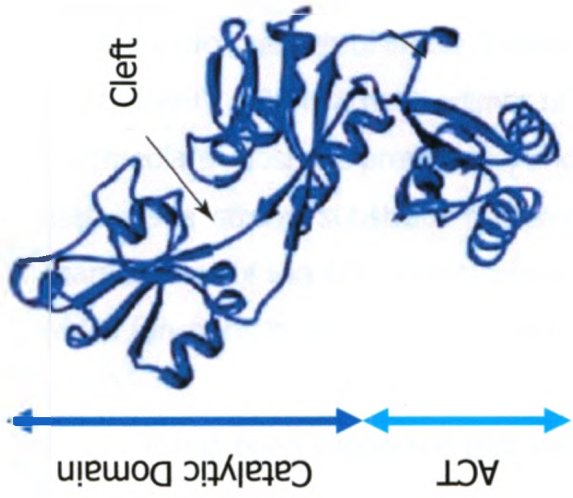
Cleft
Catalytic Domain
ACT

A.

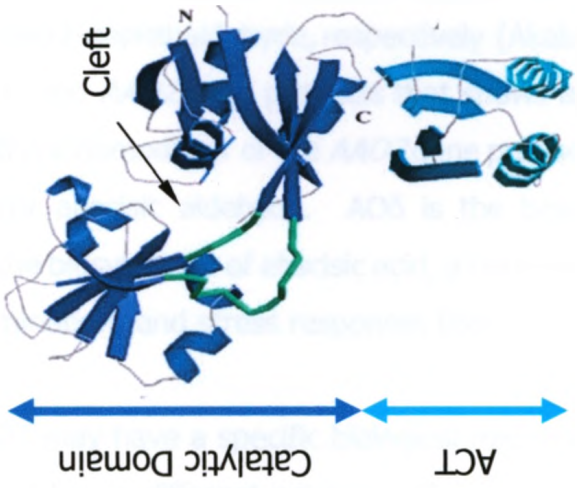
Cleft
N
C
Catalytic Domain
ACT

B.

to mediate dimerization in bacterial PDTs (Figure 3, white circles) are conserved in *Arabidopsis* ADTs. This predicted structural similarity and conservation of theoretically key amino acids suggests that *Arabidopsis* ADTs also have the potential to form dimers. However in comparison to bacterial PDTs, which are coded by a single gene and therefore are only capable of forming homodimers, the six *Arabidopsis* ADTs should be capable of forming up to 21 different homo- and heterodimers. The formation of tetramers would create even more possibilities.

1.4.2 Homo- and Heterodimer Formation in Other Enzyme Families

There are a number of examples of plant enzymes families whose members function as combinations of homo- and/or heterodimers. The formation of specific dimers is often dictated by the expression patterns of the monomers, and the functional consequences of different homo- and heterodimers can clearly be seen when the monomers have different catalytic efficiencies or substrate preferences. For example, in tomato there are three γ-glutamyl hydrolases (GGH1-3) that catalyze the removal of polyglutamate tails from folates, thereby destabilizing them. GGHs are able to form both homo- and heterodimers, however GGH3, which is inactive, is only expressed flowers (Akhtar *et al.*, 2008), decreasing the overall catalytic efficiency in flowers. Similarly, in *Arabidopsis* there are three aldehyde oxidase genes (*AAO1-3*) that give rise to four aldehyde oxidase enzymes (AOα, AOβ, AOγ, and AOδ). AOα and AOγ are homodimeric isozymes of the *AAO1* and *AAO2* gene products, respectively, that show strong substrate preferences for indole-3-aldehyde and 1-naphthaldehyde, respectively (Akaba *et al.*, 1999). AOβ is a heterodimer of *AAO1* and *AAO2* gene products that shows an intermediate substrate preference, and AOδ is a homodimer of the *AAO3* gene product that has a strong substrate preference for abscisic aldehyde. AOδ is the best-characterized of the AOs and is involved in the biosynthesis of abscisic acid, a hormone which functions in seed development, germination, and stress responses (Seo *et al.*, 2000).

It has been suggested that each ADT may have a specific biological role, and this is supported by the fact that each ADT has a different catalytic efficiency and unique expression level and pattern (Rippert *et al.*, 2009; Hood, 2008; Cho *et al.*, 2007). Furthermore, while all six ADTs preferentially use arogenate as a substrate,

ADT1 and ADT2 are also able to use prephenate both *in vitro* and *in vivo*, which may allow Phe biosynthesis in plants to proceed even in the absence of arogenate (Bross *et al.*, 2011; Cho *et al.*, 2007). As with tomato GGHs and *Arabidopsis* AOs, the enzymatic function of ADTs may be dependant both on which isozymes are present and which substrate is available.

1.5 Multi-functional Enzymes and Complex Formation

While most bacterial PDTs and plant ADTs are mono-functional enzymes, multi-functional enzymes have been identified in a number of microorganisms (Figure 5). In enterobacteria, bi-functional enzymes called P-proteins have been identified that contain domains for both CM activity and PDT activity (Zhang *et al.*, 1998; Dopheide *et al.*, 1972). More recently, tri-functional enzymes have been described in some marine bacteria (*Shewanella* species) which contain catalytic domains for CM activity, PDT activity, and DAHP synthase activity (Bross *et al.*, 2011). Another tri-functional enzyme was described in the thermophillic bacterium *Archaeoglobus fulgidus* that contains domains for CM activity, PDT activity, and PDH activity, linking the biosynthesis of phenylalanine and tyrosine (Bross *et al.*, 2011). The existence of these multi-functional proteins, composed of various enzymes involved in aromatic amino acid biosynthesis suggests that, in bacteria, these enzymatic steps are performed in close proximity. It is therefore likely that mono-functional ADTs may also function in close proximity to enzymes that catalyze other steps in the shikimate and aromatic amino acid biosynthesis pathways, as part of a larger complex which efficiently catalyzes sequential reactions.

1.6 Identifying Protein Interactions

There are many ways to study plant protein interactions, two of which are Yeast-2-Hybrid (Y2H) and co-Immunoprecipitation (co-IP). Co-IP is an *in vitro* system for identifying protein interactions. In co-IP, a protein homogenate is incubated with an antibody that recognizes a specific protein (Miernyk and Thelen, 2008). When this homogenate is passed through a column that recognizes the antibody, the protein of interest, and any other proteins which interact with it, are held back in the column and the whole complex can be eluted. This system can be used to identify whole protein

Figure 5. Schematics of ADT- and PDT-Domain Containing Enzymes. While most ADTs and PDTs are mono-functional enzymes, some bi- and tri-functional enzymes have also been identified. In addition to a PDT catalytic domain and an ACT regulatory domain, these multifunctional enzymes also contain a CM domain, and in some cases either a DAHP synthase domain, which catalyzes the first step in the shikimate pathway, or a PDH domain, which catalyzes the conversion of arogenate to tyrosine. The transit peptide region is unique to plant ADTs. Modified from Bross *et al.*, 2011.

ADT: arogenate dehydratase; CM: chorismate mutase; DAHP: 3-deoxy-7-phospho-heptulonate synthase; PDH: prephenate dehydratase; PDT: prephenate dehydratase; TP: transit peptide.

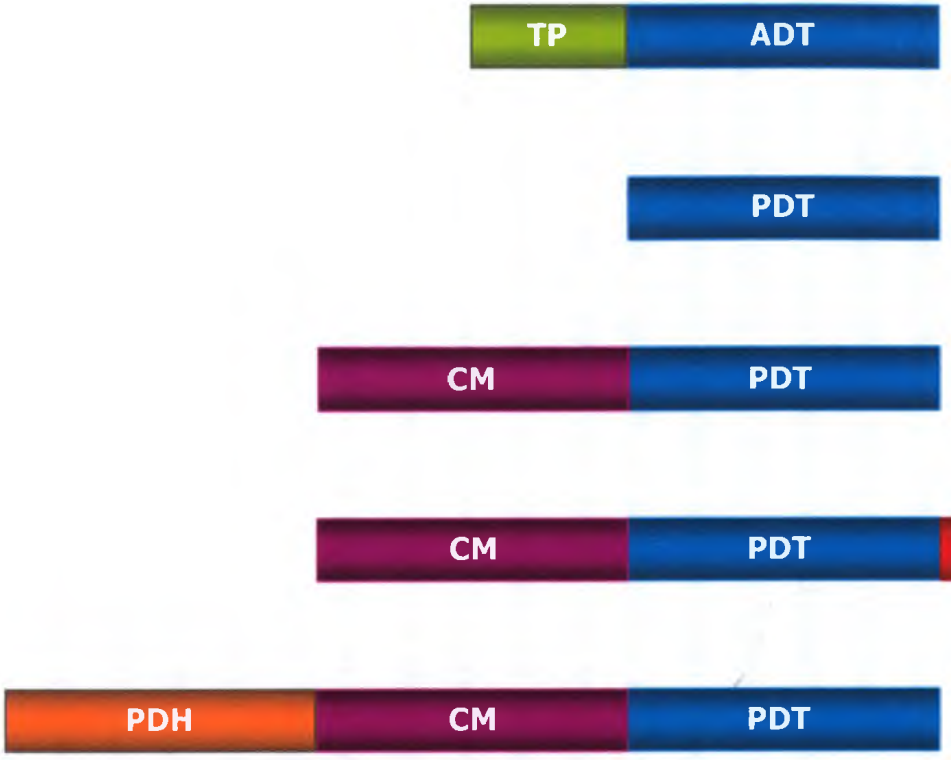

Arabidopsis ADTs

Bacterial and Yeast PDTs

Enterobacterial P-proteins
Bi-functional Enzyme

Shewanella species
Tri-functional Enzyme

Archaeoglobus fulgidus
Tri-functional Enzyme

complexes, however partial complexes are more common being that the epitope targeted by the antibody may be hidden by some interactions, in the complete complex (Moresco *et al.*, 2010). There are many variations to this technique including, but not limited to, using a second antibody in sequential co-IPs to help identify other proteins of interest in the complex. This technique can be used to demonstrate known or determine unknown interactions, however unknown interactions can be difficult to identify, as they require either mass spectrometry or protein sequencing, (Moresco *et al.*, 2010; Miernyk and Thellen, 2008).

Y2H is an *in vivo* system for identifying protein interactions which relies on the activation of specific reporter genes. In most Y2H systems, activation of the reporters is mediated by the transcription factor GAL4. In wild type yeast, GAL4 regulates galactose metabolism, and is characterized by a DNA-binding (DB) domain, and a transcription activation (TA) domain , separated by a linker region (Figure 6A; reviewed in Traven *et al.*, 2006). The DB domain interacts directly with the GAL4-specific upstream activating sequence (UAS), and the TA domain is responsible for recruitment of the transcription complex. Both the GAL4-DB and GAL4-TA domains can be separated from the rest of the GAL4 molecule and retain their function (Chevray and Nathans, 1992; Fields and Song, 1989). As they cannot interact directly, these domains can be fused individually to other proteins, and if those fusion proteins subsequently interact the resulting co-localization of the two GAL4 domains can activate transcription of UAS-controlled reporter genes, (Figure 6B and 6C; Kohalmi *et al.*, 1997; Chevray and Nathans, 1992; Fields and Song, 1989). Y2H can be used to determine whether two specific proteins interact, however one of the advantages of this system is it can also be used to identify unknown interactions. A known DB-fusion protein can be used to search a library of unknown TA-fusion proteins, without any fore-knowledge of the interactions, and the identity of an interacting protein can easily be determined by sequencing the corresponding DNA insert in the TA vector. This system is, however, limited to testing binary interactions and cannot be used to identify whole protein complexes. Furthermore, as Y2H requires that all components localize to the nucleus, some non-nuclear proteins may not fold properly in this environment. This is especially true of transmembrane proteins, which are often dependant on membrane integration for proper folding (Vidal and Legrain, 1999).

Figure 6. The GAL4-Based Yeast-2-Hybrid System. A. In wild type yeast, the GAL4 transcription factor mediates expression of galactose-induced genes. GAL4 binds to the UAS via a DB domain and recruits the transcriptional machinery via a TA domain. The DB and TA domains are separated by a linker region. **B.** The GAL4 DB and TA domains can be separated and fused to other proteins of interest (a bait or a prey) and expressed *in trans*. If the fusion proteins do not interact, reporter gene expression is not activated. **C.** When the fusion proteins interact, the DB and TA domains are co-localized and are able to activate transcription of reporter genes. Modified from Kohalmi *et al.*, 1997.

B: bait protein; DB: GAL4 DNA binding domain; L: linker region; P: prey protein; TA: GAL4 transcriptional activation domain; UAS: upstream activating sequence.

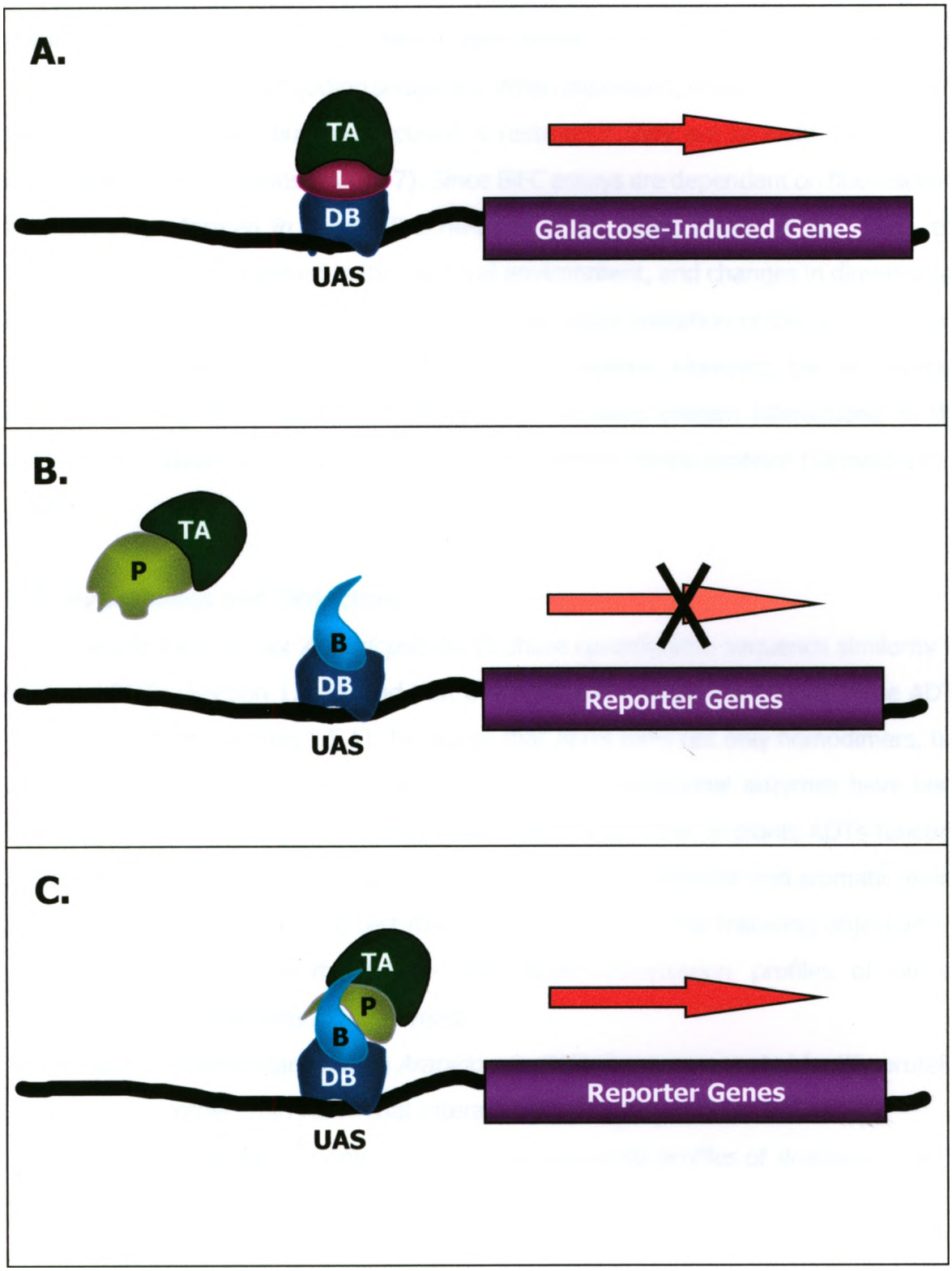
A.
TA
L
DB
UAS
Galactose-Induced Genes
B.
TA
P
B
DB
UAS
Reporter Genes
C.
TA
P
B
DB
UAS
Reporter Genes

Recently, another system has been developed which allows protein-protein interactions to be observed in living cells, called Bi-molecular Fluorescence Complementation (BiFC; reviewed in Kerppola, 2008). Similar to the Y2H system, BiFC involves fusion of a gene of interest with either an N- or C-terminal half-*Yellow Fluorescent Protein* (*YFP*) coding sequence. When expressed, neither of these half-YFPs fluoresces on its own, but fluorescence is restored if they are brought together via interacting fusion proteins (Figure 7). Since BiFC assays are dependant on fluorescence and can be performed *in planta* (Bracha-Drori *et al.*, 2004; Walter *et al.*, 2004), the interactions can be observed in their natural environment, and changes in dimerization and subcellular localization can be observed. The major limitation of this system is that like Y2H it can only be used to identify binary interactions. However, the BiFC system has successfully been used in *Arabidopsis* to visualize protein interactions in the nucleus, the cytoplasm, in organelles, and for transmembrane proteins (Citovski *et al.*, 2006).

1.7 Hypotheses and Objectives

Given that the six *Arabidopsis* ADTs share considerable sequence similarity to bacterial PDTs (Section 1.4.1), and that the predicted crystal structure of these ADTs is similar to PDTs (Section 1.5.1), I propose that ADTs form not only homodimers, but also heterodimers. In addition, since both bi- and tri-functional enzymes have been found in some bacteria (Section 1.6), I also hypothesize that in plants ADTs function as part of a larger protein complex composed of multiple shikimate and aromatic amino acid biosynthesis enzymes. To test my hypotheses, I have the following objectives:

I. Determine the homo- and heterodimerization profiles of all six *Arabidopsis* ADTs in yeast.

II. Perform large-scale *Arabidopsis* cDNA library screens to identify proteins other than ADTs that interact with a representative ADT.

III. Analyze the homo- and heterodimerization profiles of *Arabidopsis* ADTs *in planta*.

Figure 7. The Bi-molecular Fluorescence Complementation System. A protein(s) of interest can be fused with either the N- or C-terminal half of the YFP coding sequence. Neither of the half-YFPs fluoresce on their own, however fluorescence is restored when they are brought together by an interaction between the fusion proteins.

YC: C-terminal half-YFP; YN: N-terminal half-YFP.

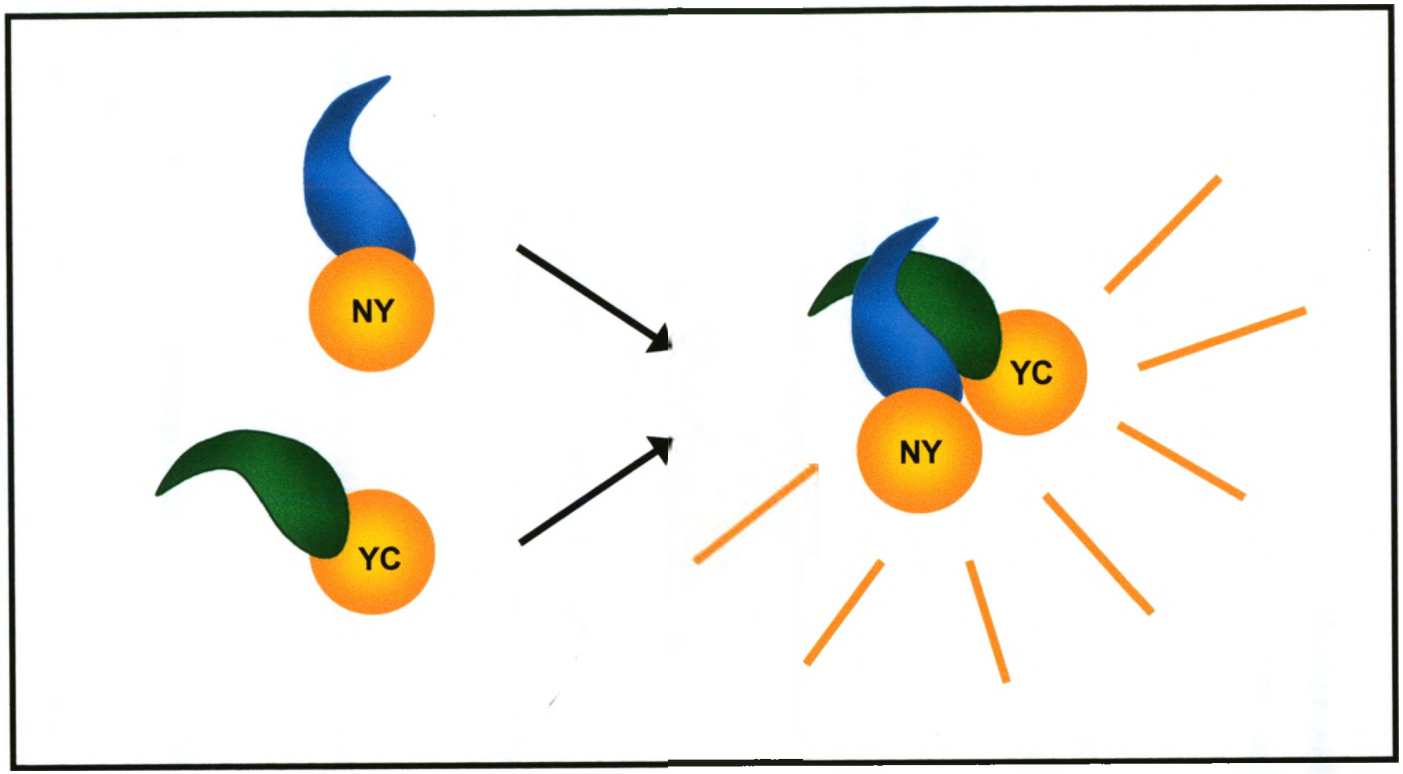
NY
YC
YC
NY

2 MATERIALS AND METHODS

2.1 Common Media, Solutions, and Reagents

2.1.1 Media

Gamborg's Solution

For 100ml: 2g sucrose and 0.32g Gamborg's B5 Medium with Vitamins (RPI Cat. No. 20200). Autoclave to sterilize. Just prior to use, add 100µl of 200mM acetosyringone and 1ml of 1M MES (see below).

Luria-Bertani (LB) Medium

For one litre: 10g tryptone, 5g yeast extract, 5g NaCl, and 200µl of 5N NaOH. Autoclave to sterilize. For solid medium, add 15g agar prior to autoclaving.

Synthetic Dextrose (SD) Medium

For one litre: 20g glucose, 6.7g yeast nitrogen base (without amino acids), and 1.5g appropriate dropout powder. Adjust to pH6.5 with 5N NaOH if necessary. Autoclave to sterilize. For solid medium, add 20g agar prior to autoclaving.

Yeast Extract and Beef (YEB) Medium

For one litre: 5g beef extract, 1g yeast extract, 5g peptone, 5g sucrose, and 0.49g $MgSO_4$. Autoclave to sterilize.

Yeast-Peptone-Dextrose-Adenine (YPDA) Medium

For one litre: 20g glucose, 10g yeast extract, 20g peptone, and 40mg adenine hemisulfate. Autoclave to sterilize.

Note: For all bacterial and yeast growth conditions, solid or liquid medium was used as appropriate.

2.1.2 Antibiotics, Hormones, Amino Acids, and Other Media Additives

Acetosyringone

For a 200mM stock solution: add 196.2mg acetosyringone (Sigma-Aldrich Cat. No. D134406) per 5ml dimethyl sulfoxide (DMSO). Store at -20°C.

Amino Acid Dropout Powder Mix

Thoroughly mix the following: 4g adenine sulfate, 2g L-argenine HCl, 10g L-aspartic acid, 10g L-glutamic acid, 2g L-histidine HCl, 3g L-isoleucine, 6g

L-leucine, 3g L-lysine HCl, 2g L-methionine, 5g L-phenylalanine, 37.4g L-serine, 20g L-threonine, 4g L-tryptophan, 3g L-tyrosine, 2g uracil, and 14.9g L-valine. For specific mixes, omit those amino acids which are necessary for selection. Add 1.5g/L medium prior to autoclaving.

3-Amino-1,2,4-Triazole (3AT)

For a 2M stock solution: add 168.16g 3-amino-1,2,4-triazole (BioShop Cat. No. ATT124) per liter ddH_2O, filter sterilize, and store at -20°C. For a final concentration of 10mM, add 5ml per liter of medium.

Ampicillin

For a 100mg/ml stock solution: add 1g ampicillin sodium salt (Sigma-Aldrich Cat. No. A9518) to 10ml ddH_2O. Filter sterilize and store at -20°C. Add 100µl per 100ml of medium.

Kanamycin

For a 60mg/ml stock solution: add 600mg kanamycin sulfate (USB Cat. No. 17924) to 10ml ddH_2O. Filter sterilize and store at -20°C. Add 100µl per 100ml of medium.

Rifampicin

For a 25mg/ml stock solution: add 250mg rifampicin (Sigma-Aldrich Cat. No. R3501) to 10ml DMSO. Store at -20°C. Add 41µl per 100ml of medium.

5-Bromo-4-chloro-3-indolyl-α-D-galactopyranoside (X-α-gal)

For a 20mg/ml stock solution: add 100mg X-α-gal (ClonTech Cat. No. 630407) to 5ml dimethyl formamide (DMF). Store in the dark at -20°C. Add 200µl per 100ml of media.

5-Bromo-4-chloro-3-indolyl-β-D-galactopyranoside (X-β-gal)

For a 100mg/ml stock solution: add 100mg X-β-gal (USB Cat. No. 12385) to 1ml DMF. Store in the dark at -20°C.

2.1.3 Buffers

Breaking Buffer

For one liter: 58.4g NaCl, 4ml of TritonX-100 (v/v) (USB Cat. No. 22686), 100ml of 10% SDS (w/v), 10ml of 1M Tris-Cl (pH8.0), and 2ml of 0.5M EDTA (pH8.0). Bring to one litre with ddH_2O.

10x Tris-Borate-EDTA (TBE) Running Buffer

For one liter: 108g Tris-base, 55g boric acid, and 40ml of 0.5M EDTA (pH8.0). Bring to one liter with ddH_2O.

10x Tris-EDTA (TE) Buffer

For 40ml: 4ml of 1M Tris-Cl (pH7.5 or pH8.0), 0.8ml of 0.5M EDTA (pH8.0), and 32.5ml sterile ddH_2O.

Z Buffer

For one litre: 8.6g Na_2HPO_4, 5.4g NaH_2PO_4, 0.75g KCl, and 0.25g $MgSO_4$ in ddH2O. Autoclave to sterilize. Just prior to use, add 2.7µl β-mercaptoethanol and 10µl X-β-gal (100mg/ml) per 1ml of Z buffer.

2.1.4 Other Solutions and Reagents

Ethylenediaminetetraacedic Acid (EDTA)

For a 0.5M stock solution: add 186.1g $Na_2EDTA•2H_2O$ to 1L ddH_2O. Adjust to pH8.0 with NaOH pellets. Autoclave to sterilize.

2-(*N*-Morpholino)-Ethanesulfonic Acid (MES)

For a 1M stock solution: add 19.5 g to 100ml ddH_20.

Sodium Dodecyl Sulfate (SDS)

For a 10% stock solution: add 100g SDS to 1L ddH_20.

Sodium Hydroxide (NaOH)

For a 5N stock solution: add 200g NaOH to 1L ddH_20.

Tris-Cl

For a 1M stock solution: add 121.1g Tris-base to 1L ddH_20. Adjust to pH 7.5 or pH8.0 with concentrated HCl. Autoclave to sterilize.

2.2 Strains and Plasmids

2.2.1 Bacteria Strains and Growth Conditions

Agrobacterium tumefaciens strain LBA4404 (NCCB accession PC2760, Hoekema *et al.*, 1983) was used for all transient expression experiments. This strain has a chromosomal rifampicin marker gene and contains the helper plasmid pAL4404. All *A. tumefaciens* cultures were grown for 16-48 hours at 28°C in YEB or LB medium supplemented with appropriate antibiotics.

Escherichia coli strain DH5α (Invitrogen Cat. No. 11319-019) was used for the maintenance and amplification of non-*ccdB* containing plasmid DNA. Plasmid DNA containing the negative selectable marker *ccdB* was maintained in the *ccdB*-insensitive *E. coli* strain DB3.1 (Invitrogen Cat. No. 11782-018). All *E. coli* cultures were grown for 16-18 hours at 37°C in LB medium supplemented with an appropriate antibiotic.

2.2.2 Yeast Strains and Growth Conditions

Saccharomyces cerevisiae strain YPB2 (Bartel *et al.*, 1993; *MATα ura3-52 his3-200 ade2-101 lys2-801 trp1-901 leu2-3,112 canR GAL4-542 gal80-538 LYS2::GAL1-UAS-LEU2*$_{TATA}$*-HIS3 URA3::GAL4-17mers(x3) CyC1*$_{TATA}$*-lacZ*) was used for initial Y2H experiments. This strain allows for GAL4-fusion protein-mediated expression of two reporter genes, *HIS3* (histidine prototrophy) and *LacZ* (β-galactosidase activity). Subsequent Y2H experiments were conducted using *S. cerevisiae* strain AH109 (ClonTech Cat. No. 630444; *MATa, trp1-901, leu2-3 112, ura3-52, his3-200, gal4Δ, gal80Δ, LYS2::GAL1-UAS-GAL1*$_{TATA}$*-HIS3, GAL2-UAS-GAL2*$_{TATA}$*-ADE2, URA3::MEL1-UAS-MEL1*$_{TATA}$*-lacZ, MEL1*). This strain allows for GAL4-fusion protein-mediated expression of three reporter genes, *HIS3, ADE2* (adenine prototrophy), and *MEL1* (α-galactosidase activity). All *S. cerevisiae* cultures were grown for 16-72 hours at 30°C or three to seven days at room temperature, on SD plates or in SD or YPDA medium supplemented with appropriate amino acids.

2.2.3 Plants and Growth Conditions

Arabidopsis (Columbia accession, CS70000) plants were vernalized for 5-7 days at 4°C, transferred to an incubator and raised under short day conditions (8 hours light, light, 16 hours dark) for 5-6 weeks. *N. benthamiana* plants (obtained from Dr. Y. Cui at Agriculture and Agri-Food Canada, London, ON) were raised under long day conditions (16 hours light, 8 hours dark) for 6-8 weeks. In both cases, light intensity was 150 μmol m^{-2} s^{-1} and temperature was maintained at 22°C.

2.2.4 Plasmids

The vectors pGEM-T (Promega Cat. No. A3600) and pDONR221 (Invitrogen Cat. No. 12536-017) were used for subcloning PCR fragments in ligation-dependant and

Gateway® cloning, respectively. pGEM-T is a linearized vector with 5' thymine overhangs which are able to capture PCR fragments via the 3' adenine overhangs generated by *Taq* polymerase. pDONR221 is a Gateway®-compatible vector containing a *ccdB* gene flanked by *attP* sites, which are compatible with an *attB*-flanked PCR product. The Y2H expression vectors pBI770 and pBI771 were used for initial yeast experiments (Kohalmi *et al.* 1997; Kohalmi *et al.*, 1998). These plasmids contain a multiple cloning site for cloning and expression of either a GAL4-DB or GAL4-TA fusion protein, respectively. The Gateway®-compatible Y2H expression vectors pGBKT7-DEST and pGADT7-DEST were used for subsequent yeast experiments (ClonTech Cat. Nos. 630489 and 630490; modified by Lu *et al.* 2010). These plasmids contain a Gateway® cassette for cloning via recombination and expression of either a GAL4-DB or GAL4-TA fusion protein, respectively. The modified Gateway®-compatible vectors pEarleyGate201-YN and pEarleyGate202-YC were used for BiFC assays (Earley *et al.* 2006; modified by Lu *et al.* 2010). These plasmids contain a Gateway® cassette for cloning via recombination and expression of a protein of interest in C-terminal fusion with either the N- or C-terminal portion of YFP, respectively. The vector p19 encodes a 19kDa tomato bushy stunt virus protein which has been shown to be a potent suppressor of post-translational gene silencing in plants (Silhavy *et al.*, 2002), and was used in this study to prevent transgene silencing in transient expression assays (Voinnet *et al.*, 2003). Other details regarding plasmids used in this study are shown in Table 1.

2.3 Cloning Procedures

2.3.1 Primer Design

For ligation-dependant cloning, PCR primers were designed to amplify full length (including the transit peptide), intermediate (intermediate region, catalytic and ACT domains), and short (only bacterial-defined catalytic and regulatory domains) *ADT1* and *ADT3* fragments based on full length coding sequence information available from TAIR (Appendix 1; accessions At1g11790 and At2g27820, respectively). All forward primers incorporate a 5′ *Sal*I site (5'GTCGAC3'), while reverse primers incorporate a 3′ *Not*I (5'GCGGCCGC3'), *Eco*RI (5'GAATTC3'), or *Xba*I (5'TCTAGA3') site, depending on existing internal restriction sites.

Table 1. Plasmid Properties.

Plasmid Name	Host(s) [a]	Selectable Marker(s) [b]	Fusion Domains [c] N	Fusion Domains [c] C	Promoter [d]	Origin(s) [e]	Sequencing Primer(s)
Plasmids for Subcloning							
pGEM-T	*E. coli*	*amp r*	-	-	-	pUC	T7/SP6
pDONR221	*E. coli*	*kan r*	-	-	-	pUC	M13 Forward/ M13 Reverse
Plasmids for Yeast-2-Hybrid							
pBI770	*E. coli*	*amp r*	Flag Tag	-	ADH1	ColE1	BC293/JN069
	Yeast	*LEU2*	GAL4-DB			*CEN6-ARS*	
pBI771	*E. coli*	*amp r*	Flag Tag	-	ADH1	ColE1	BC304/JN069
	Yeast	*TRP1*	GAL4-TA			*CEN6-ARS*	
pGBKT7-DEST	*E. coli*	*kan r*	cMyc Tag	-	ADH1	pUC	T7
	Yeast	*TRP1*	GAL4-BD			2μ	
pGADT7-DEST	*E. coli*	*amp r*	HA Tag	-	ADH1	pUC	T7
	Yeast	*LEU2*	GAL4-AD			2μ	

Table 1. (continued)

Plasmid Name	Host(s) [a]	Selectable Marker(s) [b]	Fusion Domains [c] N	Fusion Domains [c] C	Promoter [d]	Origin(s) [e]	Sequencing Primer(s)
Plasmids for Bi-molecular Fluorescence Complementation							
pEarleyGate201-YN	*E. coli*, *Agro* Plant	*kan*^{r}, *ccdB* *BAR*	HA Tag	YFP-N	*35S*	pBR322	-
pEarleyGate202-YC	*E. coli*, *Agro* Plant	*kan*^{r}, *ccdB* *BAR*	Flag Tag	YFP-C	*35S*	pBR322	-
Other Plasmids							
p19	*Agro*	*kan*^{r}	-	-	*35S*	unknown	-

[a] *Agro*: *A. tumefaciens*

[b] *amp*^{r}: ampicillin resistance; *BAR* = Basta resistance, for selection of stable plant transformants; *ccdB*: bacterial negative selectable marker; *kan*^{r}: kanamycin resisitance; *LEU2*: leucine prototrophy; *TRP1*: tryptophan prototrophy.

[c] Fusion of a tag or additional domain at the N- or C-terminus of the protein. YFP: N- or C-terminal half-YFP.

[d] *ADH1*: *ALCOHOL DEHYDROGENASE 1*, high level yeast promoter; *35S*: Cauliflower Mosaic Virus *35S*, constitutive promoter.

[e] 2μ: multi-plasmid copy yeast origin; *CEN6-ARS*: CENTROMERE 6-autonomously replicating sequence: single-plasmid copy yeast origin; ColE1, pBR322 and pUC: multi-plasmid copy bacterial origins.

For Gateway® cloning, PCR primers were designed to amplify full length *ADT1*, *ADT2* (At3g07630), *ADT3*, *ADT4* (At3g44720), *ADT5* (At5g22630), *ADT6* (At1g08250), and *CRA1* (At5g44120) fragments. All forward primers incorporate a 5'*attB1* site, while reverse primers incorporate a 3'*attB2* site, either with a stop codon (for N-terminal fusion Y2H vectors) or without a stop codon (for C-terminal fusion BiFC vectors).

All primers were analyzed for self-complementarity and compatibility using DNAMAN software (Lynnon BioSoft, version 6.0), and were obtained from Sigma or Invitrogen.

2.3.2 PCR Amplification of DNA

PCR amplification of all gene fragments was initially performed using *Tfi* DNA polymerase (Invitrogen Cat. No. 30342-024) in the TechGene Thermocycler (Fischer Scientific). Isolated plasmid DNA from existing expression vectors containing the fragment of interest was used as template DNA. Appropriate annealing temperatures were determined for amplification of each gene fragment and primer combination (Table 2). When DNA was to be used for cloning, DNA was amplified using Platinum® *Taq* High Fidelity DNA Polymerase (Invitrogen Cat. No. 10966-018). In all cases, the thermocycler program was as follows, where x°C is 45-55°C (Table 2):

> *Denature 2 min at 94°C ,followed by 10 cycles of 94°C for 15 sec, x°C for 30 sec, 72°C for 1 min, then 25 cycles of 94°C for 15 sec, x°C for 30 sec, 72°C for 1 min, adding an additional 10 sec per cycle, with a final 7 min elongation at 72°C.*

2.3.3 Gel Purification, Ligation, and Restriction Digests

PCR products and restriction enzyme digests were size-separated by gel electrophoresis in 1% agarose gel using 1x TBE running buffer, and the desired fragments were gel purified using a PureLink™ Quick Gel Extraction Kit (Invitrogen Cat. No. K2100-12), as per the manufacturer's instructions.

Ligations were performed using T4 DNA ligase (Fermentas Cat. No. EL0011), using a 3:1 insert to vector ratio, and incubated at 4°C overnight. The ligation product was transformed into *E. coli*, plasmid DNA was isolate, and a restriction digest was performed to confirm the presence of the correct ligation product.

Table 2. Annealing Temperatures for Various Primer Pairs.

Forward Primer	Reverse Primer	Annealing °C
Y2H-ADT1-F-FL	Y2H-ADT1-R-FL	50
Y2H-ADT1-F-I	Y2H-ADT1-R-FL	50
Y2H-ADT1-F-M	Y2H-ADT1-R-FL	50
D-Y2H-ADT1-F-M	D-Y2H-ADT1-R-FL	50
D-Y2H-ADT3-F-FL	D-Y2H-ADT3-R-XbaI	55
Y2H-ADT3-F-I	D-Y2H-ADT3-R-FL-XbaI	50
Y2H-ADT3-F-M	D-Y2H-ADT3-R-FL-XbaI	50
D-Y2H-ADT3-F-FL	D-Y2H-ADT3-R-FL-EcoRI	50
D-Y2H-ADT3-F-I	D-Y2H-ADT3-R-FL-EcoRI	55
D-Y2H-ADT3-F-M	D-Y2H-ADT3-R-FL-EcoRI	55
attB1-ADT1-F-FL	attB2-ADT1-R-FL	45
attB1-ADT1-F-FL	attB2-ADT1-RY-FL	45
attB1-ADT2-F-FL	attB2-ADT2-R-FL	45
attB1-ADT2-F-FL	attB2-ADT2-RY-FL	45
attB1-ADT3-F-FL	attB2-ADT3-R-FL	50
attB1-ADT3-F-FL	attB2-ADT3-RY-FL	50
attB1-ADT4-F-FL	attB2-ADT4-R-FL	55
attB1-ADT4-F-FL	attB2-ADT4-RY-FL	55
attB1-ADT5-F-FL	attB2-ADT5-R-FL	50
attB1-ADT5-F-FL	attB2-ADT5-RY-FL	50

Table 2. (continued)

Forward Primer	Reverse Primer	Annealing °C
attB1-ADT6-F-FL	attB2-ADT6-R-FL	55
attB1-ADT6-F-FL	attB2-ADT6-RY-FL	55
attB1-CRA1-F	attB2-CRA1-R	50
attB1-CRA1-F	attB2-CRA1-RY	50

All restriction enzymes were purchased from Fermentas, and digests were performed for 4-16 hours at 37°C, according to the manufacturer's instructions.

2.3.4 Gateway® Cloning

For cloning of into the Gateway® System, purified PCR products were subcloned into the vector pDONR221 via homologous recombination between the *attB* sites flanking the PCR product and *attP* sites on pDONR221, which results in the creation of an Entry Clone. This recombination reaction requires a BP Clonase (Invitrogen Cat. No. 11789020), and was performed following the manufacturer's instructions. The insert was then transferred into the Destination Vector (pGBKT7-DEST, pGADT7-DEST, pEarleyGate201-YN or pEarleyGate202-YC) via homologous recombination between the *attL* sites flanking the insert and *attR* sites on the Destination Vector. This recombination reaction requires a LR Clonase (Invitrogen Cat. No. 11791020), and was performed according to the manufacturer's instructions. Both pDONR221 and the Destination Vectors contain an *att*-flanked *ccdB* killer gene cassette, which is exchanged for the insert sequence in the recombination reaction, such that the by-products of these reactions are not viable. This reduces the number of false positives following transformation into *E. coli*.

2.3.5 Plasmid DNA Isolation from *E. coli* and Yeast

Plasmid DNA for sequencing purposes was isolated using a QIAprep Spin Miniprep Kit (QIAGEN Cat. No. 27104), following the manufacturer's instructions. Plasmid DNA for cloning was purified using an alkaline lysis-phenol:chloroform extraction protocol (modified from Ish-Horowicz and Burke, 1981).

Plasmid DNA was isolated from yeast as total DNA using a modified "Smash and Grab" protocol (Rose *et al.*, 1990). Cells were grown to stationary phase in appropriately supplemented SD medium. Cells were re-suspended in 200µl breaking buffer, 100µl buffer-saturated phenol, and 100µl chloroform:isoamyl alcohol (24:1 v/v), to which 300mg of acid-washed glass beads and 200µl TE buffer (pH8.0) were added. The suspension was vortexed using the FastPrep FP120 (Bio101 Savant) for 2 min at high speed, and centrifuged for 5 min at 14000 rpm, after which the DNA was precipitated in ice-cold 95% ethanol. DNA was re-suspended in 50µl sterile ddH_2O.

2.3.6 DNA Sequencing and *In Silico* Analyses

DNA sequencing was performed at the DNA Sequencing Facility at the Robarts Research Institute in London, ON Canada, using an ABI3730 DNA Analyzer. Details regarding sequencing primers used for each vector are available in Table 1. DNA sequencing results were analyzed using DNAMAN software (Lynnon BioSoft, version 6.0).

Following DNA isolation, Y2H library screen interactor sequences were identified using the Basic Local Alignment Search Tool (BLAST) run by the National Center for Biotechnology Information, and confirmed using The *Arabidopsis* Information Resource (TAIR). *In silico* analysis of sequences to identify potential cryptic splice sites was performed using two publicly-available eukaryotic gene structure prediction programs, GENSCAN (Burge and Karlin, 1998) and FGENESH (Softberry). Both of these programs provide a predicted peptide sequence based on analysis of the submitted gene sequence. *In silico* analysis of *ADT* sequences to identify potential nuclear localization signals was performed using the publicly-available nuclear prediction program NucPred (Brameier *et al.*, 2007), which assesses whether the protein is predicted to spend any time in the nucleus and gives this prediction a confidence value.

2.4 Bacterial Transformations

For *E. coli* transformations, ElectroMax DH5α competent cells were mixed with 100ng transforming DNA and transformed using a Gene Pulser II System (Bio-Rad) with the following settings: 2kV, 200Ω, 25μF. For *A. tumefaciens* transformations, competent LBA4404 cells were prepared according to Wise *et al.* (2006), and stored in 30% glycerol at -80°C. Thawed competent cells were mixed with 100ng transforming DNA containing the desired insert using a Gene Pulser II System (Bio-Rad) with the following settings: 2kV, 400Ω, 25μF. In both cases, transformed cells were allowed to recover for 1-2 hours in non-selective medium before plating on appropriately supplemented medium.

2.5 Introduction of DNA into Plant Tissue

DNA was introduced into *N. benthamiana* and *Arabidopsis* using *A. tumefaciens*-mediated infiltration (Wydro *et al.*, 2006; Wroblewski *et al.*, 2005). *A. tumefaciens*

infiltration cultures were prepared by inoculating 50ml YEB medium supplemented with the appropriate antibiotics, 25µl of 200mM acetosyringone, and 500µl of 1M MES. Cultures were incubated overnight at 28°C with shaking to an OD_{600} of 0.5-0.8. Cells were then re-suspended in Gamborg's Solution to an OD_{600} of 1.0-1.3. For co-infiltration of multiple constructs, re-suspended cells were combined in equal volumes just prior to infiltration. Re-suspended *A. tumefaciens* cells were injected into the lower leaf epithelium of *N. benthamiana* (Wydro *et al.*, 2006) and *Arabidopsis* (Wroblewski *et al.*, 2006) plants, which remained at room temperature under fluorescent lighting until fluorescence was evaluated every 24 hours post-infiltration, up to a maximum of 6 days.

2.6 Yeast Transformations

2.6.1 Lithium Acetate Transformations

Competent YPB2 or AH109 cells were prepared following a modified lithium acetate transformation protocol (Gietz and Woods, 2002). Competent cells were either used immediately, or stored in 30% glycerol at -80°C. Yeast were transformed with either a single plasmid, or a pair-wise combination of plasmids, using a modified polyethylene glycol (PEG)-mediated transformation method (Gietz and Woods, 2002; Kohalmi *et al.*, 1998). Transformants were then plated on appropriately supplemented SD medium. When performing large-scale library transformations, fresh competent cells containing the desired DB-fusion construct were transformed with a TA-cDNA library DNA (whole-plant, multi-developmental stage *Arabidopsis* library, Kohalmi *et al.*, 1997), rather than a single plasmid.

2.6.2 Yeast Library Mating

Diploid yeast cells were prepared following a modified Y2H Gold Mate and Plate™ library transformation protocol (ClonTech Protocol No. PT4084-1). AH109 cells (haploid *MATa*) containing pGBKT7-*ADT* construct were harvested at an OD_{600} of 0.8. The bait cells were then combined with an aliquot of TA-cDNA library (normalized universal *Arabidopsis* library, haploid *MATα* strain Y187, ClonTech Cat. No. 630487), and incubated for 24 hours in 50ml of 2xYPDA liquid medium with very slow shaking to induce mating. Using a hemocytometer, cells were evaluated for the formation of

three-lobed diploid zygotes. Once zygotes were visible, the cells were washed in 0.5xYPDA, re-suspended in TE buffer (pH8.0), and plated on appropriately supplemented SD medium.

2.7 Yeast-2-Hybrid Experiments

For this study, protein-protein interactions were tested using two different Y2H vector systems. In the first system (Kohalmi *et al.*, 1997), two reporter genes (*HIS3* and *lacZ*), in two different chromosomal locations in strain YPB2, were used to detect transcription activation. The selectable marker *HIS3* is a gene required in yeast for histidine biosynthesis, and when expressed allows the yeast to grow in the absence of histidine. Yeast cells that express *HIS3* are also resistant the toxin 3-amino-1,2,4-triazole (3AT). Resistance to 3AT can be titrated for each construct. The reporter gene *lacZ* encodes the enzyme β-galactosidase which, when expressed in the presence of a suitable substrate, produces an easily-observed color change. β-galactosidase assays were performed according to Kohalmi *et al.* (1998). Yeast were grown on appropriately supplemented SD medium and then transferred onto a nitrocellulose filter. Cells were permeabilized by submerging in liquid nitrogen, saturated with Z buffer containing X-β-gal, and incubated at 30°C for 4-6 hours, until blue pigmentation developed.

In the second system (ClonTech Cat. No. 630303), three reporter genes (*HIS3*, *ADE2*, and *MEL1*), in three different chromosomal locations in strain AH109, were used to detect transcription activation. *ADE2* is a gene required in yeast for adenine biosynthesis which can be used as both a prototrophic marker and a visual reporter (Jones and Fink, 1982). If *ADE2* expression is high, the colonies remain white, however low expression results in the accumulation of P-ribosylamino-imidazole, which is converted to a red pigment. The reporter gene *MEL1* is naturally present in some yeast strains (Naumov *et al.*, 1990) and encodes the secreted enzyme α-galactosidase which, when expressed in the presence of a suitable substrate, produces an easily-observed color change. If all reporters in the system are transcribed, then this indicates that the two proteins in question are able to interact. α-galactosidase assays were performed according to the manufacturer's instructions (ClonTech Protocol No. PT3353-2) and incubated on medium containing X-α-gal for 48 hours at room temperature, until blue pigmentation developed.

2.8 Bi-molecular Fluorescence Complementation Assays

To examine protein-protein interactions *in planta*, BiFC assays were carried out using a modified pEarleyGate vector system (Earley *et al.*, 2006; modified by Lu *et al.*, 2010). The half-YFP fusion constructs were transiently introduced into *N. benthamiana* and *Arabidopsis* using *A. tumefaciens*, and fluorescence observed using a Leica DM-IRE scanning laser confocal microscope, using the following settings:

YFP excitation at 514λ and emitance from 520-550λ.

Chloroplast autofluorescence excitation at 488λ and emitance from 630-690λ.

3 RESULTS

3.1 Determining the Appropriate *ADT* Construct Length

In preparation for cloning all six *ADT*s into the Y2H vectors, two representative ADT*s*, ADT1 and ADT3, were selected to determine the appropriate sequence length for testing protein interactions. These two isomers fall into two different phylogenetic subfamilies (Figure 2), share only 65% amino acid sequence similarity across the catalytic and ACT regulatory domains (Figure 3), and represent both intron-containing (*ADT1*) and intron-less (*ADT3*) isomers (Cho et al., 2007). As it is still unclear whether the transit peptide is required for interactions, or whether it may impede interactions, *ADT1* and *ADT3* were each amplified in three different lengths from existing constructs. The full length (FL) construct contains the entire coding region including the transit peptide sequence, while the shortest (S) contains only the coding sequence of the catalytic and ACT regulatory domains which are sufficient in bacterial PDTs. An intermediate length construct (I) was also amplified, which includes the coding sequence for the highly-conserved sequence just upstream of the bacterial-defined catalytic and regulatory domains (Figure 3). Each *ADT* was PCR amplified using primers which incorporate unique restriction sites (Appendix 1) and directionally cloned into the Y2H expression vectors pBI770 and pBI771, either directly or by first subcloning into pGEM (Figure 8; Appendix 2), and transformed into *E. coli*. Putative transformants were identified by resistance to ampicillin, and the presence of the *ADT* was confirmed by restriction analysis. To ensure sequence integrity, each expression vector was sequenced using bait- or prey-specific primers (Table 1; Kohalmi *et al.*, 1998).

3.1.1 Control Transformations for pBI770 (DB) and pBI771 (TA) Constructs

Completed FL, I, and S constructs of *ADT1* and *ADT3* were transformed into yeast strain YPB2 and tested to ensure that they are not able to activate transcription of the reporter genes in the absence of an interaction, termed self-activation. A summary of these controls is shown in Table 3. Each *DB-ADT* and *TA-ADT* fusion construct was transformed into yeast alone, and co-transformed with either a corresponding empty vector, or a *TA*- or *DB*-fusion construct containing the unrelated seed storage protein *CRUCIFERINA* (*CRA1*; accession At5g44120). Activation of the

Figure 8. Ligation-Based Cloning Strategy. Each *ADT* was PCR amplified using primers which incorporated specific restriction enzymes (tabs). The PCR amplicon was then either subcloned into pGEM-T, or digested directly and cloned into pBI770 and pBI771.

A: 3' adenine overhang; ADT: arogenate dehydratase; amp^r: ampicillin resistance; F: Flag tag; *GAL*: GAL4 domain; RE: restriction enzyme sequence; T: 5' thymine overhang.

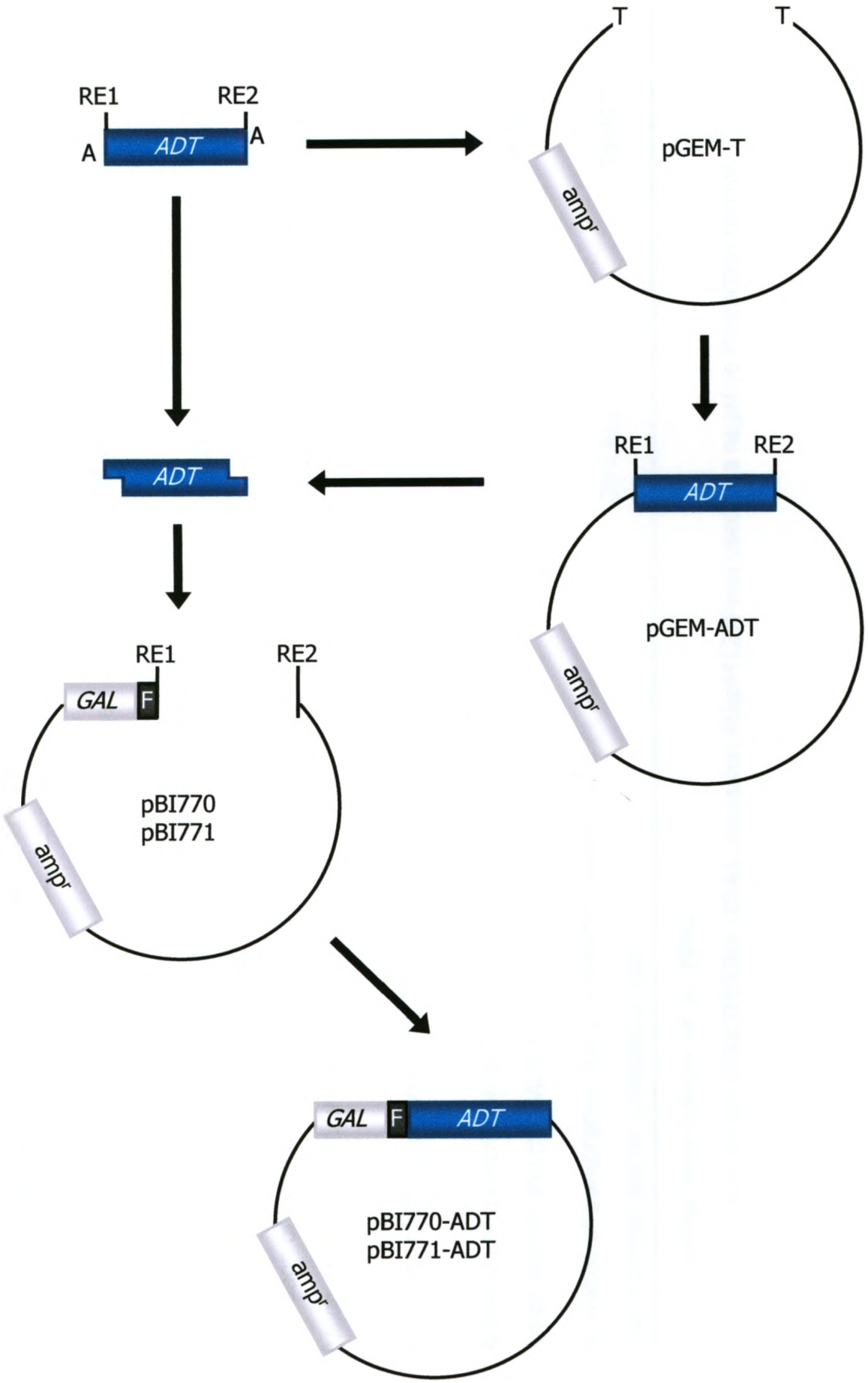
RE1
RE2
A
ADT
A
T
T
pGEM-T
ampr
RE1
RE2
ADT
pGEM-ADT
ampr
ADT
RE1
RE2
GAL
F
pBI770
pBI771
ampr
GAL
F
ADT
pBI770-ADT
pBI771-ADT
ampr

Table 3. ControlTransformations for Yeast-2-Hybrid Assays [a].

Biological Property Tested	Protein #1	Protein #2
Activation of transcription by the DB-ADT fusion protein alone	DB-ADT	-
Activation of transcription due to interaction between the DB-ADT fusion protein and the GAL4-TA domain	DB-ADT	TA
Activation of transcription due to interaction between the DB-ADT fusion protein and an unrelated protein [b]	DB-ADT	TA-CRA1
Activation of transcription by the TA-ADT fusion protein alone	-	TA-ADT
Activation of transcription due to interaction between the TA-ADT fusion protein and the GAL4-DB domain	DB	TA-ADT
Activation of transcription due to interaction between the TA-ADT fusion protein and an unrelated protein [b]	DB-CRA1	TA-ADT

[a] Table modified from Kohalmi *et al.*, 1998.

[b] The seed storage protein CRUCIFERINA (CRA1; accession At5g44120) was used as a negative interaction control.

HIS3 and *lacZ* reporter genes was then evaluated for each control transformant. While none of the ADT1 fusion proteins (both DB- and TA-fusions), nor the TA-ADT3 fusion proteins were self-activating, all three lengths of ADT3 were able to activate expression of the *HIS3* and *lacZ* reporter genes in the absence of an interaction when fused to the DB domain (Appendix 3). *In silico* analysis showed that all six *Arabidopsis* ADTs contain a cryptic GAL4-type nine amino acid transactivation domain (Piskacek *et al.*, 2007), however since ADT1 is not self-activating, it is likely that only ADT4, ADT5, and ADT6, which are closely related to ADT3, will also be self-activating. For detailed description of this activation domain, see Section 4.1.1.

3.1.2 ADT1 and ADT3 Form Dimers in Most Lengths

Full length, intermediate and short *ADT1* constructs were co-transformed into yeast strain YPB2 along with either *TA-ADT1* or *TA-ADT3* constructs in all possible pair-wise combinations (Figure 9). ADT1 is able to form homodimers and activate both the *HIS3* and *lacZ* reporters in most combinations tested, except when ADT1-FL is fused to the GAL4-TA domain (Figure 9A). While TA-ADT1-FL is able to dimerize with DB-ADT1-S, activation of the reporters is absent with DB-ADT1-FL and weak with DB-ADT1-I. Interestingly, the DB-ADT1-FL fusion is still able to form heterodimers with ADT3 (Figure 9B), so it is not likely that the TA-ADT1-FL construct itself is defective. Similarly, ADT3 is able to form heterodimers and activate both reporters with all three lengths of ADT1, except where ADT3-S is fused to the GAL4-TA domain (Figure 9B). ADT3 homodimers were not tested, nor were the reciprocals of the ADT1-ADT3 heterodimers, as the DB-ADT3 fusion proteins are self-activating (Section 3.1.1). These results show that *Arabidopsis* ADTs are able to form homo- and heterodimers. These results also indicate that, with the exception of the TA-ADT1-FL fusion protein, inclusion of the transit peptide sequence does not limit interaction ability, and so all subsequent Y2H experiments were performed with full length ADTs.

3.2 Determining the Dimerization Profiles of all Six ADTs

Initial cloning of *ADT1* and *ADT3* was performed using traditional ligation-based protocols, however subsequent cloning was performed using Invitrogen Gateway®

Figure 9. Dimerization of Full Length, Intermediate, and Short ADT1 and ADT3 Constructs. Each dimer combination was transformed into yeast and assayed for growth, histidine prototrophy, and β-galactosidase activity. Growth of white colonies in the absence of histidine and production of a blue pigment in the presence of X-β-gal indicates an interaction. A summary of the assay results is shown to the right of each panel. **A.** ADT1 forms homodimers in all combinations tested, except for the full length dimer. **B.** ADT1 and ADT3 form heterodimers in all combinations tested, except when the ADT3-S construct is fused to the TA domain.

+: interaction; –: no interaction; DB: GAL4 DNA binding domain; FL: full length construct; G: growth assay; H: histidine prototrophy assay; I: intermediate length construct; L: lacZ; S: short length construct; TA: GAL4 transactivation domain.

A.

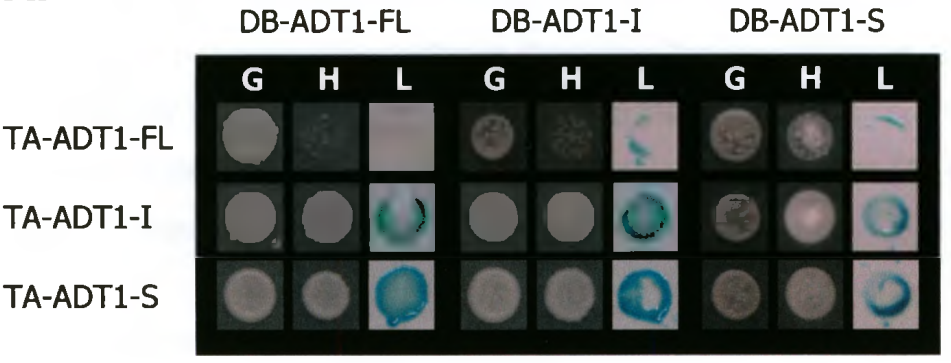

	1FL	1I	1S
1FL	-	+	+
1I	+	+	+
1S	+	+	+

B.

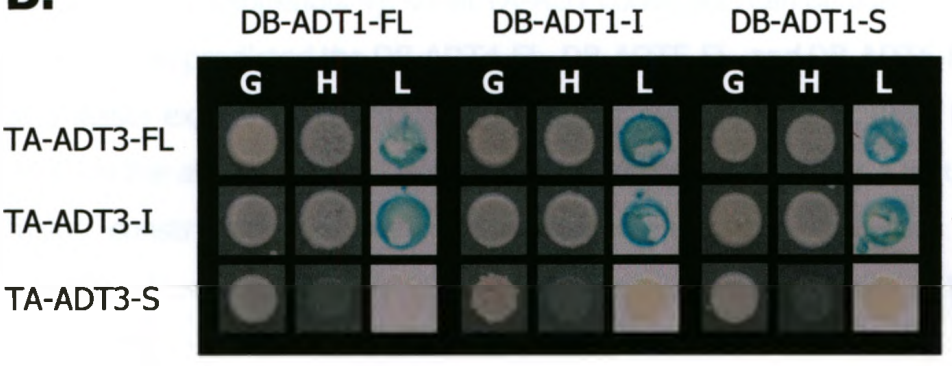

	1FL	1I	1S
3FL	+	+	+
3I	+	+	+
3S	-	-	-

cloning technology, which allows for efficient transfer of insert sequences from one vector to another via homologous recombination (Figure 10). All six full length *ADT*s were PCR amplified using primers which are compatible with the Gateway® cloning system (Appendix 3), recombined into Entry Vector pDONR221 (producing an Entry Clone for each *ADT*), and transformed into *E. coli*. Sequence integrity for each *ADT* was confirmed by DNA sequencing, following which each *ADT* was transferred from the Entry Clones to the Destination Vectors pGBKT7-DEST (DB-fusion) and pGADT7-DEST (TA-fusion) via recombination. Being that both pDONR221 and pGBKT7-DEST are selected for by kanamycin resistance, the Entry Clones were linearized using either *MluI* or *AseI* prior to recombination to prevent the transformation of non-recombined Entry Clones. For each completed construct, the junction between the *DB-* or *TA*-domain and the *ADT* sequence was confirmed by DNA sequencing.

3.2.1 Control Transformations for pGBKT7 (DB) and pGADT7 (TA) Constructs

Completed pGBKT7 and pGADT7constructs were transformed into yeast strain AH109 and tested for self-activation (Table 3). None of the TA-fusion proteins were self-activating (Appendix 4), so all TA-ADT constructs can be used to test dimerization. However, as predicted the DB-ADT4-FL, DB-ADT5-FL, and DB-ADT6-FL constructs, and to a lesser extent the DB-ADT3-FL construct, were able to activate the reporter gene *MEL1* in the absence of an interacting protein (Appendix 5). As a result, these four DB-fusion constructs were not used to test dimerization. Only the DB-ADT1-FL and DB-ADT2-FL constructs, which are not self-activating, were used to test dimerization.

3.2.2 ADT1, but not ADT2, Can Form Heterodimers with All Other ADTs

Using DB-ADT1-FL and DB-ADT2-FL in combination with all six TA-fusion constructs, all possible homo- and heterodimer combinations were co-transformed into yeast strain AH109 and the ability of the fusion proteins to interact was tested by evaluating reporter gene activation (Figure 11). As with the previous yeast system, TA-ADT1-FL is not able to form a homodimer with DB-ADT1-FL (Figure 11). However, DB-ADT1-FL is able to form heterodimers with ADT3, ADT4, ADT5 and ADT6, in each case activating all three reporter genes. Since the TA-ADT1-FL construct is able to form a heterodimer with DB-ADT2-FL (see below), it can be concluded that while the

Figure 10. Gateway® Cloning Strategy. Each ADT was PCR amplified using primers which incorporated *attB* sites (light grey boxes). Each PCR amplicon was then subcloned into pDONR221 before being transferred to the appropriate destination vector via recombination. Positions of restriction enzyme sites used to linearize the entry clones prior to LR reactions are marked.

ADT: arogenate dehydratase; amp^r: ampicillin resistance; *att*: attenuation site; BP: BP clonase reaction; *ccdB*: negative selectable marker; *Cm*: chloramphenicol resistance; kan^r: kanamycin resistance; LR: LR clonase reaction; RE: restriction enzyme sequence.

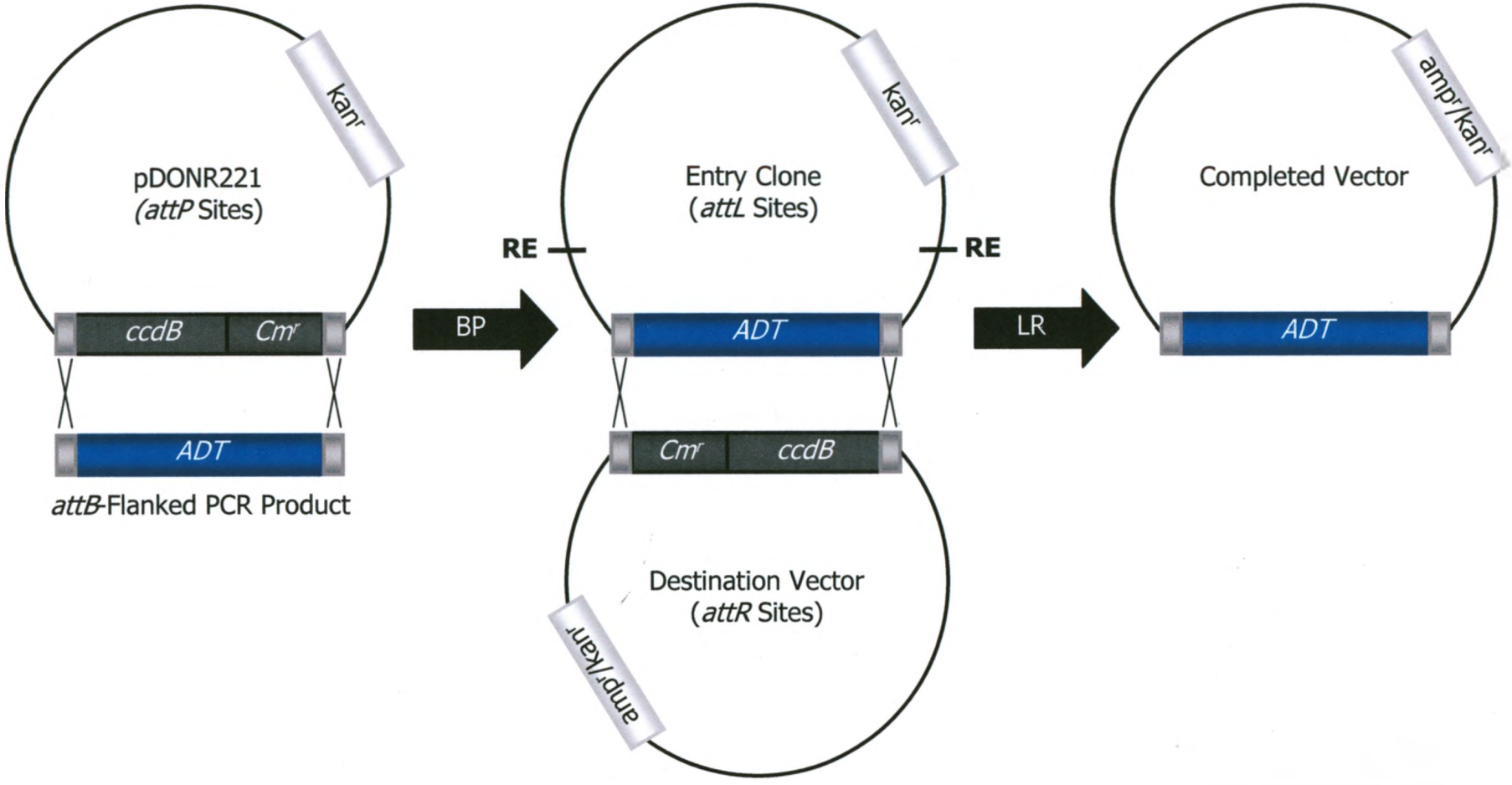
pDONR221
(attP Sites)
kanr
ccdB
Cmr
ADT
attB-Flanked PCR Product
BP
RE
Entry Clone
(attL Sites)
kanr
ADT
Cmr
ccdB
RE
Destination Vector
(attR Sites)
ampr/kanr
LR
Completed Vector
ampr/kanr
ADT

Figure 11. Dimerization of Full Length ADT1 and ADT2 Constructs with all Six ADTs in Yeast. Each dimer combination was assayed for growth, histidine prototrophy, adenine prototrophy, and α-galactosidase activity. Growth of white colonies in the absence of histidine, growth of white or red colonies in the absence of adenine, and production of a blue pigment in the presence of X-α-gal indicates an interaction. While ADT1 is able to form heterodimers with all other ADTs (see text for details), ADT2 is only able to form a heterodimer with ADT1. Note that the ADT2-ADT1 dimer activates expression of the *ADE2* and *MEL1* reporters, but not the *HIS3* reporter. Neither ADT1 nor ADT2 are able to form homodimers in this system. A summary of the assay results is shown to the right of the panel.

+: interaction; –: no interaction; A: adenine prototrophy; DB: GAL4 DNA binding domain; FL: full length construct; G: growth; H: histidine prototrophy; M: *MEL1*, α-galactosidase; TA: GAL4 transactivation domain.

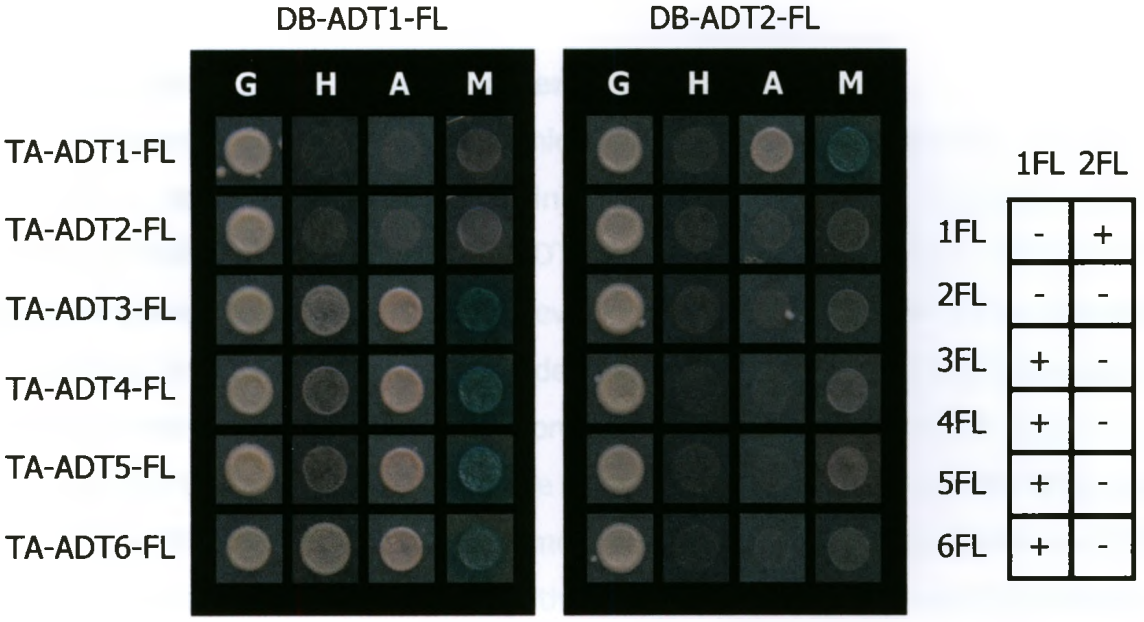
DB-ADT1-FL
DB-ADT2-FL
G H A M
G H A M
TA-ADT1-FL
TA-ADT2-FL
TA-ADT3-FL
TA-ADT4-FL
TA-ADT5-FL
TA-ADT6-FL
1FL 2FL
1FL - +
2FL - -
3FL + -
4FL + -
5FL + -
6FL + -

TA-ADT1-FL construct is not able to form homodimers, it is able to form at least one heterodimer a yeast system.

DB-ADT2-FL is not able to form a homodimer in yeast, nor is it able to form heterodimers with any of the other ADTs, except for TA-ADT1-FL (Figure 11). It is interesting to note that this ADT1-ADT2 dimer activates the *ADE2* and *MEL1* reporters, but not the *HIS3* reporter. As each of the reporters is controlled by a different promoter, sharing only the GAL4-UAS, it is possible that the ADT1-ADT2 dimer may be unable to activate the *HIS3* reporter, without affecting expression of *ADE2* or *MEL1*. However, due to the self-activation properties of ADT3, ADT4, ADT5, and ADT6, the ADT2 heterodimers were not tested in reciprocal configurations.

3.3 Large-Scale cDNA Library Screens

To identify any other proteins which interact with ADTs, three different large-scale library screens were performed in this study, using two independent cDNA libraries. Initially, DB-ADT1-FL and DB-ADT1-I (both cloned using vector pBI770) were screened against a whole-plant, multi-developmental stage TA-cDNA library (Kohalmi *et al.* 1997). Only two interactors were identified: a putative aminotransferase (which was not processed further as the fusion protein is out of frame) and ADT1 (Figure 12). The same ADT1 fragment, which lacks the transit peptide sequence, was identified four times. While this confirms the ADT1 homodimer, it does not provide evidence of the formation of a larger protein complex. As this cDNA library has been amplified a number of times (S. Kohalmi, personal communication), it is possible that the diversity of the library is diminished. To address this, an additional DB-ADT1-FL (using vector pGBKT7) screen was performed using a commercially available library which is compatible with the Gateway® Y2H constructs. This commercial library is a universal *Arabidopsis* cDNA library which has been normalized, such that the quantity of highly-expressed transcripts (such as actin) have been reduced, increasing the likelihood that interactions with the products of transcripts with low expression levels might be identified (ClonTech PT4084).

Figure 12. Interactions Identified Using the Kohalmi *et al.* (1997) cDNA Library. Two screens were performed, using either DB-ADT1-FL or DB-ADT1-I. Five interactors were identified, all of which were identified by DNA sequencing as ADT1 except for DB-ADT1-I-T03, which is a putative aminotransferase (At5g27410). However, only the ADT1 fragments produce in-frame TA-fusion proteins. Growth of white colonies in the absence of histidine and production of a blue pigment in the presence of X-β-gal indicates an interaction. A summary of the interactions is shown to the right of the panels.

+: interaction; DB: GAL4 DNA binding domain; FL: full length construct; G: growth; H: histidine prototrophy; L: *lacZ*, β-galactosidase; T: transformant number; TA: GAL4 transactivation domain.

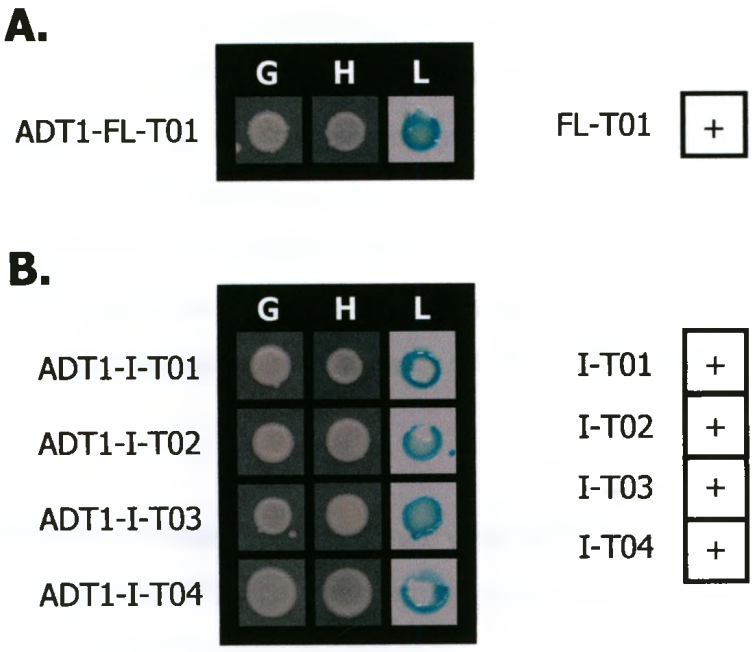
A.
G
H
L
ADT1-FL-T01
FL-T01
+
B.
G
H
L
ADT1-I-T01
ADT1-I-T02
ADT1-I-T03
ADT1-I-T04
I-T01
I-T02
I-T03
I-T04
+
+
+
+

3.3.1 Processing of Interactors and Control Transformations for Y2H cDNA Library Screens

DNA was successfully isolated from 54 of 72 putative positive colonies in the normalized cDNA library screen (Appendix 6), and subjected to a diagnostic restriction digest using *Hind*III and *Eco*RI (example shown in Figure 13). All interactors with unique digest patterns were sent for DNA sequencing, however for interactors with identical digest patterns only one representative sample was analyzed. Fusion proteins in which the interactor sequence is not in frame with the TA- or DB-domain sequence were not processed further (Table 4). Representatives of each in-frame interactor were transformed back into yeast strain AH109 (see controls described in Table 3) to determine whether they are self-activating, and those which activated transcription of either *ADE2*, *HIS3*, or both in the absence of DB-ADT1-FL were not processed further (Table 4; Appendix 7). The third reporter gene in this system, *MEL1*, was not informative for analyzing interactions as, even in the absence of an interacting protein, all of the isolated interactors were able to activate transcription of *MEL1* (Appendix 7). Interactors which were not able to activate expression of *HIS3* and *ADE2* on their own (Table 5) were co-transformed along with DB-ADT1-FL to confirm the interaction (Figure 14).

3.3.2 Confirmation of Interactions Involving ADTs

The large-scale DB-ADT1-FL screen against the normalized universal *Arabidopsis* cDNA library confirmed the formation of both ADT1-ADT4 and ADT1-ADT6 heterodimers (Table 5; Figure 14). The interaction with ADT4 was identified once and sequencing revealed that the interaction was mediated by an N-terminally truncated ADT4 which included the entire ACT regulatory domain and most of the catalytic domain. This interaction activated transcription of *ADE1*, but not *HIS3*. Interactions with three types of ADT6 fragments were also identified in this screen. Two different N-terminally truncated ADT6 fragments, which include the entire catalytic and ACT regulatory domains, and part of the transit peptide were identified (once each), and a full length sequence was identified 13 times (Table 5). Surprisingly, the truncated *ADT6* sequences are both out of frame with the TA-fusion domain, and the full length *ADT6* sequence contains a stop codon in between the TA-domain sequence and the *ADT6* sequence,

Figure 13. Representative Restriction Digest of DB-ADT1-FL Interactors Recovered from the Normalized Commercial cDNA Library Screen. Diagnostic restriction digests were performed using *Hind*III and *Eco*RI. Similar digest patterns are marked by red and yellow boxes, respectively, and only one representative of each pattern was sent for sequencing. All unique patterns were sent for sequencing. Transformant numbers are indicated across the top of the gel, and ladder sizes are given on the left. Vector-derived fragments (2.4kb and 5.0kb, respectively) are indicated on the right of the gel.

ADT: arogenate dehydratase; DB: DNA binding domain; FL: full length; kb: kilo base; L: ladder.

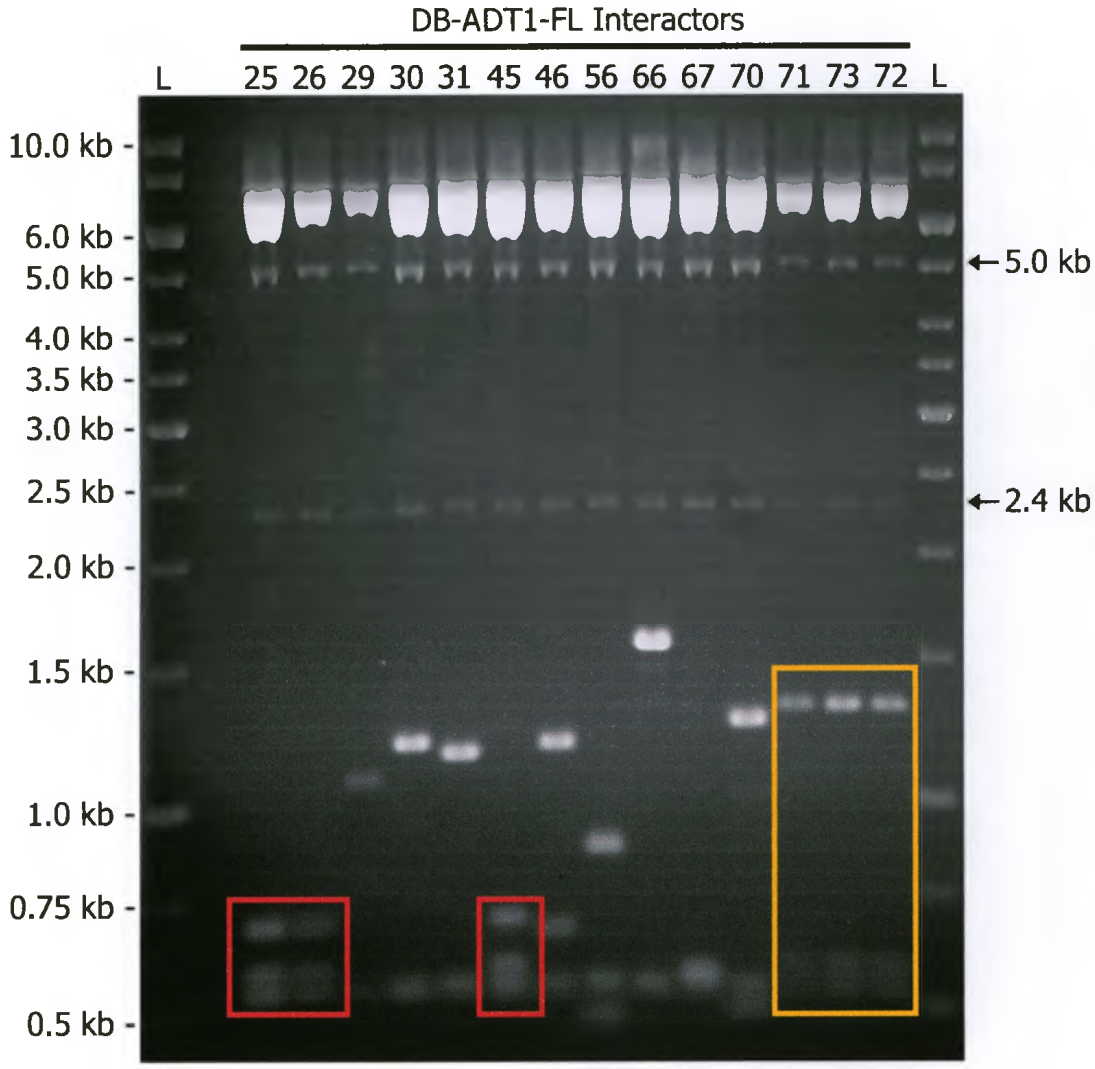
DB-ADT1-FL Interactors
L
25 26 29 30 31 45 46 56 66 67 70 71 73 72
L
10.0 kb -
6.0 kb -
5.0 kb -
4.0 kb -
3.5 kb -
3.0 kb -
2.5 kb -
2.0 kb -
1.5 kb -
1.0 kb -
0.75 kb -
0.5 kb -
←5.0 kb
←2.4 kb

Table 4. Putative ADT1 Interactors Which Were Not Processed.

Interactor Name	Abbr.	TAIR	Function	Interaction Frequency	Unique Fragments	Correct Frame	SA. [a]
Proteins that Localize to the Chloroplast							
Putative Acid Phosphatase		At5g44020	Unknown	2	1	Yes	Yes
FK506-BINDING PROTEIN 16	FKBP16	At4g39710	Protein Folding	1	1	Yes	Yes
EPITHIOSPECIFIER MODIFIER 1	ESM1	At3g14120	Glucosinolate Catabolism	1	1	No*	-
Plastid-lipid Associated Protein		At4g22240	Unknown	4	1	No	-
Unknown Protein		At1g13990	Unknown	1	1	No	-
CHLORORESPIRATORY REDUCTION 23	CRR23	At1g70760	NAD(P)H Complex	4	1	No	-
NUCLEAR-ENCODED CLP PROTEASE P7	NCLPP7	At5g23140	Caseinolytic Protease	1	1	No	-
Proteins that Localize to the Cell Wall							
GDSL-like Lipase		At5g14450	Lipid Metabolism	2	1	Yes	Yes
BETA GALACTOSIDASE 9	BGAL9	At2g32810	Putative β-galactosidase	1	1	Yes	Yes
Pathogenesis-related Thaumatin Protein		At2g28790	Response to other organisms	1	1	No	-
Proteins that Localize to the Plasma Membrane							
Unknown Protein, proline rich		At2g41420	Unknown	1	1	Yes	Yes
RAB GTPase Homolog G3F	RAB7B	At3g18820	Signal Transduction	5	1	No	-
Proteins that Localize to the Nucleus							
Wound Responsive Protein		At1g19660	DNA-binding, Nuclease Activity	1	1	Yes	Yes

Table 4. (continued)

Interactor Name	Abbr	TAIR	Function	Interaction Frequency	Unique Fragments	Correct Frame	SA. [a]
Proteins that Localize to the Endosome							
ESCRT-like Complex, Ubiquitin Binding Protein	ELC	At3g12400	Protein Sorting	1	1	Yes	Yes
Protein that Localize to the Endomembrane System							
PATHOGENESIS-RELATED 4	PR4	At3g04720	Chitin Binding	1	1	Yes	Yes
Unknown Protein		At5g25410	Unknown	1	1	Yes	Yes
Proteins that Localize to the Cytoplasm							
MYO-INOSITOL-PHOSPHATE SYNTHASE	MIPS1	At4g39800	Inositol Biosynthesis	1	1	Yes	Yes
Proteins with Unknown Localization Patterns							
Putative Class IV Aminotransferase		At5g27410	Unknown	1	1	No	-
RHAMNOSE BIOSYNTHESIS 1	RHM1	At1g78570	UDP-L-Rhamnose Biosynthesis	1	1	Yes	Yes
Putative Transmembrane Amino Acid Transporter		At1g25530	Unknown	1	1	No	-

[a] SA: self-activation. Only fusion proteins which are in frame were evaluated for self-activation properties.

* These sequences are either out of frame, contain a premature stop codon prior to the start of the interactor sequence, or both.

Table 5. Putative ADT1 Interactors.

Interactor Name	Abbr.	TAIR	Function	Interaction Frequency	Unique Fragments	Correct Frame	SA. [a]	Confidence [b]
Proteins that Localize to the Chloroplast								
AROGENATE DEHYDRATASE 1	ADT1	At1g11790	Phe Biosynthesis	4	1	Yes	No	High
AROGENATE DEHYDRATASE 4	ADT4	At3g44720	Phe Biosynthesis	1	1	Yes	No	High
AROGENATE DEHYDRATASE 6	ADT6	At1g28050	Phe Biosynthesis	15	3	Yes*	No	High
BRANCHED CHAIN AMINOTRANSFERASE 3	BCAT3	At3g49680	Ile/Leu/Val Biosynthesis	1	1	Yes	No	High
CHLOROPLASTOS ALTERADOS 1	CLA1	At4g15560	Isoprenoid Biosynthesis	1	1	Yes	No	Low
Putative Elongation Factor		At5g08650	Small GTP-binding Protein	1	1	Yes	No	Low
ADENYLOSUCCINATE SYNTHASE	ADSS	At3g57610	AMP Biosynthesis	1	1	Yes	No	Low
Proteins that Localize to the Mitochondrion								
SUCCINYL-CoA LIGASE, alpha subunit		At5g08300	TCA Cycle	1	1	Yes	No	Low
Proteins that Localize to the Plasma Membrane								
Putative Protein Kinase		At2g36350	Protein Phosphorylation	2	1	Yes	No	Low

[a] SA: self-activating properties.

[b] High confidence interactions either activate two reporters or have been identified in binary interaction assays. Low confidence interactions activate only one reporter.

* These sequences are either out of frame, contain a premature stop codon prior to the start of the interactor sequence, or both.

Figure 14. Confirmation of Interactors Identified in the Normalized Commercial cDNA Library Screens. All DB-ADT1-FL interactors recovered from the normalized cDNA library screen which are in frame and are not self-activating were co-transformed back into yeast with DB-ADT1-FL to confirm the original interaction. Each dimer combination was assayed for growth, histidine prototrophy, adenine prototrophy, and α-galactosidase activity. Growth of white colonies in the absence of histidine, growth of white or red colonies in the absence of adenine, or production of a blue pigment in the presence of X-α-gal would indicates an interaction. Details regarding each interactor can be found in Table 5. TA-fusion proteins are listed along the left, and a summary of the interactions are shown in to the right of the panel. Note that expression of the *MEL1* reporter gene is activated by all interactors alone (see Appendix 7) and so it is not informative in this interaction study.

+: interaction; −: no interaction; A: adenine prototrophy; DB: GAL4 DNA binding domain; FL: full length construct; G: growth; H: histidine prototrophy; M: *MEL1*, α-galactosidase; TA: GAL4 transactivation domain.

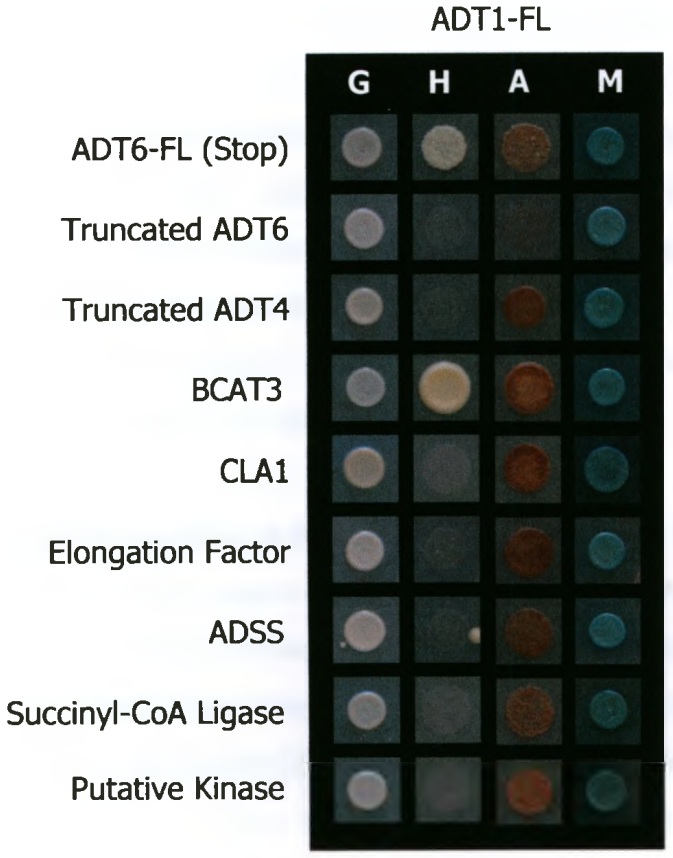

	1FL
ADT6-FL	+
ADT6 (t)	-
ADT4 (t)	+
BCAT3	+
CLA1	+
EF	+
ADSS	+
S-CoA	+
Kinase	+

just one amino acid prior to the start codon of the *ADT6* sequence. These interactors would normally not have been processed, as they should not produce a biologically relevant fusion protein, however as the ADT1-ADT6 heterodimer has already been shown in yeast (Section 3.2.2), these interactions warrant further investigation (see Sections 3.3.4 and 4.4.2).

3.3.3 ADT1 Interacts with Many Other Proteins

Six putative non-ADT interactors were confirmed in yeast using DB-ADT1-FL, a summary of which is shown in Table 5. These interactions include a branched-chain aminotransferase (BCAT3), and a putative elongation factor, as well as proteins involved in isoprenoid biosynthesis (CLA1), and AMP biosynthesis (ADSS), all of which localize to the chloroplast. DB-ADT1-FL is also able to interact with a Succinyl-CoA Ligase α subunit, which localizes to the mitochondrion, and a putative protein kinase which is predicted to localize to the plasma membrane. Twenty putative interactors were eliminated because they were not in frame with the GAL4-TA domain, or they exhibited self-activation properties (Table 4).

3.3.4 *In Silico* Analysis of Potential Cryptic Splice Sites in TA-ADT6

The TA-ADT6-FL fusion construct identified in the normalized commercial cDNA library screen contains a premature stop codon in between the GAL4-TA domain and the start of the *ADT6* sequence, which would prevent the translation of the *ADT6* sequence. Being that the ADT1-ADT6 heterodimer had already been demonstrated in yeast (Section 3.2.2), it was speculated that some kind of splicing event may be occurring which removes the premature stop codon. To determine whether a cryptic spicing event could potentially be affecting some DB-ADT1-FL interactors, the full length DNA sequence of the TA-ADT6-FL fusion protein recovered from the cDNA library was submitted to two eukaryotic gene structure prediction programs: GENSCAN (Bruge and Karlin, 1998) and FGENESH (Softberry). However, as neither of these prediction programs offers *S. cerevisiae* as an organism setting, analysis was performed using the closest available settings: *Arabidopsis* for GENSCAN, and *Schizosaccharomyces pombe* for FGENESH. Both of these programs predicted the removal of a small intron which would include the premature stop codon and maintain the frame of the TA-ADT6 fusion

protein (Figure 15A and 15B). Since the predicted donor site is in the linker region between the HA tag and the start of the ADT6 sequence, it is shared by all constructs in the library. To examine how this may affect other interactors, the full length TA-fusion sequence of a non-ADT interactor (At1g25530, a putative amino acid transporter), which was out of frame, was also submitted to GENSCAN for analysis. GENSCAN predicted the removal of an intron which includes most of the HA tag, the entire linker region, and a small part of the At1g25530 sequence (Figure 15C). Following removal of this predicted intron, the TA-At1g25530 sequence is in frame.

3.4 *In Planta* Dimerization Profiles of all Six ADTs

As an alternative to the GAL4 Y2H system, where four of the six ADTs are self-activating, all six *ADT*s were cloned into the BiFC vectors pEarleyGate21-YN and pEarleyGate202-YC. Since this system relies on the reconstitution of fluorescence, rather than transcriptional activation of reporters, the self-activation properties of these ADTs in yeast will not pose a problem *in planta*. Another advantage of BiFC is that it not only allows for the detection of protein interactions, it can also detect the subcellular localization of those interactions. Each of the six *ADT*s was cloned in fusion with the N- and C-terminal halves of the YFP protein, respectively, and transformed into *A. tumefaciens*. Since the N-terminal transit peptide of the ADTs may be cleaved upon entry into the chloroplast (Li and Chiu, 2010), the half-YFPs are fused to the C-terminus of the ADT. Prior to transformation, the identity of each *ADT* insert was confirmed by restriction enzyme digestion using *MluI-AseI* and *HindIII-XhoI* (Figures 16 and 17).

3.4.1 Control Infiltrations for BiFC

Prior to co-infiltration with another *Arabidopsis* ADT, each construct was co-infiltrated with appropriate controls to ensure that it can be used in the BiFC system (Table 6; Appendices 8 and 9). Each *YN-ADT* and *YC-ADT* construct was infiltrated individually to ensure that it was not able to fluoresce in the absence of a corresponding half-YFP construct. To determine the amount of fluorescence which results from random collisions (ie. not based on an interaction) of the fusion proteins, each *YN-ADT* and *YC-ADT* construct was also co-infiltrated with a *YC-CRA1* or *YN-CRA1* construct. CRA1 is an unrelated seed storage protein and is often used as a negative interaction control

Figure 15. Select Examples of Fusion Proteins Resulting from Predicted Cryptic Splicing Events in Yeast. Portions of each sequence which are relevant to the potential splicing events are shown for the TA-ADT6 and TA-amino acid transporter sequences. Each alignment was performed using the sequence of the interactor alone, the sequence of the fusion protein from the library as indicated by the transformant number, and the sequence predicted by either the GENSCAN or FGENESH gene structure prediction programs. While splicing occurs on the transcript-level, the resulting proteins sequences are shown. The numbers on the right-hand side are in reference to the N-terminal end of each sequence. **A.** The ADT6 fusion protein predicted by GENSCAN results from the a small intron from the original sequence, which removes the premature stop codon (shown here by a red star) and maintains the frame of the fusion protein. **B.** The ADT6 fusion protein predicted by FGENESH results from the removal of one intron from the original sequence, which removes the premature stop codon and maintains the frame of the fusion protein. **C.** The putative amino acid transporter fusion protein sequence predicted by GENSCAN results from the removal of a large intron from the original sequence which restores the frame of the fusion protein to that of the original sequence.

Light Blue: vector-derived sequences common to all TA-fusion proteins in the library; Green: ADT6 sequence; Dark Blue: putative amino acid transporter sequence. Black Shading: amino acids shared in all sequences; Grey Shading: amino acids shared in >50% of sequences; Red Star: stop codon.

AA: amino acid; ADT: arogenate dehydratase; FL: full length; T: transformant number; TA: transcription activation domain.

A.


ADT6
ADT1FL-T02
GenScan
Linker Sequence
ADT6 Sequence

B.


ADT6
ADT1FL-T02
FGENESH
Linker Sequence
ADT6 Sequence

C.

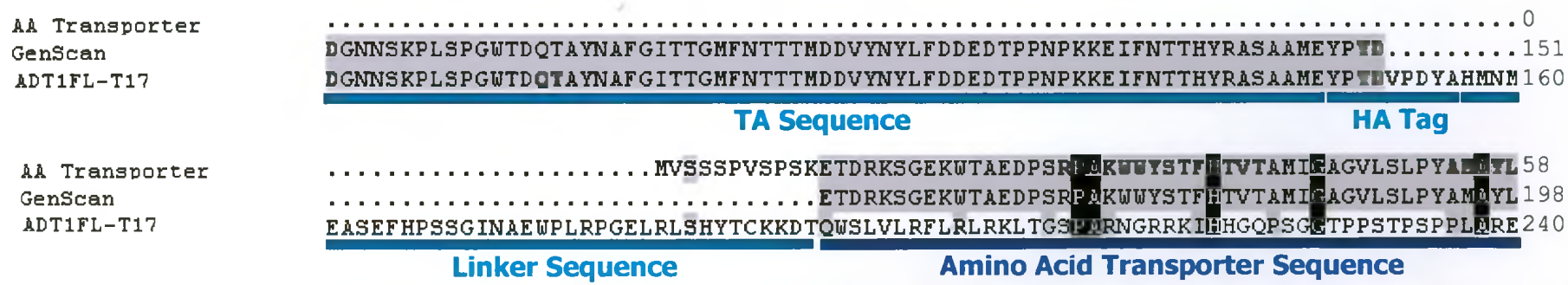
AA Transporter
GenScan
ADT1FL-T17
TA Sequence
HA Tag
AA Transporter
GenScan
ADT1FL-T17
Linker Sequence
Amino Acid Transporter Sequence

Figure 16. Restriction Enzyme Analysis of pEarleyGate201-YN Constructs. **A.** Diagram of pEarleyGate 201-YN with all cloned inserts shown above, and insert sizes to the right. Following a successful insertion via recombination, the *ADT* sequence replaces the *Cm^r* and *ccdB* sequences in the vector. Relevant restriction enzyme sites are shown, and reference positions along the vector sequence are boxed. All positions are given in kb. **B.** Gel electrophoresis of pEarleyGate201-YN restriction digests. Ladder fragment sizes are labeled on the left, and approximate sizes of relevant restriction fragments are shown on the right. Inserts are identified across the top of each gel (ADT1-ADT6, CRA1). Observed fragment sizes differ slightly (by approx. 100-200bp) from calculated sizes as the modified vector sequences available are not completely accurate. Expected fragment sizes (in bp) from each digest are listed below.

*Hind*III- *Xho*I digest:

Empty 201-YN: 3162, 9159
ADT1: 3035, 9159
ADT2: 1430, 1572, 9159
ADT3: 765, 2366, 9159
ADT4: 777, 2354, 9159
ADT5: 780, 2354, 9159
ADT6: 750, 2348, 9159
CRA1: 125, 354, 547, 674, 1575, 9159

*Ase*I-*Mlu*I digest:

Empty 201-YN: 1444, 2127, 8750
ADT1: 1444, 10750
ADT2: 1444, 10717
ADT3: 1444, 1571, 9275
ADT4: 1444, 10846
ADT5: 1444, 2642, 8207
ADT6: 1444, 1815, 8998
CRA1: 1444, 10990

Restriction Enzymes: *A*: *Ase*I; *H*: *Hind*III; *M*: *Mlu*I; *M**: *Mlu*I is a methylation sensitive enzyme, and this site may be methylated as it was not recognized in this digest; *X*: *Xho*I.

bp: base pairs; C: *CRA1*, *CRUCIFERINA*; *ccdB*: negative selectable marker; *Cm^r*: chloramphenicol resistance gene; E: empty vector; kb: kilobase; L: 1kb DNA ladder; YC: C-terminal half of YFP; YN: N-terminal half of YFP.

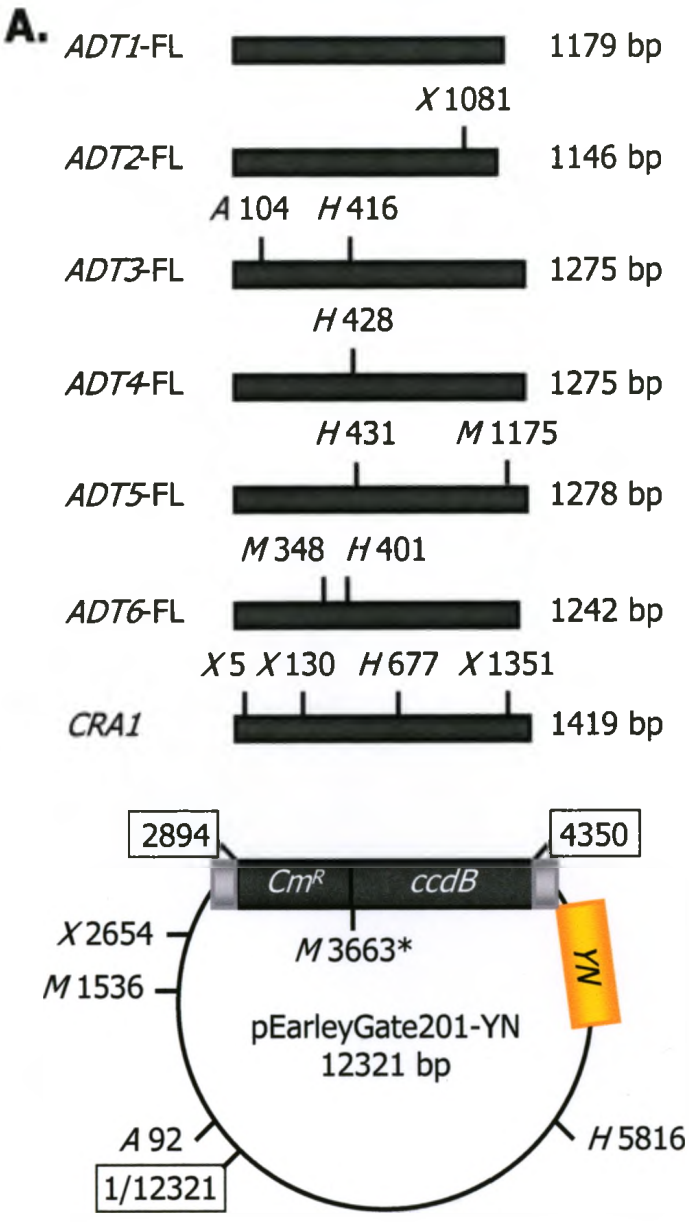
A.
ADT1-FL
1179 bp
X 1081
ADT2-FL
1146 bp
A 104
H 416
ADT3-FL
1275 bp
H 428
ADT4-FL
1275 bp
H 431
M 1175
ADT5-FL
1278 bp
M 348
H 401
ADT6-FL
1242 bp
X 5
X 130
H 677
X 1351
CRA1
1419 bp
2894
4350
CmR
ccdB
YN
X 2654
M 3663*
M 1536
pEarleyGate201-YN
12321 bp
A 92
H 5816
1/12321

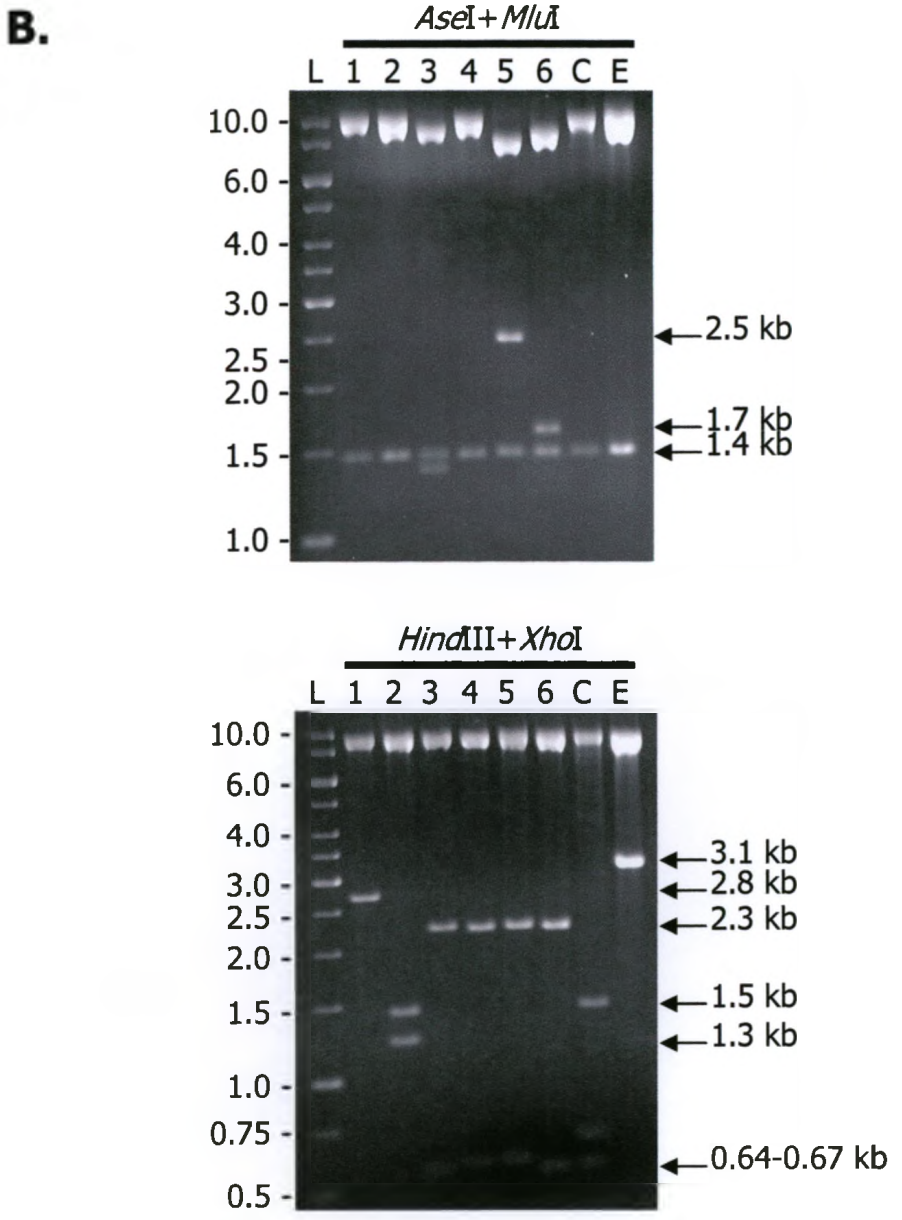
B.
AseI+MluI
L 1 2 3 4 5 6 C E
10.0
6.0
4.0
3.0
2.5
2.0
1.5
1.0
2.5 kb
1.7 kb
1.4 kb
HindIII+XhoI
L 1 2 3 4 5 6 C E
10.0
6.0
4.0
3.0
2.5
2.0
1.5
1.0
0.75
0.5
3.1 kb
2.8 kb
2.3 kb
1.5 kb
1.3 kb
0.64-0.67 kb

Figure 17. Restriction Enzyme Analysis of pEarleyGate201-YN Constructs. **A.** Diagram of pEarleyGate 202-YC with all cloned inserts shown above, and insert sizes to the right. Following a successful insertion via recombination, the *ADT* sequence replaces the *Cm*^{r} and *ccdB* sequences in the vector. Relevant restriction enzyme sites are shown, and reference positions along the vector sequence are boxed. All positions are given in kb. **B.** Gel electrophoresis of pEarleyGate202-YC restriction digests. Ladder fragment sizes are labeled on the left, and approximate sizes of relevant restriction fragments are shown on the right. Inserts are identified across the top of each gel (ADT1-ADT6, CRA1). Observed fragment sizes differ slightly (by approx. 100-200bp) from calculated sizes as the modified vector sequences available are not completely accurate. Expected fragment sizes (in bp) from each digest are listed below:

*Hind*III-*Xho*I digest:

Empty 202-YC: 2868, 9159
ADT1: 2741, 9159
ADT2: 1427, 1281, 9159
ADT3: 762, 2075, 9159
ADT4: 774, 2063, 9159
ADT5: 777, 2063, 9159
ADT6: 747, 2057, 9159
CRA1: 125, 351, 547, 674, 1284, 9159

*Ase*I-*Mlu*I digest:

Empty 202-YC: 1444, 2124, 8459
ADT1: 1444, 10456
ADT2: 1444, 10423
ADT3: 1444, 1568, 8984
ADT4: 1444, 10552
ADT5: 1444, 2639, 7916
ADT6: 1444, 1812, 8707
CRA1: 1444, 10696

Restriction Enzymes: *A*: *Ase*I; *H*: *Hind*III; *M*: *Mlu*I; *M**: *Mlu*I is a methylation sensitive enzyme, and this site may be methylated as it was not recognized in this digest; *X*: *Xho*I.

bp: base pairs; C: *CRA1*, *CRUCIFERINA*; *ccdB*: negative selectable marker; *Cm*^{r}: chloramphenicol resistance gene; E: empty vector; kb: kilobase; L: 1kb DNA ladder; YC: C-terminal half of YFP; YN: N-terminal half of YFP.

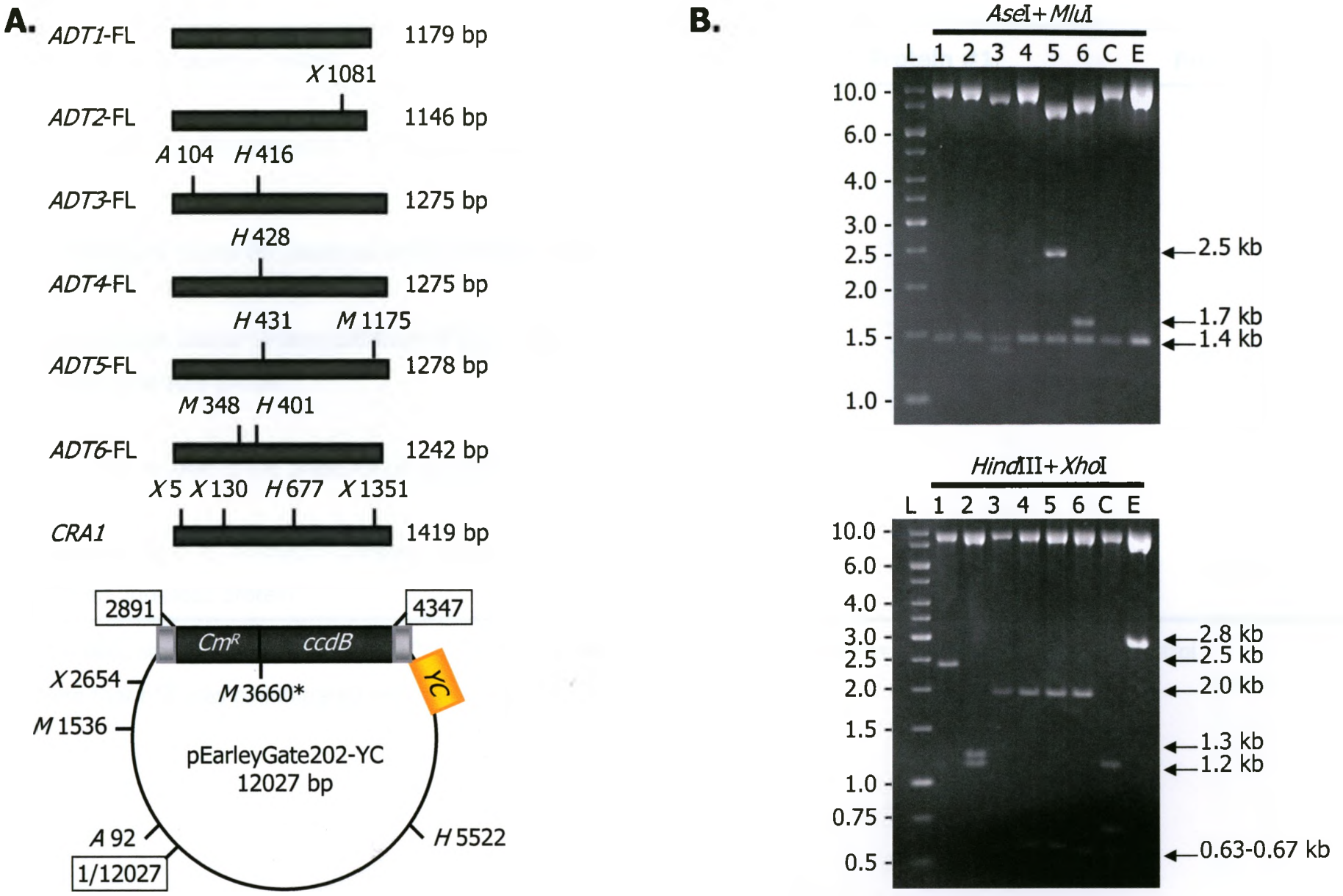
A.
ADT1-FL
1179 bp
X 1081
ADT2-FL
1146 bp
A 104
H 416
ADT3-FL
1275 bp
H 428
ADT4-FL
1275 bp
H 431
M 1175
ADT5-FL
1278 bp
M 348
H 401
ADT6-FL
1242 bp
X 5
X 130
H 677
X 1351
CRA1
1419 bp
2891
4347
CmR
ccdB
YC
X 2654
M 3660*
M 1536
pEarleyGate202-YC
12027 bp
A 92
H 5522
1/12027
B.
AseI+MluI
L 1 2 3 4 5 6 C E
10.0
6.0
4.0
3.0
2.5
2.0
1.5
1.0
2.5 kb
1.7 kb
1.4 kb
HindIII+XhoI
L 1 2 3 4 5 6 C E
10.0
6.0
4.0
3.0
2.5
2.0
1.5
1.0
0.75
0.5
2.8 kb
2.5 kb
2.0 kb
1.3 kb
1.2 kb
0.63-0.67 kb

Table 6. Control Infiltrations for Bi-molecular Fluorescence Complementation Assays.

Biological Property Tested	Protein #1	Protein #2
Fluorescence in the absence of YFP fusion proteins	p19 [b]	-
Fluorescence due to the presence of the YN-ADT fusion protein alone	YN-ADT	-
Fluorescence due to random collisions of the YN-ADT fusion protein and an unrelated protein [a]	YN-ADT	YC-CRA1
Fluorescence due to the presence of the YC-ADT fusion protein alone	-	YC-ADT
Fluorescence due to random collisions of the YC-ADT fusion protein with an unrelated protein [a]	YN-CRA1	YC-ADT

[a] The seed storage protein CRUCIFERINA (CRA1; accession At5g44120) was used as a negative interaction control.

[b] Note that p19 was co-infiltrated with all controls.

in Y2H assays (Kohalmi *et al.*, 1998). None of the *Arabidopsis* ADTs were able to fluoresce on their own, and any fluorescence which resulted from random collisions with CRA1 was fleeting. To enhance expression of the fusion constructs, all infiltrations included p19, a potent viral suppressor of post-transcriptional gene silencing in plants (Voinnet *et al.*, 2003; Silhavy *et al.*, 2002).

3.4.2 ADTs Form All Possible Homo- and Heterodimers *In Planta*

Initially, all homo- and heterodimer combinations were transiently expressed in *N. benthamiana*, as these plants have large, sturdy leaves which are easy to infiltrate. *Arabidopsis* leaves are smaller and much more delicate than *N. benthamiana*, and are easily damaged during infiltration, making it difficult to perform transient expression assays. When expressed in *N. benthamiana* leaves under a 35S promoter, *Arabidopsis* ADTs formed all 36 possible homo- and heterodimers. Representative images of all possible ADT dimers are shown in Figures 18-24. While some ADT dimers were detectable within 24 hours post-infiltration, all were detectable by 48 hours post-infiltration, with the exception of dimers involving ADT2, which took up to five days. Furthermore, the fluorescence signal from these ADT2 dimers was not as bright as for other ADT dimers.

3.4.3 ADT Homodimers Predominantly Localize to the Chloroplasts

As all ADTs have an N-terminal transit peptide, it was not surprising that homo- and heterodimers of all six ADTs localize predominantly to the chloroplasts in *N. benthamiana*. However, the ADT localization patterns are not typical chloroplast localization patterns, as the YFP signal does not completely overlay the chloroplast autofluorescence (due to the green pigments of the thylakoid grana). Rather, ADT dimers localize in a punctate pattern outside of the area of autofluorescence (for clear examples see Figure19F, Figure 21C, and Figure24F). This pattern is associated with all six ADTs, and is consistent with localization to chloroplast stromules (described in Section 4.3.1). What was surprising, however, was the localization pattern of dimers which involve ADT5. While these dimers do associate with chloroplasts (Figure 22), they also exhibit a nuclear-like localization pattern, which can be characterized by either diffuse YFP fluorescence (Figure 23D), or diffuse fluorescence which also contains

Figure 18. Homo- and Heterodimerization of ADT1 in *N. benthamiana* Leaves. Transient expression of YN- and YC-ADT constructs in *N. benthamiana* leaves results in the accumulation of yellow fluorescence in some cells, which indicates dimer formation in these areas. **A-F.** ADT1 forms homodimers and heterodimers which localize to the chloroplast in a stromule-like pattern. **E.** ADT1-ADT5 heterodimers also localize in a nuclear-like pattern. Dimers are identified to the left of each row, and columns represents the YFP channel, chloroplast autofluorescence (red), and overlay, respectively. In images which show multiple patterns, the open arrows mark a stromule-like pattern and the closed arrows mark a nuclear-like pattern. Scale bars in panels A, B, D, and E are 10μm, and 25μm in panels C and F.

ADT: arogenate dehydratase; YC: C-terminal half YFP; YN: N-terminal half YFP.

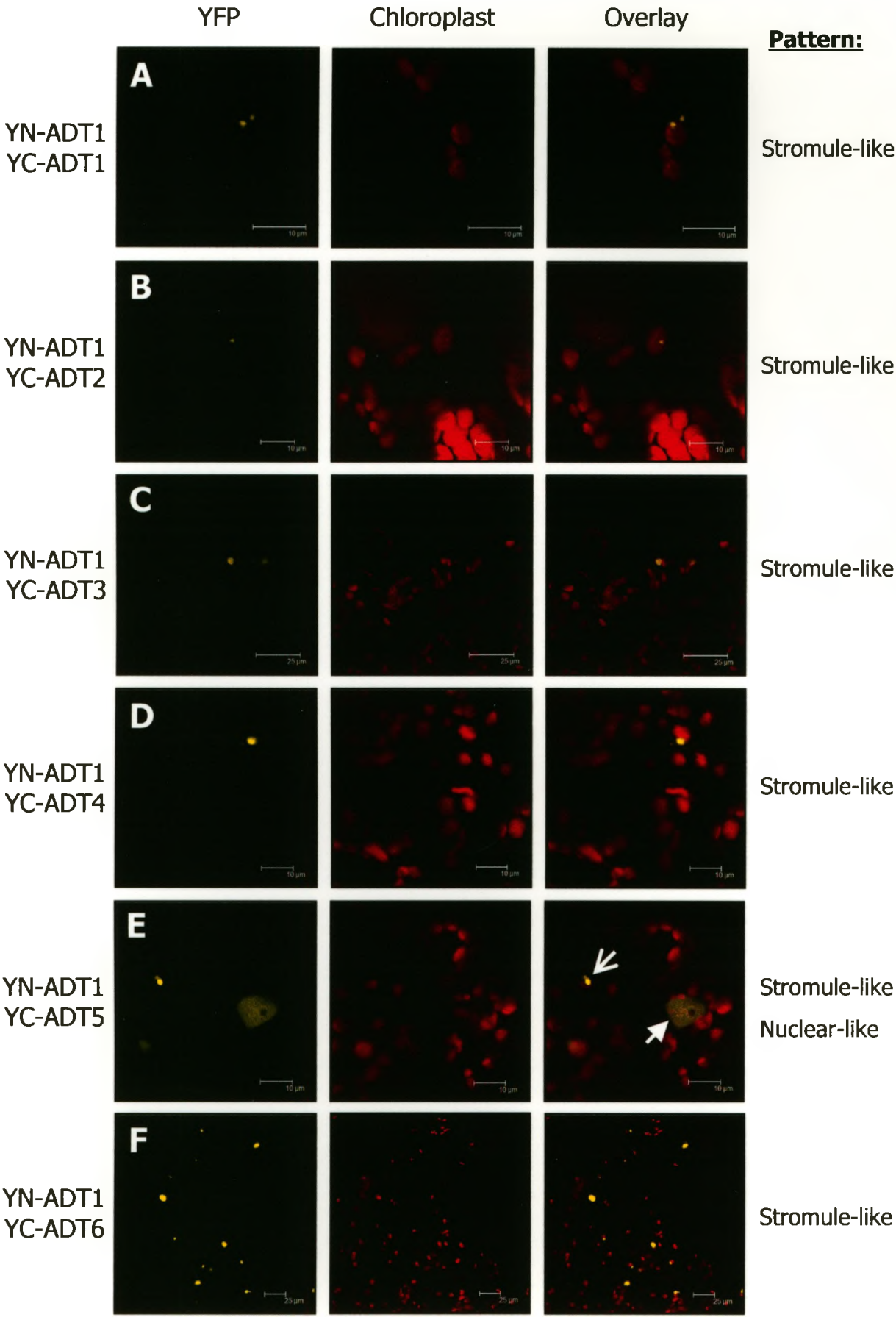
YFP
Chloroplast
Overlay
Pattern:
A
YN-ADT1
YC-ADT1
Stromule-like
B
YN-ADT1
YC-ADT2
Stromule-like
C
YN-ADT1
YC-ADT3
Stromule-like
D
YN-ADT1
YC-ADT4
Stromule-like
E
YN-ADT1
YC-ADT5
Stromule-like
Nuclear-like
F
YN-ADT1
YC-ADT6
Stromule-like

Figure 19. Homo- and Heterodimerization of ADT2 in *N. benthamiana* Leaves. Transient expression of YN- and YC-ADT constructs in *N. benthamiana* leaves results in the accumulation of yellow fluorescence in some cells, which indicates dimer formation in these areas. **A-D, F.** ADT2 forms homodimers and heterodimers which localize to the chloroplast in a stromule-like pattern. **E.** ADT2-ADT5 heterodimers localize in a nuclear-like pattern. Dimers are identified to the left of each row, and columns represents the YFP channel, chloroplast autofluorescence (red), and overlay, respectively. Scale bars in all panels are 10μm.

ADT: arogenate dehydratase; YC: C-terminal half YFP; YN: N-terminal half YFP.

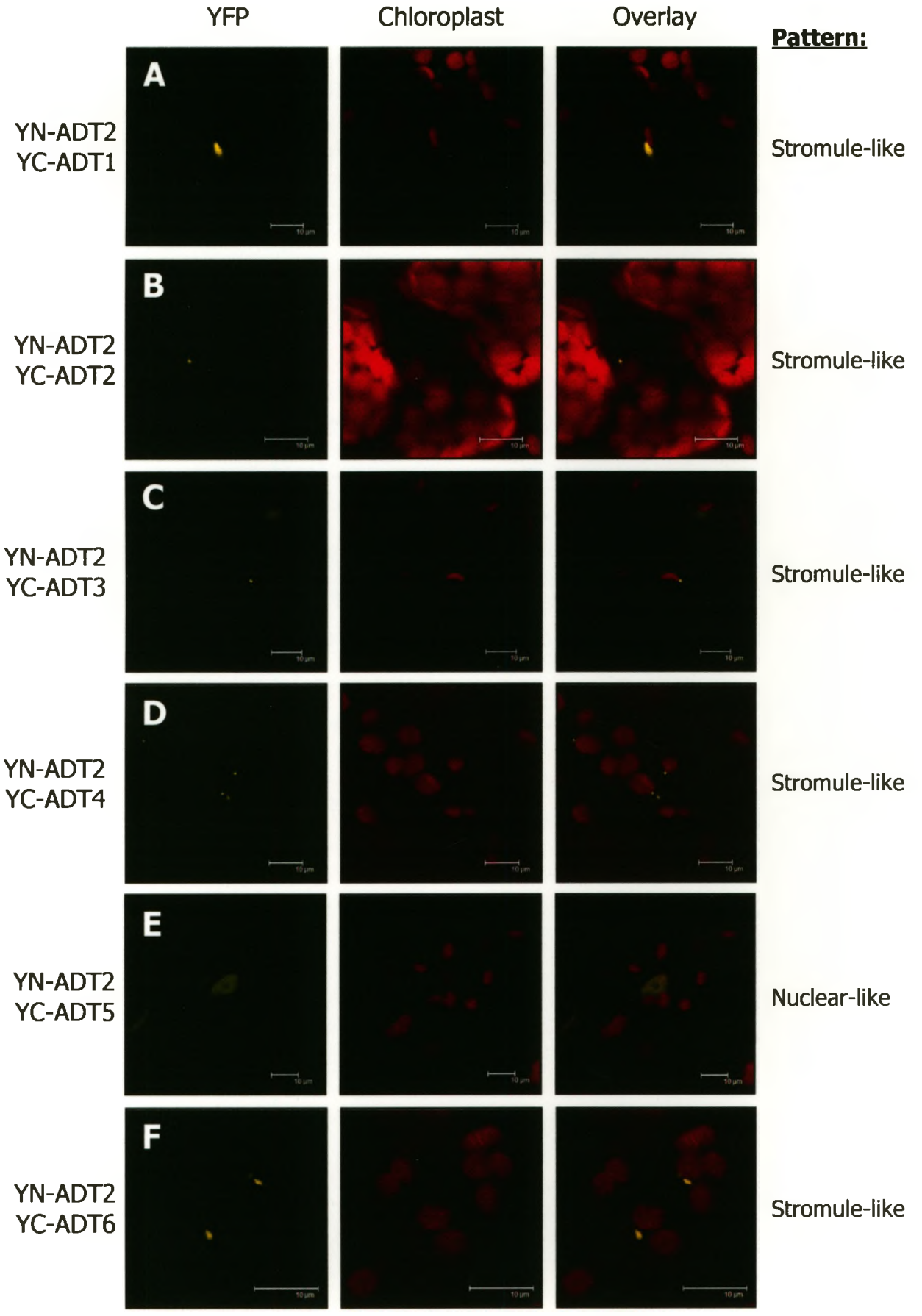
YFP
Chloroplast
Overlay
Pattern:
A
YN-ADT2
YC-ADT1
Stromule-like
B
YN-ADT2
YC-ADT2
Stromule-like
C
YN-ADT2
YC-ADT3
Stromule-like
D
YN-ADT2
YC-ADT4
Stromule-like
E
YN-ADT2
YC-ADT5
Nuclear-like
F
YN-ADT2
YC-ADT6
Stromule-like

Figure 20. Homo- and Heterodimerization of ADT3 in *N. benthamiana* Leaves. Transient expression of YN- and YC-ADT constructs in *N. benthamiana* leaves results in the accumulation of yellow fluorescence in some cells, which indicates dimer formation in these areas. **A-D, F.** ADT3 forms homodimers and heterodimers which localize to the chloroplast in a stromule-like pattern. **E.** ADT3-ADT5 heterodimers also localize in a nuclear-like pattern. Dimers are identified to the left of each row, and columns represents the YFP channel, chloroplast autofluorescence (red), and overlay, respectively. Scale bars in all panels are 10μm, and the overlay in panel C includes the brightfield image.

ADT: arogenate dehydratase; YC: C-terminal half YFP; YN: N-terminal half YFP.

Figure 20. Homo- and Heterodimerization of ADT3 in *N. benthamiana* Leaves. Transient expression of YN- and YC-ADT constructs in *N. benthamiana* leaves results in the accumulation of yellow fluorescence in some cells, which indicates dimer formation in these areas. **A-D, F.** ADT3 forms homodimers and heterodimers which localize to the chloroplast in a stromule-like pattern. **E.** ADT3-ADT5 heterodimers also localize in a nuclear-like pattern. Dimers are identified to the left of each row, and columns represents the YFP channel, chloroplast autofluorescence (red), and overlay, respectively. Scale bars in all panels are 10μm, and the overlay in panel C includes the brightfield image.

ADT: arogenate dehydratase; YC: C-terminal half YFP; YN: N-terminal half YFP.

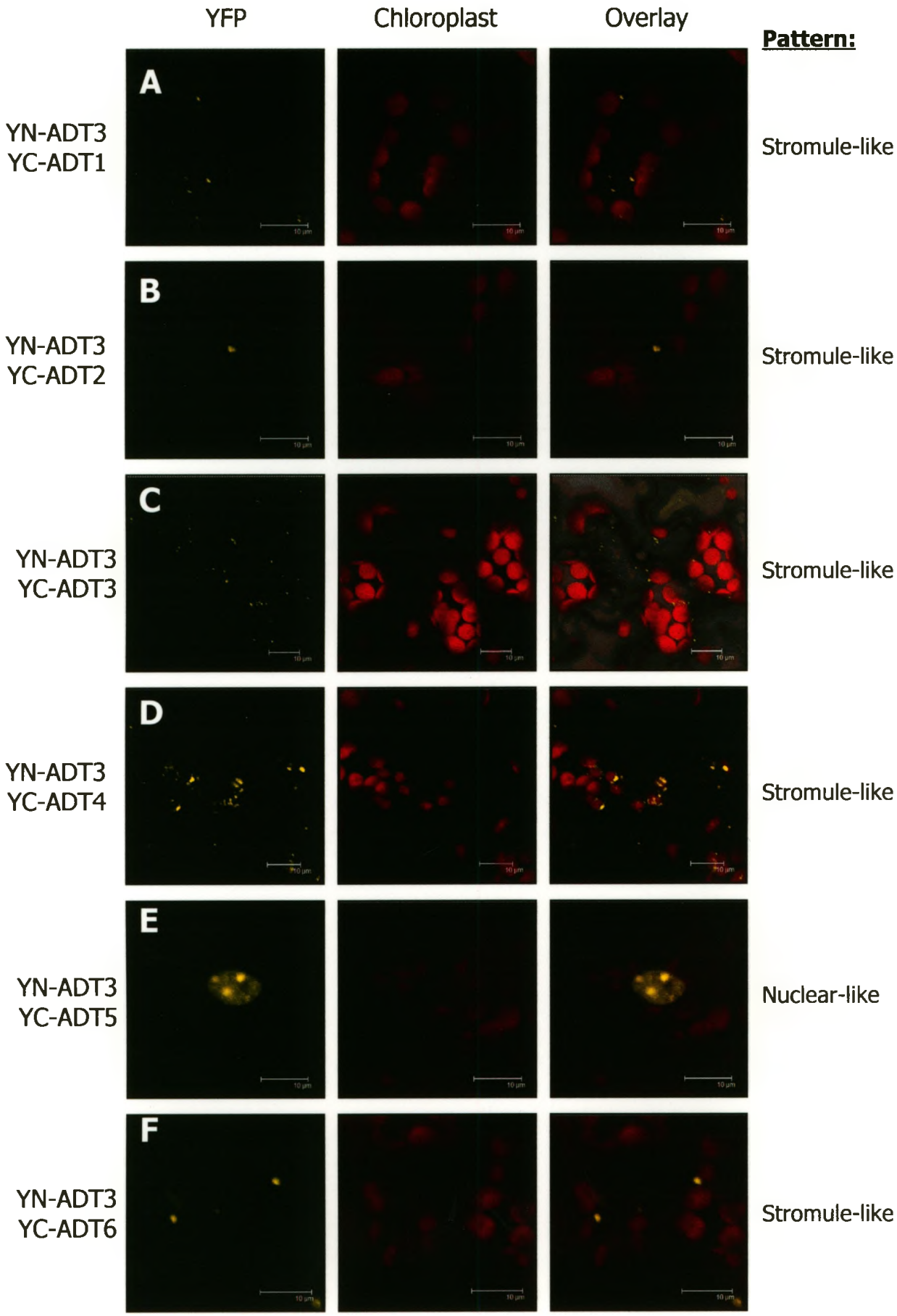
YFP
Chloroplast
Overlay
Pattern:
A
YN-ADT3
YC-ADT1
Stromule-like
B
YN-ADT3
YC-ADT2
Stromule-like
C
YN-ADT3
YC-ADT3
Stromule-like
D
YN-ADT3
YC-ADT4
Stromule-like
E
YN-ADT3
YC-ADT5
Nuclear-like
F
YN-ADT3
YC-ADT6
Stromule-like

Figure 21. Homo- and Heterodimerization of ADT4 in *N. benthamiana* Leaves.
Transient expression of YN- and YC-ADT constructs in *N. benthamiana* leaves results in the accumulation of yellow fluorescence in some cells, which indicates dimer formation in these areas. **A-F.** ADT4 forms homodimers and heterodimers which localize to the chloroplast in a stromule-like pattern. **E.** ADT4-ADT5 heterodimers also localize in a nuclear-like pattern. Dimers are identified to the left of each row, and columns represents the YFP channel, chloroplast autofluorescence (red), and overlay, respectively. In images which show multiple patterns, the open arrows mark a stromule-like pattern and the closed arrows mark a nuclear-like pattern. The scale bar in panel C is 5μm, and all other panels are 10μm.

ADT: arogenate dehydratase; YC: C-terminal half YFP; YN: N-terminal half YFP.

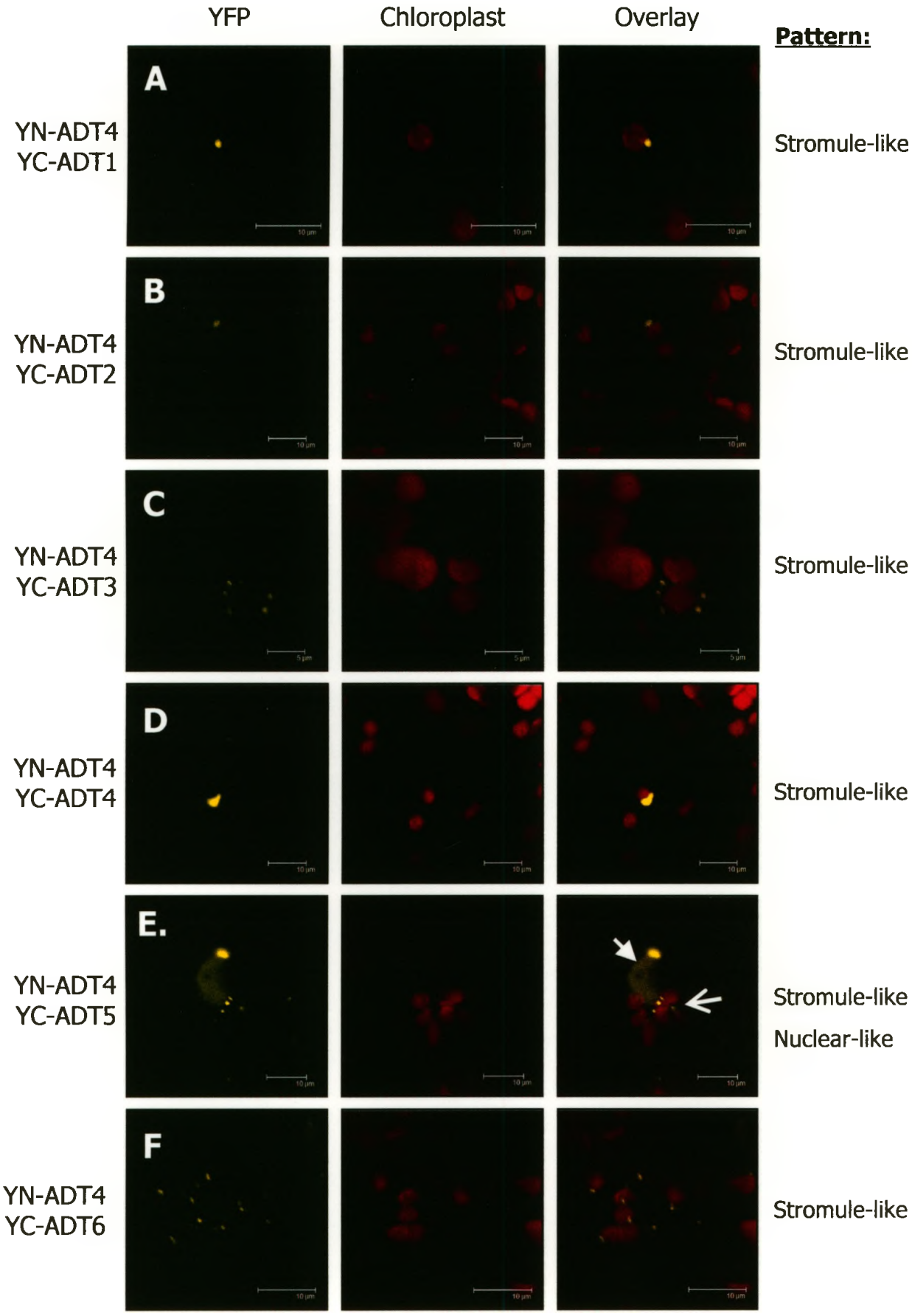
YFP
Chloroplast
Overlay
Pattern:
A
YN-ADT4
YC-ADT1
Stromule-like
B
YN-ADT4
YC-ADT2
Stromule-like
C
YN-ADT4
YC-ADT3
Stromule-like
D
YN-ADT4
YC-ADT4
Stromule-like
E.
YN-ADT4
YC-ADT5
Stromule-like
Nuclear-like
F
YN-ADT4
YC-ADT6
Stromule-like

Figure 22. Stromule-like Localization Pattern of ADT5 Homo- and Heterodimers in *N. benthamiana* Leaves. Transient expression of YN- and YC-ADT constructs in *N. benthamiana* leaves results in the accumulation of yellow fluorescence in some cells, which indicates dimer formation in these areas. **A-F.** ADT5 forms homodimers and heterodimers which localize to the chloroplasts in a stromule-like pattern. Dimers are identified to the left of each row, and columns represents the YFP channel, chloroplast autofluorescence (red), and overlay, respectively. Scale bars in panels A-E are 10μm, and 25μm in panel F.

ADT: arogenate dehydratase; YC: C-terminal half YFP; YN: N-terminal half YFP.

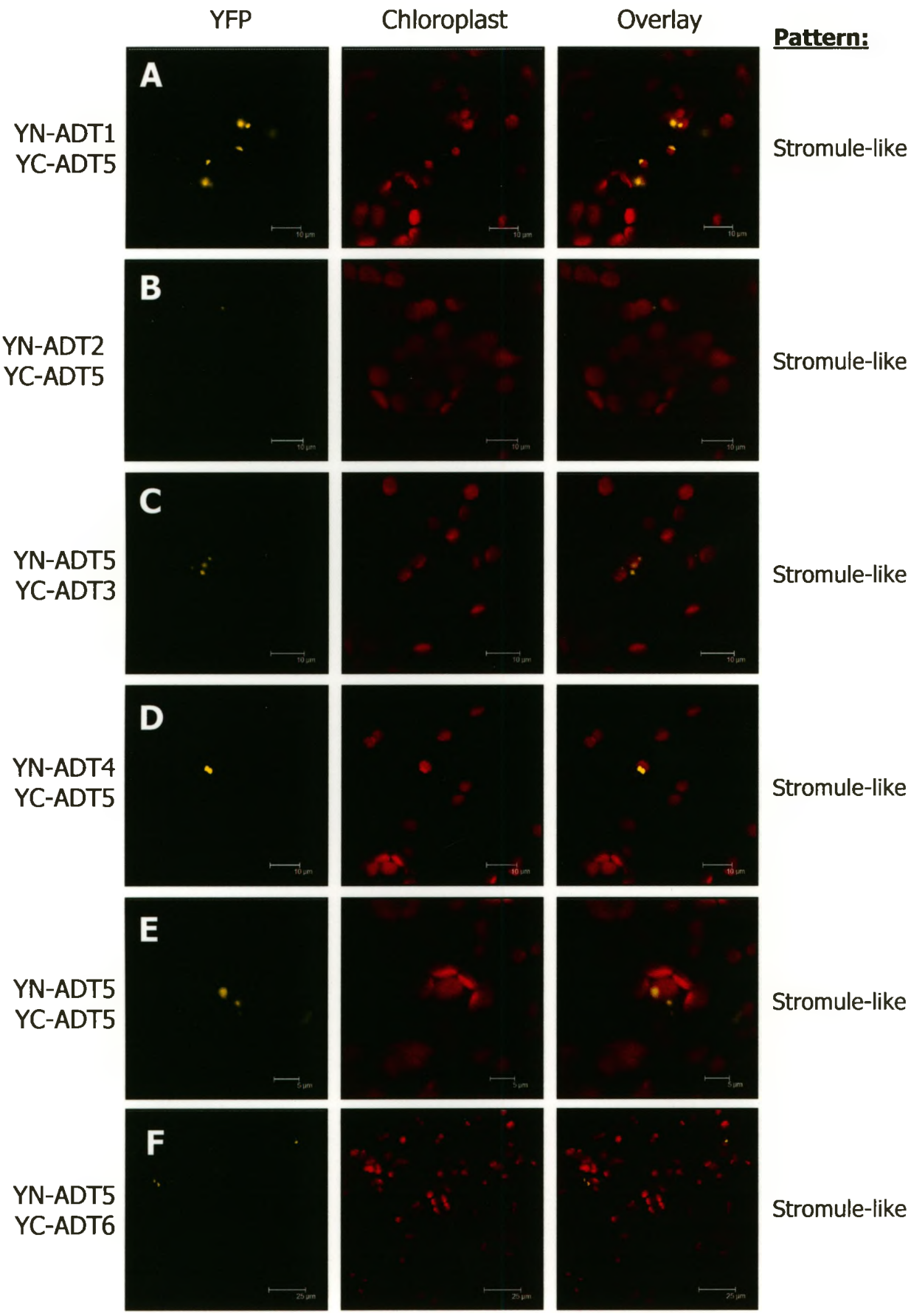
YFP
Chloroplast
Overlay
Pattern:
A
YN-ADT1
YC-ADT5
Stromule-like
B
YN-ADT2
YC-ADT5
Stromule-like
C
YN-ADT5
YC-ADT3
Stromule-like
D
YN-ADT4
YC-ADT5
Stromule-like
E
YN-ADT5
YC-ADT5
Stromule-like
F
YN-ADT5
YC-ADT6
Stromule-like

Figure 23. Nuclear-like Localization Pattern of ADT5 Homo- and Heterodimers in *N. benthamiana* Leaves. Transient expression of YN- and YC-ADT constructs in *N. benthamiana* leaves results in the accumulation of yellow fluorescence in some cells, which indicates dimer formation in these areas. **A-E.** ADT5 forms homodimers and heterodimers which localize in a nuclear-like pattern. Dimers are identified to the left of each row, and columns represents the YFP channel, chloroplast autofluorescence (red), and overlay, respectively. Scale bars in panels A-D are 10μm, 5μm in panel E, and 25μm in panel F. The overlay in panels A and D includes the brightfield image.

ADT: arogenate dehydratase; YC: C-terminal half YFP; YN: N-terminal half YFP.

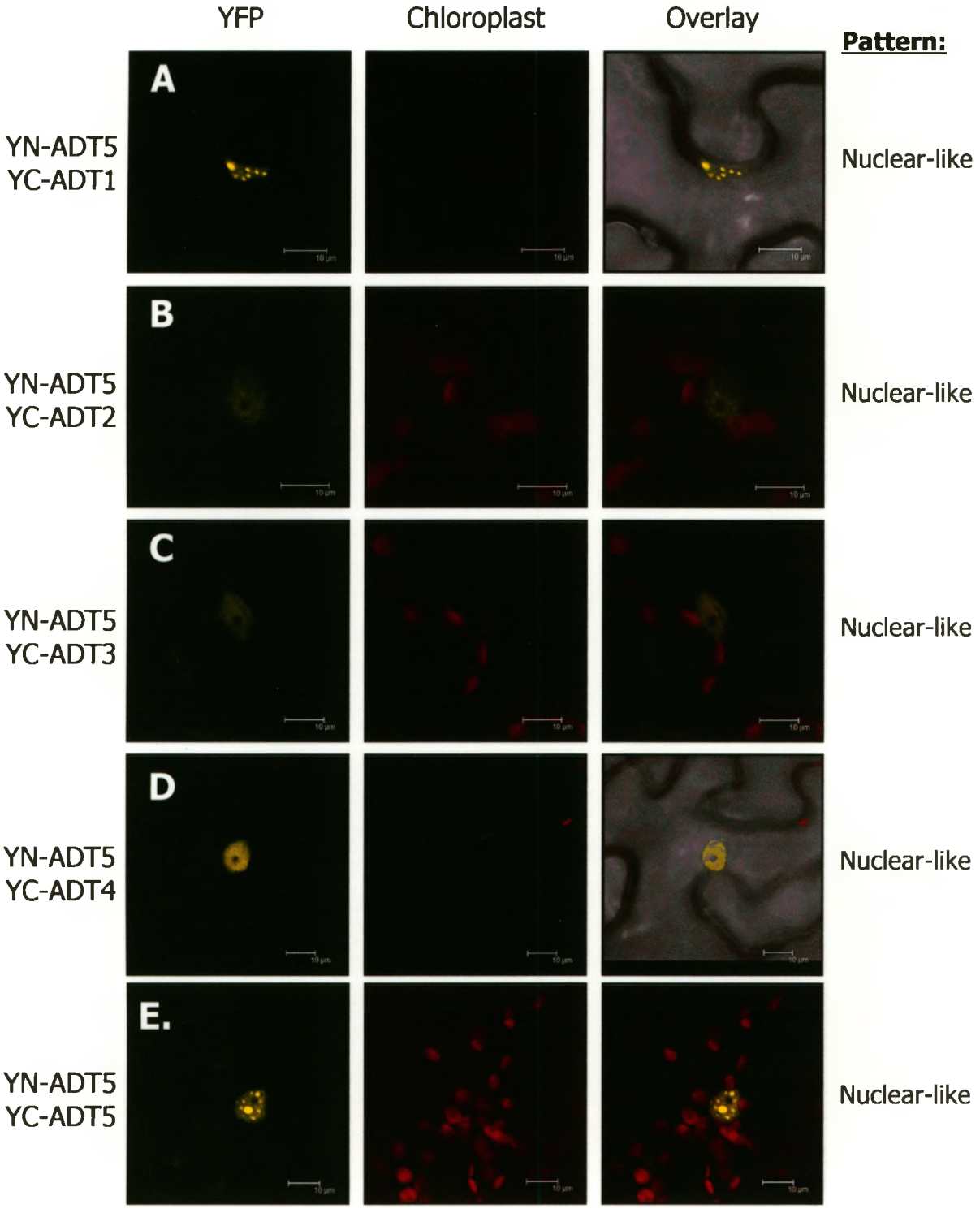
YFP
Chloroplast
Overlay
Pattern:
A
YN-ADT5
YC-ADT1
Nuclear-like
B
YN-ADT5
YC-ADT2
Nuclear-like
C
YN-ADT5
YC-ADT3
Nuclear-like
D
YN-ADT5
YC-ADT4
Nuclear-like
E.
YN-ADT5
YC-ADT5
Nuclear-like

Figure 24. Homo- and Heterodimerization of ADT6 in *N. benthamiana* Leaves.
Transient expression of YN- and YC-ADT constructs in *N. benthamiana* leaves results in the accumulation of yellow fluorescence in some cells, which indicates dimer formation in these areas. **A-D, F.** ADT6 forms homodimers and heterodimers which localize to the chloroplast in a stromule-like pattern. **E.** ADT6-ADT5 heterodimers also localize in a nuclear-like pattern. Dimers are identified to the left of each row, and columns represents the YFP channel, chloroplast autofluorescence (red), and overlay, respectively. Scale bars in panels A-C, E, and F are 10μm, and 25μm in panel D. The overlay in panel E includes the brightfield image.

ADT: arogenate dehydratase; YC: C-terminal half YFP; YN: N-terminal half YFP.

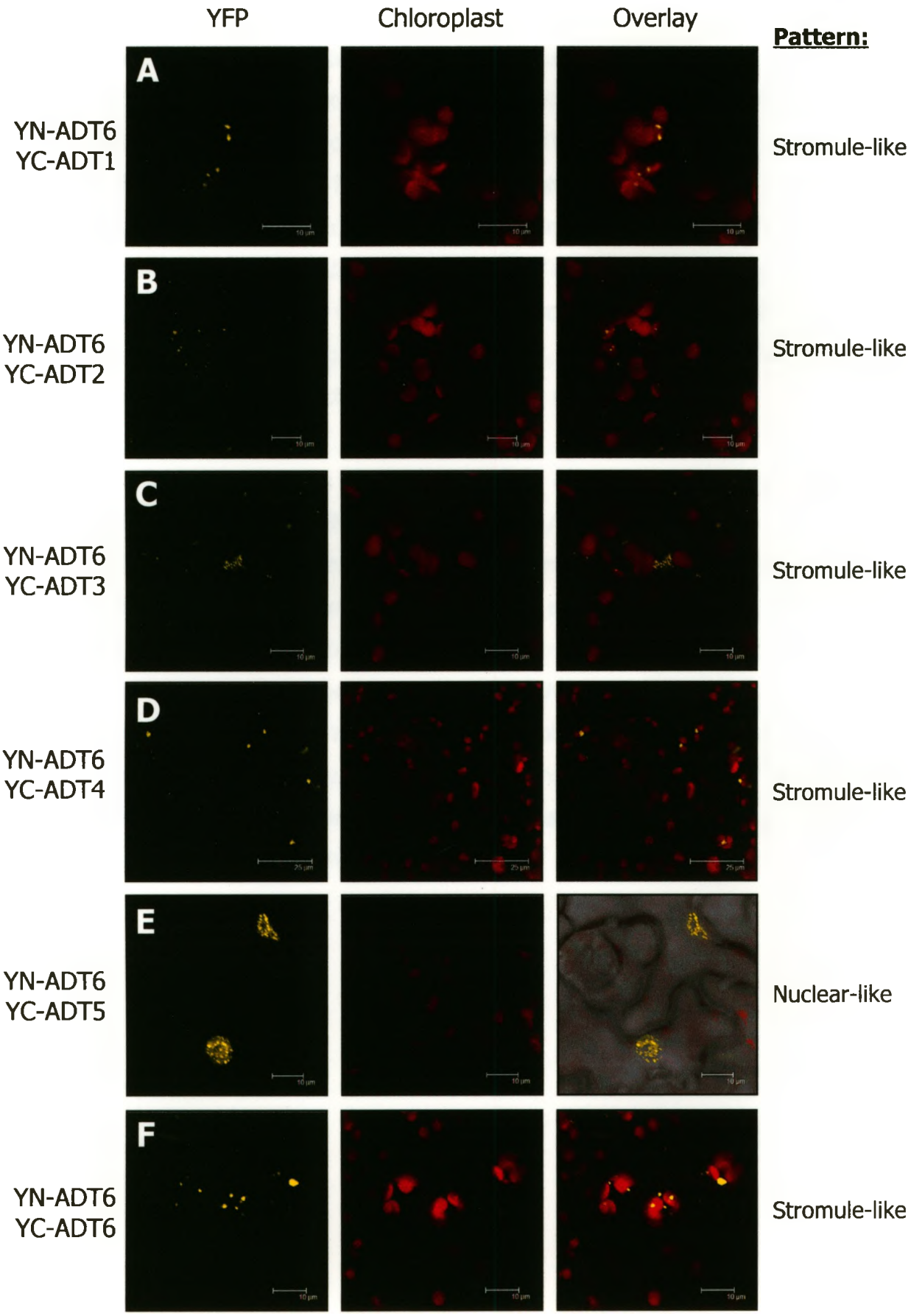
YFP
Chloroplast
Overlay
Pattern:
A
YN-ADT6
YC-ADT1
Stromule-like
B
YN-ADT6
YC-ADT2
Stromule-like
C
YN-ADT6
YC-ADT3
Stromule-like
D
YN-ADT6
YC-ADT4
Stromule-like
E
YN-ADT6
YC-ADT5
Nuclear-like
F
YN-ADT6
YC-ADT6
Stromule-like

brighter accumulations of YFP (Figure 23F).

3.4.4 *In Silico* Analysis of Potential ADT Nuclear Localization Signals

Since ADT5 dimers localize in a nuclear-like pattern in *N. benthamiana*, it was necessary to determine whether *Arabidopsis* ADTs might have a nuclear localization signal (NLS). Full length ADT sequences were submitted to NucPred (Brameier *et al.*, 2007) for analysis. ADT1 and ADT3 had moderate prediction scores of 0.52 and 0.40, respectively, while ADT2, ADT4, ADT5, and ADT6 all had very low prediction scores (0.10, 0.11, 0.11, and 0.13, respectively). As NucPred suggests a minimum threshold of 0.80 or higher for strong nuclear predictions, it was concluded that none of the *Arabidopsis* ADTs are predicted to localize to the nucleus.

3.4.5 Dimer Formation and Localization Patterns in *Arabidopsis* are in Agreement with Those Identified in *N. benthamiana*

To determine whether the dimerization profiles observed in *N. benthamiana* are representative of what occurs in the natural host system, select ADT dimers were also tested in *Arabidopsis*. Due to the difficulty in infiltrating *Arabidopsis* leaves, only ADT1 and ADT3 homo- and heterodimers were tested. As with *N. benthamaina*, both homo- and heterodimers of ADT1 and ADT3 were visible in *Arabidopsis* by 72 hours post-infiltration (Figure 25). The localization patterns are punctate and predominantly chloroplast-associated, confirming that *N. benthamiana* is an appropriate system for determining the *in planta* dimerization profiles of *Arabidopsis* ADTs.

Figure 25. Homo- and Heterodimerization of ADT1 and ADT3 in *Arabidopsis* Leaves. Transient expression of YN- and YC-ADT constructs in *Arabidopsis* leaves results in the accumulation of yellow fluorescence in some cells, which indicates dimer formation in these areas. **A.** ADT1 forms homodimers localize to the chloroplast in a stromule-like pattern. **B.** ADT3 also forms homodimers which localize to the chloroplast in a stromule-like pattern. **C-E.** ADT1 and ADT3 form heterodimers which localize in a stromule-like pattern. Dimers are identified to the left of each row, and columns represents the YFP channel, chloroplast autofluorescence (red), and overlay, respectively. Scale bars in panels A, C, E, are 10μm, and 5μm in panel D.

ADT: arogenate dehydratase; YC: C-terminal half YFP; YN: N-terminal half YFP.

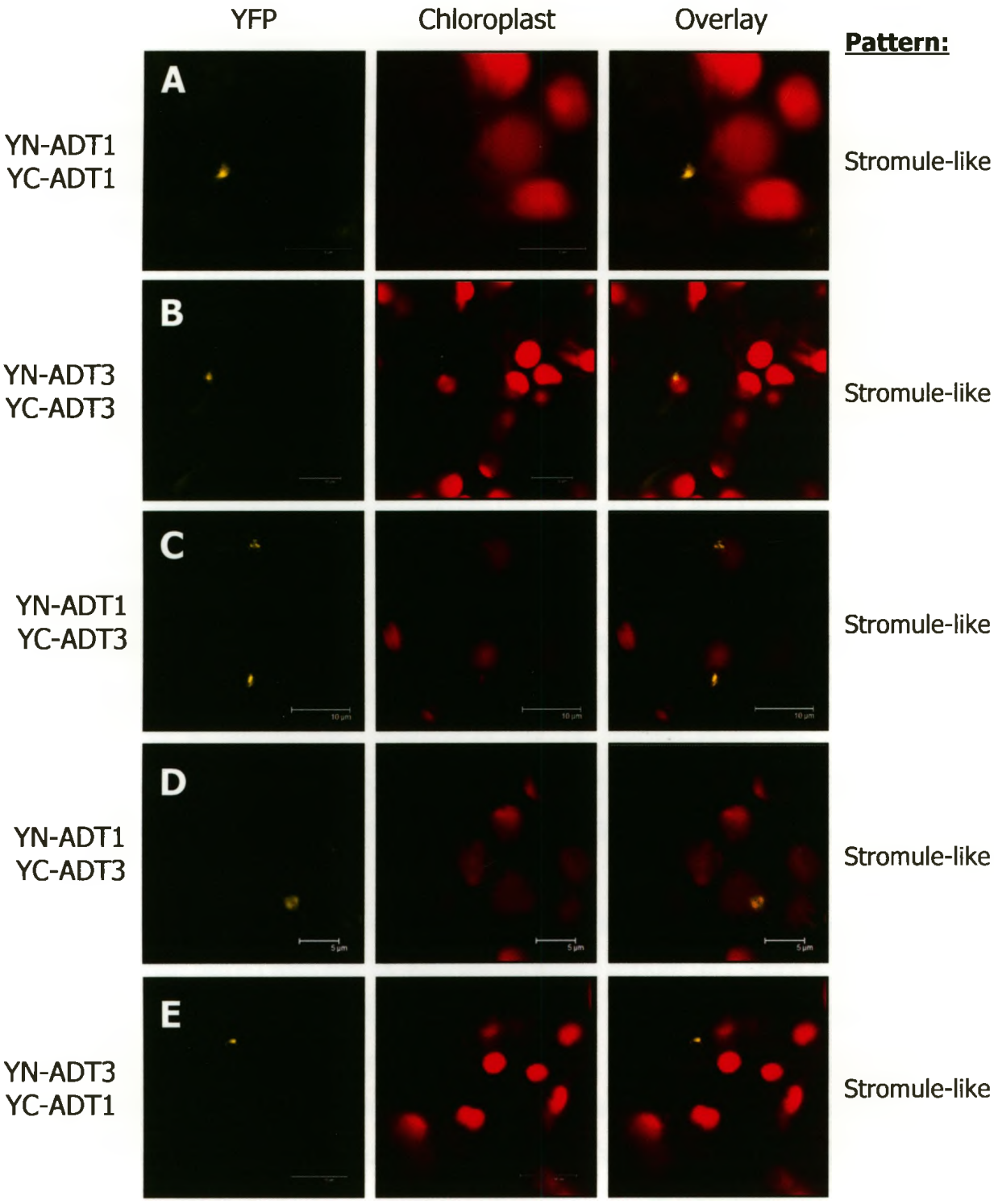
YFP
Chloroplast
Overlay
Pattern:
A
YN-ADT1
YC-ADT1
Stromule-like
B
YN-ADT3
YC-ADT3
Stromule-like
C
YN-ADT1
YC-ADT3
Stromule-like
D
YN-ADT1
YC-ADT3
Stromule-like
E
YN-ADT3
YC-ADT1
Stromule-like

4 DISCUSSION

This study examined the protein-protein interaction profiles of *Arabidopsis* ADTs using a combination of *in vivo* and *in planta* approaches. The formation of twelve *Arabidopsis* ADT homo- and heterodimers were successfully tested in yeast, and 36 different dimers were successfully examined *in planta*. In *N. benthamiana*, these dimers have two distinct subcellular localization patterns, and are either closely associated with the chloroplast, or localized in a nuclear-like pattern. Three Y2H cDNA library screens were also performed, which confirmed the ADT1-ADT1 homodimer as well as the ADT1-ADT4 and ADT1-ADT6 heterodimers. These cDNA library screens also identified a number of other potential ADT interactors.

4.1 ADT1 and ADT3 form Dimers in all Construct Lengths Tested

To determine whether the transit peptide should be included when testing ADT dimers, three coding sequence variants (FL, I, and S) of *ADT1* and *ADT3* were cloned into Y2H vectors and transformed into yeast. ADT1 is able to form homodimers in all combinations tested, however when ADT1-FL is fused to the TA domain activation of the reporters is either weaker or absent (Figure 9A). Since the DB-ADT1-FL construct is able to form dimers with itself and with ADT3, it is likely that the lack of full length homodimer is due to the presence of the TA domain itself, which could impede interactions by preventing appropriate folding of the protein or by blocking the site of inter-molecular interactions through an intra-molecular interaction (van Aelst *et al.*, 1993).

ADT1 is also able to form a heterodimer with ADT3 in all combinations tested, except when paired with the TA-ADT3-S construct (Figure 9B). Since ADT3 can only be used as a TA-fusion (see below), it is difficult to say whether the lack of interaction between the TA-ADT3-S construct and DB-ADT1 is due to similar TA-fusion-induced impediments, or due to the lack of the intermediate region. Most transit peptides are cleaved upon entry into the chloroplast (Li anc Chiu, 2010; Bédard and Jarvis, 2005), however if the ADT transit peptide is not cleaved and is required for interaction, then this could explain why the bacterial-defined ADT3 short construct is unable to interact. As the intermediate length ADTs are able to interact, the intermediate region may contain amino acids which are required for interactions at least in some ADTs. Since it

is still not known if and where the ADT transit peptide is cleaved, and since the presence of the complete transit peptide only affects the ability of ADT1 to interact as a TA-fusion protein, and since omission of the complete transit peptide impedes the ability of ADT3 to interact with ADT1, subsequent experiments were carried out using full length ADTs.

4.1.1 Some ADTs are Self-Activating in a Yeast System

Control transformations showed that ADT3, but not ADT1, activated reporter expression in the absence of a TA construct (Appendix 3). Such self-activation is a common problem when testing transcription factors (Kovacs, 2003), as these proteins are independently capable of recruiting the transcription complex. However, being that ADTs are enzymes, interaction with the yeast transcription complex was not expected. Sequence analysis of all six ADTs revealed the presence of a protein motif which showed a high degree of sequence identity to a GAL4-type transactivation domain in the N-terminal region of the ADT catalytic domain (Table 7; Figure 2). The motifs in ADT3, ADT4, ADT5, and ADT6 match the consensus sequence at six of the nine amino acid positions, and therefore resemble a cryptic GAL4-TA domain more than ADT1 and ADT2, which match at only four and three amino acids, respectively. It is not surprising, therefore, that all four of these ADTs were self-activating (Appendix 5). However, unlike the DB-ADT3 constructs in yeast strain YPB2, which activated expression of both reporters (Appendix 3), the DB-ADT3 constructs in strain AH109 only activated expression of one of the three reporters (*MEL1*; Appendix 5). While this type of activation domain is common in yeast and bacteria, there is no evidence to suggest that it is a functional activation domain in plants (Piskacek *et al.*, 2007). It is therefore likely that, for *Arabidopsis* ADTs, this motif is only a cryptic activation domain.

4.2 ADTs Form Different Homo- and Heterodimer Combinations

4.2.1 ADT1, but Not ADT2, Interacts with All Other ADTs in Yeast

Only DB-ADT1 and DB-ADT2 fusion proteins could be used to test possible homo- and heterodimers in yeast, as ADT3, ADT4, ADT5, and ADT6 are all self-activating as DB-fusion proteins (Appendix 5). When testing full length constructs, ADTs are not all equally able to form dimers in a yeast system (Figure 11). ADT1 is able

Table 7. Consensus Sequence of a Cryptic GAL4-type Nine Amino Acid Transactivation Domain Present in *Arabidopsis* ADTs.

Position	Consensus[a]	ADT1[b]	ADT2	ADT3	ADT4	ADT5	ADT6
1	DGT	E	E	**D**	**D**	**D**	**D**
2	FLVAD	Q	E	Q	Q	Q	Q
3	FLV	**F**	**F**	**F**	**F**	**F**	**F**
4	WDEY	**E**	**D**	**E**	**D**	**D**	**E**
5	FVYENS	A	T	**V**	**V**	**V**	**V**
6	FLDEY	A	A	A	A	A	A
7	FLIY	**F**	**F**	**F**	**F**	**F**	**F**
8	LQGF	**Q**	E	**Q**	**Q**	**Q**	**Q**
9	FLERD	A	A	A	A	A	A

[a] Consensus sequence from Piskacek *et al.*, 2007.

[b] Bold: amino acids which match the consensus sequence.

to form dimers with all other ADTs, but not itself, whereas ADT2 is only able to interact with ADT1, but not any other ADT. This suggests either (1) that not all ADTs form homo- and heterodimers, or (2) that there is some inherent aspect of the yeast system that is preventing interactions from occurring, such as improper folding. Since the reciprocal interactions cannot be tested in yeast due to the self-activation properties of ADT3, ADT4, ADT5, and ADT6 DB-fusion proteins, the Y2H system cannot be used to determine which of these explanations is correct.

4.2.2 All ADTs Form Homo- and Heterodimers *In Planta*

Since the self-activation properties of ADT3, ADT4, ADT5, and ADT6 significantly limited the homo- and heterodimer combinations which can be tested in yeast, all six *ADT*s were cloned into the BiFC system, which can be used both to test dimerization and to determine the subcellular localization pattern of those dimers. All possible ADT homo- and heterodimer combinations were tested in both configurations (N- and C-terminal half-YFPs) in *N. benthamiana*. Only full length ADTs were used, to ensure that each was processed and localized in the plant cells as naturally as possible. Since it is still not known whether the ADT transit peptide is cleaved, the half-YFP was fused to the C-terminus of each ADT so that it would not be separated from the ADT if cleavage occurred. In contrast to the Y2H dimerization profiles, all six ADTs were able to form homo- and heterodimers *in planta* (Figures 18-24). This indicates that the lack of interactions in yeast was likely a consequence of working in a heterologous system, rather than an inability to form dimers. In the Y2H system, the GAL4-TA and GAL4-DB domains were fused to the N-terminus of the ADTs, as this was thought to be the least disruptive fusion location. The crystal structures of bacterial PDTs showed that dimerization is likely mediated by amino acids in the catalytic and ACT regulatory domains (Tan *et al.*, 2008; Vivan *et al.*, 2008), and so it was thought that if the transit peptide sequence is not required for interaction, it would act as a hinge region separating the GAL4 domain and the ADT. However, as this N-terminal fusion appears to impede interactions more than the C-terminal fusion, it may be that the transit peptide sequence is required for dimerization of, or at least proper folding of, plant ADTs.

4.2.3 ADT Dimers: Implications for Function

In all likelihood, the use of a constitutive 35S promoter in this BiFC system creates an artificially ADT-saturated cellular environment (Benfey and Chua, 1990), which does not reflect the naturally varying expression patterns of *Arabidopsis* ADTs (Rippert *et al.*, 2009; Hood, 2008; Cho *et al.*, 2007). While high expression levels do test the potential of two proteins to interact given that they are both expressed, and track their subcellular localization, it does not provide any information on how these dimers form under natural conditions. The most common way to regulate the formation of specific dimers in natural systems is spatiotemporal segregation of the monomers (Tsuchisaka *et al.*, 2009; Akhtar *et al.*, 2008; Akaba *et al.*, 1999). If two monomers are expressed in different tissues, at different developmental stages, or in response to different environmental conditions, then their ability to dimerize is negated by the inability to make contact. Even if multiple monomers are present in the same place at the same time, their relative levels may dictate which type of dimer is most abundant. Similarly, competition amongst the monomers can also affect which dimers form, as a monomer with a high affinity for a specific interaction partner can out-compete a monomer with a low affinity for that same interaction.

*Arabidopsis ADT*s are expressed in all tissues and under all conditions tested thus far (Rippert *et al.*, 2009; Hood, 2008; Cho *et al.*, 2007), and when co-expressed are able to form all possible homo- and heterodimers, suggesting that the formation of specific dimers may be dependant on the relative abundance of monomers, competition between monomers, or both. This type of interaction profile has been described for aminocyclopropane-1-carboxylate synthases (ACSs), which catalyze the second step of ethylene biosynthesis in *Arabidopsis* (Tsuchisaka *et al.*, 2009; Yamagami *et al.*, 2003). Ethylene is a key regulator of developmental processes in plants, and in *Arabidopsis* there are nine ACS isozymes. Like ADTs, ACS isozymes function as dimers, have tissue-specific expression patterns and exhibit a variety of substrate affinities, although one ACS isoform is inactive. In tissues where levels of the ACS substrate, S-adenosyl-methionine, are low, expression levels of high-affinity enzymes are increased. ACS isozymes are capable of forming 45 different dimers, although due to interactions with the inactive monomer only 25 dimers are active, and it is the relative ratios and activities of all 45 dimers which allows for the precise regulation of ethylene production

throughout development (Tsuchisaka et al., 2009). There is clearly functional redundancy in this family, as the expression levels of the remaining ACS isozymes are altered in all of the knockout lines, and only the full nine-ACS-knockout is embryonic lethal.

If, like ACS isozymes, all 21 possible *Arabidopsis* ADT dimers are present all the time, and only their relative levels change, then the activity of ADTs likely depends on the combined activity of all dimers present and the relative abundance of specific dimers at any given time. Small changes in abundance would allow either for very precise control or for a lot of flexibility. The catalytic activities of *Arabidopsis* ADTs have been evaluated *in vitro* and in yeast, and they do show some variability in substrate use and catalytic efficiency. All six ADTs are able to use arogenate as a substrate, however only ADT1, ADT2, and ADT6 are able to use prephenate as a substrate (Cho *et al.*, 2007), and ADT6 is not able to use prephenate efficiently enough to support growth *in vivo* (Bross *et al.*, 2011). Furthermore, *in vitro* catalytic efficiency in the presence of arogenate is variable among ADTs, with ADT2 and ADT6 being the most efficient and ADT4 and ADT5 the least (Cho *et al.*, 2007). However, these data only account for the activities of the ADT homodimers, as the activities of heterodimers have not been tested.

Furthermore, ADTs are differentially-expressed in a tissue-specific manner and in response to different environmental conditions (Hood, 2008; Cho *et al.*, 2007). A recent characterization of *Arabidopsis adt* knockouts has shown that, while most single- and double-knockouts do not have an obvious phenotype, the *adt4-adt5* knockouts have impaired lignificaiton, suggesting that these ADTs have a specific role in lignification (Corea *et al.*, 2010). This is consistent with the suggestion that each ADT has a distinct biological function (Bross *et al.*, 2011; Rippert *et al.*, 2009; Cho *et al.*, 2007). However, the fact that all six *Arabidopsis* ADT are expressed at some level in all tissues and under all conditions tested, and that the formation of all 21 dimers is possible suggests that the response of ADTs to changing phenylalanine requirements may be more complex than initially proposed.

The availability of specific ADTs for dimerization may dictate which dimers are more or less abundant, which is important because changes in dimer abundance would impact on the combined enzymatic activity of the system, and this combined enzymatic

activity may be what allows the organism to precisely respond to changes in Phe demand. Being that Phe is a precursor for the components of so many important cellular processes (such as protein synthesis, reproduction, environmental stress responses, and pathogen defense), regulating Phe biosynthesis is very important for plant welfare.

4.3 ADTs Exhibit Different Subcellular Localization Patterns

Interestingly, although all of the ADT constructs used in the BiFC system were full length and included the complete N-terminal transit peptide, two different subcellular localization patterns were observed. While all six ADTs are predominantly associated with the chloroplasts, this pattern does not overlay with the chlorophyll autofluorescence (ie. Figure 21). The second pattern is specific to ADT5 and appears to be nuclear (ie. Figure 23), which is surprising given that none of the ADTs are predicted to contain a nuclear localization signal (Section 3.4.4).

4.3.1 ADT Dimers Localize Predominantly to the Periphery of the Chloroplast

All ADT dimers predominately localize to the periphery of the chloroplast, where they form punctate foci. These foci can be found all around the chloroplast, and are always outside of the chlorophyll autofluorescence. There are a number of possible explanations for this type of localization pattern. First, the YFP may be accumulating in mitochondria, as mitochondria have long been shown to occur in close association with chloroplasts (Wildman *et al.*, 1962). This may be the case for ADT1, as the ADT1 transit peptide sequence least resembles a chloroplast targeting sequence (Crawley, 2004). However, all other ADTs are strongly predicted to localize to the chloroplast, and it would be difficult to explain why ADT dimers accumulate only in mitochondria which are directly adjacent to chloroplasts.

Second, the foci may represent peroxisomes, which are often visualized in close association with chloroplasts (Mano *et al.*, 2002). However, initial co-localization of fluorescently-tagged ADT monomers with a peroxisome marker show that, while these two localization patterns are similar when viewed separately, ADT fluorescence does not overlay with the peroxisome marker (C.D. Bross, personal communication).

A third explanation for this localization pattern is that ADTs are accumulating at

import pores around the chloroplast. Chloroplast targeting is usually mediated by proteins of the TIC-TOC complex in the membrane of the chloroplast (Li and Chiu, 2010; Bédard and Jarvis, 2005). If the ADT transit peptide is recognized by TOC proteins, but the preprotein is unable to pass through the channel into the stroma, the fusion proteins may accumulate in the TIC-TOC complex (Hinnah *et al.*, 2002). This accumulation could place the two half-YFPs in close proximity such that the YFP signal is reconstituted. However, there are many more TIC-TOC complexes in the membrane of a chloroplast than there are ADT-YFP accumulations (Li and Chiu, 2010). It would be difficult to explain why the ADT preproteins are only accumulating in certain pores but not others.

Finally, the foci may represent an accumulation of dimers in stromules (stroma-containing tubules), which are projections of the chloroplast membrane (Natesan *et al.*, 2005; Gray *et al.*, 2001). These membrane extensions contain stroma but do not usually contain thylakoid grana, and so do not autofluoresce as they do not contain any chlorophyll (Figure 26). Stromules increase the surface area of the chloroplast (Natesan *et al.*, 2005), and have been shown to form connections with other chloroplasts, the endoplasmic reticulum (Schattat *et al.*, 2011), peroxisomes and mitochondria (Kwok and Hanson, 2004a), and the nucleus (Kwok and Hanson, 2004b). Stromules are highly motile and are capable of shuttling protein complexes of up to 550kDa between chloroplasts (Kwok and Hanson, 2004d). They are abundant in epidermal cells where they can form thin extensions up to 200µm long, but in mesophyll cells they tend to be less abundant and more beak-like in appearance (Waters *et al.*, 2004). Under stress conditions, stromules have also been shown to bud off and transport their contents to the vacuole (Ishida *et al.*, 2008). There is, however, currently no known targeting sequence for stromule-specific localization of proteins. The chloroplast-associated ADT localization patterns strongly resemble other stromule-localized proteins (Shaw and Gray, 2011; Sattarzadeh *et al.*, 2009; Hanson and Sattarzadeh, 2008; Holzinger *et al.*, 2007; Kwok and Hanson, 2004c and 2004d). Localization of ADTs to stromules would provide a mechanism for efficient transport of Phe both within the chloroplast and to the cytosol and mitochondria, where it is required for protein synthesis and for the production of many secondary metabolites.

Figure 26. Diagram of a Chloroplast Stromule. Stromules are projections of the chloroplast membrane which contain stroma but not thylakoid grana (Natesan *et al.*, 2005). The area of autofluorescence within the chloroplast, due to chlorophyll within the thylakoid grana, is shaded green in this figure. Stromules have been visualized in close proximity to the nucleus (Kwok and Hanson, 2004a), as well as mitochondria and peroxisomes (Kwok and Hanson, 2004b).

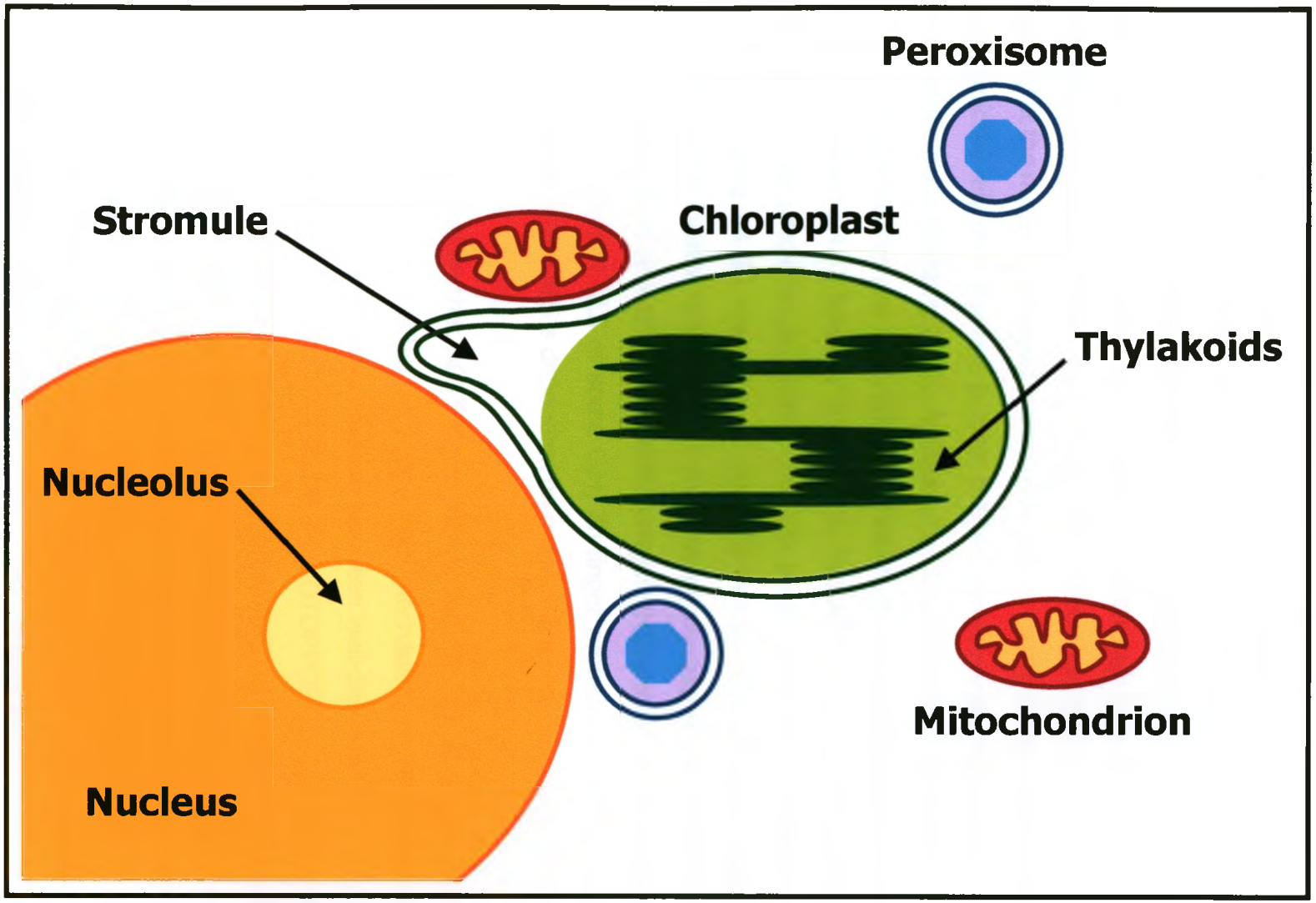
Peroxisome
Stromule
Chloroplast
Thylakoids
Nucleolus
Nucleus
Mitochondrion

4.3.2 ADT5 Dimers have a Nuclear-like Localization Pattern

Dimers which contain ADT5 display a completely unexpected localization pattern. While both the ADT5 homo- and heterodimers localize to the chloroplast in a stromule-like pattern much like that of other ADTs (Figure 22), they also localize in a nuclear-like pattern (Figure 23). This was not expected, since ADTs are enzymes and are unlikely to act as transcription factors. Nuclear import can be accomplished either passively, by which proteins less than 40kDa diffuse through the nuclear envelope, or actively through the interaction of a nuclear localization signal (NLS) with importin α or importin β at the nuclear envelope (Meier and Brkljacic, 2010). Plant nuclear localization signals typically rely on either one (classic NLS) or two (bipartite NLS) short stretches of basic amino acids (Raikhel, 1992). Analysis of all six ADTs using the NucPred nuclear prediction program (Brameier *et al.*, 2007) did not identify any putative NLSs in the ADT sequences (Section 3.4.4), however it is possible that ADT5 contains an NLS that is not recognized by the prediction programs. This has been shown for a number of other proteins, including all 36 members of the DOF family of transcription factors in *Arabidopsis*, which localize to the nucleus via an atypically-spaced bipartite NLS that is not recognized by publicly-available prediction programs (Krebsa *et al.*, 2010). Similarly, the atypical interspersed NLS of some C_2H_2 Zn-finger proteins is difficult to predict because formation of the NLS is dependant on proper folding of the protein (Hatayama *et al.*, 2008).

It is also possible that ADT5 does not contain an NLS at all, but rather is translocating to the nucleus either via a piggyback mechanism, or via stromules. The piggyback mechanism of nuclear localization has been well-described for a number of plant proteins, including the PHYTOCHROME A PHOTORECEPTOR (PHYA), which is transported to the nucleus via an interaction with FAR-RED ELONGATED HYPOCOTYL 1 (FHY1; Genoud *et al.*, 2008). Similarly, stromules have been shown in close proximity to nuclei, sometimes even embedded in the folds of the nuclear envelope (Kwok and Hanson, 2004b), so if ADTs do localize to the stromules, ADT5 could also be transported to the nucleus by the stromules themselves. While it is not known yet whether stromules are able to connect directly to the nucleus, if the transit peptide is cleaved upon entry into the chloroplast, the processed ADT5 protein is less than 40kDa in size (Bross *et al.*, 2011), making passive diffusion a possible mechanism of entry into

the nucleus.

The nuclear-like localization pattern of ADT5 homo- and heterodimers is usually characterized by a diffuse accumulation of YFP, which is associated with the nucleoplasm (Lorkovic *et al.*, 2004). Some nuclei also have larger accumulations of YFP within the area of diffuse fluorescence which suggests accumulation in a specific subnuclear compartment. However, the bright foci do not seem to correspond to the nucleolus, as the nucleolus is visible in most of the nuclei as a single, dark, circular area within the diffuse fluorescence. Many subnuclear compartments have been described in plants to which specific proteins localize (Shaw and Brown, 2004). The two localization patterns which most resemble the ADT5 pattern are associated with Cajal bodies (Li *et al.*, 2006) and nuclear speckles (Lorkovic *et al.*, 2008), both of which contain proteins involved in mRNA splicing. However, being that the relative size, number, and distribution of each of these nuclear compartments is dependant on the physiological and transcriptional states of the cell, and its position in the cell cycle, it is difficult to distinguish one type of nuclear body from another based on pattern alone.

The role of ADT5 in the nucleus is currently a mystery. If ADT5 is transported from the chloroplast to the nucleus, it may be involved in regulating the expression of genes required for Phe biosynthesis in *Arabidopsis*, such as the *ADT*s. It is also possible that ADT5 could be involved in RNA processing, however the mechanism by which this would occur is wholly unknown. Regardless, there is some evidence to suggest that the function of ADT5 is of particular importance to the plant. While none of the single ADT knockouts have a visible phenotypes, the *adt4-adt5* double knockout lines show significantly impaired lignin biosynthesis (Corea *et al.*, 2010), suggesting that these two ADTs may be important either for maintaining adequate Phe levels, or for directing Phe into specific metabolic pathways.

4.4 ADT1 Interacts with a Wide Variety of Other Proteins

It was initially hypothesized that ADTs would interact with proteins other than themselves. The existence of multi-functional ADT/PDT-containing enzymes in enterobacteria (Zhang *et al.*, 1998; Dopheide *et al.*, 1972), *Shewanella* species, and *Archaeglobis fulgides* (Bross *et al.*, 2011) suggests that ADTs may act as part of a larger protein complex which facilitates aromatic amino acid biosynthesis. Y2H screens

of two cDNA libraries identified thirty different putative ADT1 protein interactors, only ten of which were in frame fusion proteins which met the control requirements (Section 3.1.1). Other than confirming interactions between ADT1 and ADT1, ADT4, and ADT6, none of the other identified proteins are known to be involved in aromatic amino acid biosynthesis.

4.4.1 cDNA Library Screens Confirm ADT1 Homo- and Heterodimers

Three of the ADT1 interactors recovered from the Y2H cDNA library screens are known homo- and heterodimers (ADT1, ADT4, and ADT6), which is consistent with the binary interactions previously determined. The ADT1 and ADT4 fragments recovered, as well as two of the three ADT6 fragments, were shorter than the full length sequences, suggesting that these sequences are sufficient to interact with ADT1. Each of the truncated ADT sequences contained a complete ACT regulatory domain, but only the ADT1 and ADT6 fragments contained a complete catalytic domain and, in the case of ADT6, part of the transit peptide. The ADT4 fragment is missing the first 63 amino acids of the catalytic domain. This portion of the catalytic domain includes three amino acids which are predicted to be involved in intermolecular interactions (Figure 3; Bross *et al.*, 2011; Tan *et al.*, 2008), suggesting that these three amino acids may not be critical for dimerization.

4.4.2 The TA-ADT6 Fusion Protein may Undergo a Splicing Event in the Heterologous Yeast System

Using DB-ADT1-FL, interactions with ADT6 were identified a number of times, however in each case the fusion protein was either out of frame, or contained a stop codon immediately prior to the start of the full length, in-frame *ADT6* sequence. As a general rule, fusion proteins which are not in frame would be disregarded because they translate into non-functional proteins. However, as the ADT1-ADT6 heterodimer has already been demonstrated (Section 3.2.2), there was cause for further investigation. Based on the position of the stop codon in the full length fusion proteins, only the GAL4-AD domain, the HA tag and the linker region are predicted to be translated. If these components alone were responsible for the interaction, then every fusion protein in the library should give a positive result as these are shared vector-derived sequences.

Since this is not the case, it was speculated that some modification must be occurring which removes the stop codon and allows some portion of the *ADT6* sequence to be translated to mediate the interaction. While *ADT6* itself does not contain any introns (Cho *et al.*, 2007), it is possible that the yeast system is recognizing and removing a perceived intron. One of the most well known examples of cryptic splicing in a heterologous system is Green Fluorescent Protein (GFP). The *GFP* sequence had to be modified for expression in plants, as plant systems recognized and removed a cryptic intron from the GFP transcript, resulting in a non-functional protein (Haselhoff *et al.*, 1997). If removal of this hypothetical intron in the TA-ADT6 fusion protein also removes the stop codon and maintains the frame of the fusion protein, this would explain the frequent recovery of this interaction in the screen.

To test the feasability of this solution, the complete coding sequence for the fusion protein was analyzed using two different eukaryotic gene structure prediction programs. Both GENSCAN (Burge and Karlin, 1998) and FGENESH predicted the removal of a small intron which includes the premature stop codon (Figure 15A and 15B). The original sequence of the fusion protein is in frame, and both of the predicted introns maintain that frame while removing the premature stop codon. The presence of this predicted splice product still needs to be confirmed by isolating the processed RNA from yeast and sequencing it.

Since the predicted donor site is part of the vector sequence, which is shared by all constructs in the library, the sequences of other interactors identified in this screen may also have similar cryptic introns. For example, At1g25530 is a putative amino acid transporter which was initially discarded because the sequence of the predicted fusion protein is out of frame. However, when this sequence was analyzed using GENSCAN, an intron was predicted which removes part of the HA tag and the entire linker sequence (Figure 15C), correcting the frame of the downstream sequence.

4.4.3 Why are Interactions with known Shikimate Pathway Enzymes Absent from the cDNA Library Screens?

Since a number of multi-functional enzymes have been described in bacteria which catalyze multiple steps of the shikimate and aromatic amino acid biosynthesis pathways (Bross *et al.*, 2011; Zhang *et al.*, 1998; Dopheide *et al.*, 1972), it was

hypothesized that *Arabidopsis* ADTs, which are mono-functional enzymes, would interact with other enzymes from these pathways. Even though the cDNA library screens performed in this study did not identify any other enzymes from the shikimate or aromatic amino acid biosynthesis pathways, this does not necessarily mean that the complex does not exist. When performing cDNA library screens, it is important ensure that as much of the library was screened as is possible, to decrease the possibility that an interactor was missed. It is difficult to determine whether adequate library coverage was achieved for the first cDNA library (Kohalmi *et al.*, 1997), as it has been amplified and its current diversity is not known, however 5.5 million transformants were screened using the normalized commercial cDNA library. This figure is close to what the manufacturer recommends for each screen, and since use of the normalized library is comparable to screening three times as many transformants as a non-normalized library (ClonTech PT4084), low library coverage is not likely to be an issue in this study.

Although the Y2H system is useful both for testing known interactions and for identifying completely unknown interactions, it does have one major limitation: it only tests binary interactions. If multiple simultaneous interactions are required to mediate an interaction, individual interactions may not be recovered in the Y2H system. Similarly, since ADT form dimers, formation of a larger complex could be dependant on formation of a specific ADT dimer. The TA-cDNA libraries also have limitations. In regards to the libraries used in this study, both are poly-A primed, which results in an over-representation of the 3' end of the transcripts and an under-representation of the 5' end. There is, therefore, an over-representation of the C-termini of the resulting proteins and an under-representation of the N-termini. If an interaction domain is in the N-terminal portion of a protein and is rarely found in the library, that interaction may be difficult to identify. Any one of these limitations could explain why no other interactors were identified in this study.

4.4.4 ADT1 Interacts with Proteins From Many Cellular Processes

While no other enzymes of the shikimate pathway were identified in this study, a number of other putative interactors were identified (Table 5). However, the biological significance of these interactions is not clear. Three of these candidate DB-ADT1-FL interactors localize to the chloroplast. ADENYLO-SUCCINATE SYNTHASE (ADSS)

catalyzes the conversion of L-aspartate to adenylosuccinate during *de novo* biosynthesis of adenosine monophosphate (AMP), a precursor of adenosine triphosphate (ATP; Prade *et al.*, 2000). A *lepA*-like translation elongation factor was also recovered. In bacteria, *lepA* encodes a translation elongation factor with GTPase activity which is critical for efficient protein synthesis (Youngman and Green, 2007). ADT1 also putatively interacts with CHLOROPLASTOS ALTERADOS 1 (CLA1) a 1-deoxy-D-xylulose-5-phosphate synthase which catalyzes the first step of the methylerythritol phosphate (MEP) pathway (Rodríquez-Concepción and Boronat, 2002). The end product of the MEP pathway, isopentenyl diphosphate, is required for isoprenoid biosynthesis. Chlorophyll, carotenoids, tocopherols, and gibberellins are all important isoprenoid-derived compounds. While none of these compounds is phenylalanine-derived, some phenylpropanoids are prenylated (Yazaki *et al.*, 2009), including flavonoids and isoflavonoids, which are potent antioxidants and antimicrobial agents.

ADT1 is also putatively able to interact with two proteins which do not localize to the chloroplast: a putative protein kinase which localizes to the plasma membrane (At2g36350), and a Succinyl CoA Ligase α subunit, which localizes to the mitochondria (At5g08300). While it is not surprising for ADT1 to interact with a kinase, as it is common for proteins to be post-translationally modified and such modifications of ADTs have not yet been determined. Succinyl-CoA ligase functions in the tricarboxylic acid (TCA) cycle (Sweetlove *et al.*, 2002), potentially linking ADT1 to energy production, however this interaction would require the localization of ADT1 to the mitochondrion. ADT1 is predicted to localize to the chloroplast, and the YFP localization data presented in this study support this prediction, however at least 50 proteins have been identified which are dual-targeted to chloroplasts and the mitochondria (Carrie *et al.*, 2009).

4.4.5 ADT1 Interacts with BCAT3 in Yeast

Approximately 1% of the metabolism-related genes in the *Arabidopsis* genome are aminotransferases (ATs), which are divided into four classes based on evolutionary relationships (Liepman and Olsen, 2004). ATs function as homodimers, and are usually able to use multiple similar substrates for catalysis (Liepman and Olsen, 2004). In Phe biosynthesis, an AT is required for the conversion of prephenate to arogenate, and a gene encoding a confirmed prephenate-specific Class Ib AT has recently been identified

in Arabidopsis (At2g22250; Maeda *et al.*, 2011) and tomato (Graindorge *et al.*, 2010). The cDNA library screens in this study did not identify this particular AT, however ADT1 does interact with one of the Class III branched-chain ATs (BCAT3) which localizes to the chloroplast and is involved in leucine, isoleucine, and valine biosynthesis, as well as methionine chain elongation in glucosinolate biosynthesis (Knill *et al.*, 2008). There was no significant change in Phe levels in either the seeds or rosette leaves of *bcat3* plants, however BCAT3 function is partially redundant with other BCATs (Knill *et al.*, 2008), so it may be that the effects were masked by the activity of other ATs. It is currently not clear whether BCAT3 could function in the transmination of prephenate or arogenate, as neither was tested as a substrate (Knill *et al.*, 2008).

4.5 Concluding Remarks and Future Directions

This study provides the first identification and initial characterization of the protein-protein interactions of plant ADTs. The BiFC assays performed in this study showed (1) that *Arabidopsis* ADTs are able to form all possible homo- and heterodimers *in planta*, and (2) that these dimers present two different subcellular localization patterns. While all ADT dimers localize predominantly to the chloroplast in what appears to be a stromule-like pattern, dimers which contain ADT5 also show a nuclear-like localization pattern. That being said, this study relied on a constitutive 35S promoter to drive high-level expression of the YFP-fusion proteins (Benfey and Chua, 1990), which might create an artificially ADT-saturated cellular environment. It would be more informative in the future to produce stable plant transformants for each possible dimer, using the native ADT promoters, to examine the natural dimerization profiles in specific tissues, developmental stages, and in response to different environmental stresses. This will require the identification and cloning of each ADT promoter, which may present some challenges as there are other open reading frames within 0.6-2.0kb upstream of four of the six *ADT*s (Hood, 2008).

It will also be useful to co-localize these dimers with fluorescent markers for specific subcellular compartments, such as the mitochondria, peroxisomes, and stromules, as well as proteins which localize to specific subnuclear compartments, to definitively determine where the ADTs are localizing. ADT5 is of particular interest, as its possible role in the nucleus is not understood. This could be examined using a Y2H

cDNA library screen, as such a screen could help to identify any proteins which could help ADT5 to localize to the nucleus. However, use of ADT5 as a GAL4 DB-fusion protein would require modification of the cryptic GAL4-type activation domain. This could be accomplished through site-directed mutagenesis of the activation domain to convert the self-activating sequence to one of the two non-self-activating sequences (Table 7). Only two nucleotides need to be altered by site-directed mutagenesis to produce the two amino acid codon changes, D1E and V5A, that are required. As these amino acids are not predicted to be involved in mediating protein interactions (Figure 2), mutagenesis should not interfere with the ability to dimerize, however this would have to be confirmed before screening began.

Although no strong evidence for the formation of a Phe biosynthetic protein complex was presented in this study, I still believe there is a good chance that it exists. If a larger aromatic amino acid biosynthetic complex exists, its formation would positively impact on the overall efficiency of the Phe biosynthetic pathway by allowing for quick shuttling of intermediates between enzymes. Co-IP with total protein extracts from *Arabidopsis* is an alternative approach to addressing this question as this method is not limited to binary interactions. This would increase the chances of finding these interactors, if they exist, because it is possible to isolate whole or partial protein complexes using this system (Moresco *et al.*, 2010; Miernyk and Thellen, 2008). As the ADT-YFP fusion proteins include either Flag or HA epitope tags (Earley *et al.*, 2006), these constructs could be used to perform co-IP experiments with commercially-available antibodies, however it would also be beneficial to perform these co-IPs with ADT-specific antibodies. To avoid the cross-reactivity of traditional antibodies between all of the ADTs (described by Rippert *et al.*, 2009), these antibodies should be based on peptides.

Dimer formation requires intermolecular interactions which involve specific amino acids in each monomer. While the recent crystallization of select bacterial PDTs has allowed researchers to predict which amino acids might be involved in mediating these intermolecular interactions (Tan *et al.*, 2008; Vivan *et al.*, 2008), none of these predictions have been experimentally confirmed. Determining which amino acids are required for the dimerization *Arabidopsis* ADTs could be accomplished a number of ways. Site-directed mutagenesis could be used to alter specific amino acid codons,

namely the 18 amino acids thus far predicted to be involved in these interactions. However it is likely that more than one substitution will be required to completely abolish dimerization, although in most cases small changes are sufficient to destroy an interaction site (Libereles *et al.*, 2010). The drawback of this approach is that to specifically engineer all possible combinations of the 18 predicted amino acids would be time consuming, and would not take into account any other amino acids which may also be required. It may be more efficient to begin with an unbiased approach, such as a Reverse Y2H screen (Vidal and Legrain, 1999). This approach would require the creation of a library of *ADT*s with varying combinations of randomly generated nucleotide substitutions which, when expressed, could be screened against a wild-type ADT, and only those which do not interact will survive. This would help to both narrow down which predicted amino acids are involved in mediating the interactions, as well as identify any new amino acids of interest.

If ADTs do perform an important regulatory step in Phe biosynthesis, then understanding when and how ADTs function is critical for understanding Phe biosynthesis and in turn the regulation and production of Phe-derived secondary metabolites. Phe is one of the most commercially-produced amino acids, with sales reaching $1 billion US annually (Sprenger, 2007). The ability to manipulate Phe biosynthesis in plants also has a number of potential biotechnological applications. Lignin, a phenylpropanoid which accounts for up to 30% of the vascular plant cell wall (Laskar *et al.*, 2010), gives plant stems structure and stability and, in order to increase lignin deposition and produce sturdier, more wind-resistant crops, it is first necessary to increase Phe levels. Lignin degradation is also one of the major obstacles facing cellulosic ethanol biofuel production, and modifying lignin deposition has been shown to improve fermentable sugar yields (Chen and Dixon, 2007). Furthermore, increasing the levels of antioxidants in food crops could have a major impact on human health, but to increase the production of Phe-derived antioxidants it is necessary to first increase the amount of Phe available. Although this particular study only breaks the surface of what there is to learn about ADTs, their interactions, and the implications for Phe biosynthesis, it is an important stepping stone to the possible downstream applications of this knowledge. More work is clearly needed to understand the significance of these interactions and to apply this information in a physiologically relevant manner.

5 REFERENCES

Akaba, S., Seo, M., Dohmae, N., Takio, K., Sekimoto, H., Kamiya, Y., Furuya, N., Koman, T., and Koshiba, T. (1999). Production of homo- and hetero-dimeric isozymes from two aldehyde oxidase genes of *Arabidopsis thaliana*. Biochem. *126*: 395-401.

Akhtar, T.A., McQuinn, R.P., Naponelli, V., Gregory, J.F. III, Giovannoni, J.J. and Hanson, A.D. (2008). Tomato γ-glutamyl hydrolases: Expression, characterization, and evidence for heterodimer formation. Plant Physiol. *148*: 775-785.

Armbruster, U., Hertle, A., Makarenko, E., Zühlke, J., Pribil, M., Dietzmann, A., Schliebner, I., Aseeva, E., Fenino, E., Scharfenberg, M., Voigt, C., and Leister, D. (2009). Chloroplast proteins without cleavable transit peptides: Rare exceptions or a major constituent of the chloroplast proteome? Mol. Plant. *2*: 1325-1335.

Bartel, P., Chien, C.T., Sternglanz, R., and Fields, S. (1993). Elimination of false positives that arise in using the 2-hybrid system. Biotechniques *14*: 920-924.

Bédard, J., and Jarvis, P. (2005). Recognition and envelope translocation of chloroplast preproteins. J. Exp. Bot. *56*:2287-2320.

Benfey, P.N., and Chua, N-H. (1990). The Cauliflower Mosaic virus 35S promoter: combinatorial regulation of transcription in plants. Science *250*: 959-966.

Binder, S. (2010). Branched-chain amino acid metabolism in *Arabidopsis thaliana*. The *Arabidopsis* Book *8*: e0138. doi:10.1199/tab.0137.

Bracha-Drori, K., Shichrur, K., Katz, A., Oliva, M., Angelovici, R., Yalovsky, S., and Ohad, N. (2004). Detection of protein–protein interactions in plants using bimolecular fluorescence complementation. Plant J. *40*: 419-427.

Brameier, M., Krings, A., and MacCallum, R.M. (2007). NucPred—Predicting nuclear localization of proteins. Bioinform. *23*:1159-1160.

Bross, C.D., Corea, O.R.A., Kaldis, A., Menassa, R., Bernards, M.A., and Kohalmi, S.E. (2011). Complementation of the *pha2* yeast mutant suggests functional differences for arogenate dehydratases from *Arabidopsis thaliana*. Plant Physiol. Biochem. Epub ahead of print. doi:10.1016/j.plaphy.2011.02.010.

Burge, C.B., and Karlin, S. (1998). Finding the genes in genomic DNA. Curr. Opin. Struct. Biol. *8*: 346-354.

Carrie, C., Giraud, E., and Whelan, J. (2009). Protein transport in organelles: Dual targeting of proteins to mitochondria and chloroplasts. FEBS J. *276*: 1187-1195.

Chen, F., and Dixon, R.A. (2007). Lignin modification improves fermentable sugar yields for biofuel production. Nature Biotech. *25*: 759-761.

Chevray, P.M. and Nathans, D. (1992). Protein interaction cloning in yeast: Identification of mammalian proteins that react with the leucine zipper of Jun. Proc. Natl. Acad. Sci. USA. *89*: 5789-5793.

Cho, M., Corea, O.R.A., Yang, H., Bedgar, D.L., Laskar, D.D., Anterola, A.M., Moog-Anterola, F.A., Hood, R.L., Kohalmi, S.E., Bernards, M.A., Kang, C., Davin, L.B., and Lewis, N.G. (2007). Phenylalanine biosynthesis in *Arabidopsis thaliana*. Identification and characterization of arogenate dehydratases. J. Biol. Chem. *282*: 30827-30835.

Corea, O.R.A., Chanyoung, K., Patten, A., Cardenas, C., Davin, L., and Lewis, N. (2010). Upstream genes encoding phenylalanine biosynthesis: Differential control of protein and lignin formation in *Arabidopsis*. Plant Biology 2010, Monréal, Canada. July 31 - August 4 2010.

Citovsky, V., Lee, L., Vyas, S., Glick, E. Chen, M., Vainstein, A., Gafni, Y., Gelvin, S.B., and Tzfira, T. (2006). Subcellular localization of interacting proteins by bimolecular fluorescence complementation *in planta*. J. Mol. Bio. *362*: 1120-1131.

Crawley, C.D. (2004). Characterization of six prephenate dehydratase-like genes in *Arabidopsis thaliana*. M.Sc. Thesis: University of Western Ontario, Department of Biology.

Curien, G., Biou, V., Mas-Droux, C., Robert-Genthon, M., Ferrer, J-L., and Dumas, R. (2008). Amino acid biosynthesis: New architectures in allosteric enzymes. Plant Physiol. Biochem. *46*: 325-339.

Dopheide, T.A., Crewther, P., and Davidson, B.E. (1972). Chorismate mutase-prephenate dehydratase from *Escherechia coli* K-12. II. Kinetic properties. J. Biol. Chem. *247*: 4447-4452.

Earley, K., Haag, J.R., Pontes, O., Opper, K., Juehne, T., Song, K., and Pikaard, C.S. (2006). Gateway-compatible vectors for plant functional genomics and proteomics. Plant J. *45*: 616-629.

Ehlting, J., Mattheus, N., Aeschliman, D.S., Li, E., Hamberger, B., Cullis, I.F., Zhuang, J., Kaneda, M., Mansfield, S.D., Samuels, L., Ritland, K., Ellis, B.E., Bohlmann, J., and Douglas, C.J. (2005). Global transcript profiling of primary stems from *Arabidopsis thaliana* identifies candidate genes for missing links in lignin biosynthesis and transcriptional regulators of fiber differentiation. Plant J. *42*: 618-640.

Fields, S., and Song, O. (1989). A novel genetic system to detect protein interactions. Nature. *340*: 245-246.

Fürst, P., and Stehle, P. (2004). What are the essential elements needed for the determination of amino acid requirements in humans? J. Nutr. *134*: 1558S-1565S.

Genoud, T., Schweizer, F., Tscheuschler, A., Debrieux, D., Casal, J.J., Schäfer, E., Hiltbrunner, A., and Fankhauser, C. (2008). FHY1 mediates nuclear import of the light-activated phytochrome A photoreceptor. PloS Genetics *4*: e1000143. doi:10.1371/journal.pgen.1000143.

Gietz, R.D., and Woods., R.A. (2002). Transformation of yeast by the LiAc/SS Carrier DNA/PEG Method. Meth. Enzym. *350*: 87-96.

Görlach, J., Beck, A., Henstrand, J.M., Handa, A.K., Herrmann, K.M., Schmid, J., and Amrhein, N. (1993a). Differential expression of tomato (*Lycopersicon esculentum* L.) genes encoding shikimate pathway isoenzymes. I. 3-Deoxy-D-arabinoheptulosonate 7-phosphate synthase. Plant Mol. Biol. *23*: 697-706.

Görlach, J., Schmid, J., and Amrhein, N. (1993b). Differential expression of tomato (*Lycopersicon esculentum* L.) genes encoding shikimate pathway isoenzymes. II. Chorismate mutase. Plant Mol. Biol. *23*: 707-716.

Graindorge, M., Giustini, C., Jacomin, A.C., Kraut, A., Curien, G., Matringe, M. (2010). Identification of a plant gene encoding glutamate/aspartate-prephenate aminotransferase: The last homeless enzyme of aromatic amino acids biosynthesis. FEBS Letters *584*: 4357-4360.

Gray, J.C., Sullivan, J.A., Hibberd, J.M., and Hansen, M.R. (2001). Stromules: Mobile protrusions and interconnections between plastids. Plant Biol. *3*:223-233.

Hamberger, B., Ehlting, J. Barbazuk, B., and Douglas, C. (2006). Comparative genomics of the shikimate pathway in *Arabidopsis*, *Populus trichocarpa* and *Oryza sativa*: Shikimate pathway gene family structure and identification of candidates for missing links in phenylalanine biosynthesis. *In*: Recent Advances in Phytochemistry. Volume 40. Integrative Plant Biochemistry (J.T. Romeo, ed). Elsevier Ltd, Amsterdam, pp. 85-113.

Hanson, M.R., and Sattarzadeh, A. (2008). Dynamic morphology of plastids and stromules in angiosperm plants. Plant Cell Environ. *39*: 646-657.

Haselhoff, J. Siemering, K.R., Prasher, D.C., and Hodge, S. (1997). Removal of a cryptic intron and subcellular localization of green fluorescent protein are required to mark transgenic *Arabidopsis* plants brightly. Proc. Natl. Acad. Sci. USA. *94*: 2122-2127.

Hatayama, M., Tomizawa, T., Sakai-Kato, K., Bouvagnet, P., Kose, S., Imamoto, N., Yokoyama, S., Utsunomiya-Tate, N., Mikoshiba, K., Kigawa, T., and Aruga, J. (2008). Functional and structural basis of the nuclear localization signal in the ZIC3 zinc finger domain. Hum. Mol. Genet. *17*: 3459-3473.

Hell, R., Jost, R., Berkowitz, O., and Wirtz, M. (2002). Molecular and biochemical analysis of the enzymes of cysteine biosynthesis in the plant *Arabidopsis thaliana*. Amino Acids, *22*: 245-257.

Herrmann, K.M. and Weaver, L.M. (1999). The shikimate pathway. Annu. Rev. Plant Physiol. Plant Mol. Biol. *50*: 473-503.

Hinnah, S.C., Wagner, R., Sveshnikova, N., Harrer, R., and Soll, J. (2002). The chloroplast protein import channel Toc75: Pore properties and interaction with transit peptides. Biophysical J. *83*: 899-911.

Hoekema, A., Hirsch, P.R., Hooykaas, P.J.J., and Schilperoort, R.A. (1983). A binary plant vector strategy based on separation of *vir*- and T-region of the *Agrobacterium tumefaciens* Ti-plasmid. Nature *303*: 179-180.

Holzinger, A., Buchner, O., Lütz, C., and Hanson, M.R. (2007). Temperature-sensitive formation of chloroplast protrusions and stromules in mesophyll cells of *Arabidopsis thaliana*. Protoplasma *230*: 23-30.

Hood, R.L. (2008). RNA expression of six arogenate dehydratases in *Arabidopsis*. MSc. Thesis: University of Western Ontario, Department of Biology.

Ish-Horowicz, D. and Burke, J.F. (1981). Rapid and efficient cosmid cloning. Nucleic Acids Res. *10*: 2989-2998.

Ishida, H., Yoshimoto, K., Izumi, M., Reisen, D., Yano, Y., Makino, A., Ohsumi, Y., Hanson, M.R., and Mae, T. (2008). Mobilization of rubisco and stroma-localized fluorescent proteins of chloroplasts to the vacuole by an ATG gene-dependent autophagic process. Plant Physiol. *148*: 142-155.

Jander, G., and Joshi, V. (2009). Aspartate-Derived Amino Acid Biosynthesis in *Arabidopsis thaliana*. The *Arabidopsis* Book *7*: e0121. 10.1199/tab.0121.

Jones, E.W., and Fink, G.R. (1982). Regulation of amino acid and nucleotide biosynthesis in yeast. *In*: The Molecular Biology of the Yeast *Saccharomyces*: Metabolism and Gene Expression (J.N. Strathern, E.W. Jones, and J.R. Broach, eds). Cold Spring Harbor Laboratory Press, Cold Spring Harbor, New York. pp.181-299.

Jung, E., Zamir, L.O., and Jensen, R.A. (1986). Chloroplasts of higher plants synthesize L-phenylalanine via L-arogenate. Proc. Natl. Acad. Sci. *83*: 7231-7235.

Keith, B., Dong, X., Ausuble, F.M., and Fink, G.R. (1991). Differential induction of 3-deoxy-D-arabino-heptulosonate 7-phosphate synthase genes in *Arabidopsis thaliana* by wounding and pathogenic attack. Proc. Natl. Acad. Sci. USA. *88*: 8821-8825.

Kerppola, T.K. (2008). Bimolecular fluorescence complementation (BiFC) analysis as a probe of protein interactions in living cells. Annu. Rev. Biophys. *37*:465-487.

Kliebenstein, D.J., Kroymann, J., Brown, P., Figuth, A., Pedersen, D., Gershenzon, J., and Mitchell-Olds, T. (2001). Genetic control of natural variation in *Arabidopsis* glucosinolate accumulation. Plant Physiol. *126*:811-825.

Knill, T., Schuster, J., Reichelt, M., Gershenzon, J., and Binder, S. (2008). *Arabidopsis* branched-chain aminotransferase 3 functions in both amino acid and glucosinolate biosynthesis. Plant Physiol. *146*: 1028–1039.

Kohalmi, S.E., Nowak, J., and Crosby, W.L. (1997). The yeast two-hybrid system. *In*: Differentially Expressed genes in Plants: A Bench Manual (G. Harper and E. Hansen, eds). Taylor and Francis, UK. 63-82.

Kohalmi, S.E., Reader, L.V., Samach, A., Nowak, J., Haughn, G.W., and Crosby, W.L. (1998). Identification and characterization of protein interactions using the yeast 2-hybrid system. *In*: Plant Molecular Biology Manual (S.B. Gelvin and R.A. Schilperoort, eds.). Kluwer Academic, Netherlands. pp. 1-30.

Kovacs, K.M. (2003). Molecular characterization of a homeotic protein in *Arabidopsis thaliana.* MSc. Thesis: University of Western Ontario, Department of Biology.

Krebsa, J., Mueller-Roeber, B., and Ruzicic, S. (2010). A novel bipartite nuclear localization signal with an atypically long linker in DOF transcription factors. J. Plant Physiol. *167*: 583-586.

Kwok, E.Y. and Hanson, M.R. (2004a). *In vivo* analysis of interactions between GFP-labeled microfilaments and plastid stromules. BMC Plant Biol. *4*: 2.

Kwok, E.Y. and Hanson, M.R. (2004b). Plastids and stromules interact with the nucleus and cell membrane in vascular plants. Plant Cell Rep. *23*: 188-195.

Kwok, E.Y. and Hanson, M.R. (2004c). Stromules and the dynamic nature of plastid morphology. J. Microscopy *214*: 124-137.

Kwok, E.Y. and Hanson, M.R. (2004d). GFP-labelled Rubisco and aspartate aminotransferase are present in plastid stromules and traffic between plastids. J. Exp. Bot. *55*: 595-604.

Laskar, D.D., Corea, O.R.A., Patten, A.M., Kang, C.H., Davin, L.B., and Lewis, N.G. (2010). Vascular plant lignification: Biochemical/structural biology considerations of upstream aromatic amino acid and monolignol pathways. *In*: Comprehensive Natural Products II: Chemistry and Biology. Volume 6. Carbohydrates, Nucleosides & Nucleic Acids (L. Mander and H-W Liu, eds). Elselvier Ltd. pp.541-604.

Li, H-M., and Chiu, C.C. (2010). Protein transport in to chloroplasts. Ann. Rev. Plant Biol. *61*: 157-180.

Li, C.F., Pontes, O., El-Shami, M., Henderson, I.R., Bernatavichute, Y.V., Chan, S.W-L., Lagrange, T., Pikaard, C.S., and Jacobsen, S.E. (2006). An ARGONAUTE4-containing nuclear processing center colocalized with Cajal bodies in *Arabidopsis thaliana*. Cell *126*: 93-106.

Libereles, D.A., Kolesov, G., and Dittmar, K. (2010). Understanding gene duplication through biochemistry and population genetics. *In*: Evolution after gene duplication (K. Dittmar and D.A. Libereles, eds.). Wiley-Blackwell, Hoboken, New Jersey, USA.

Liepman, A.H., and Olsen, L.J. (2004). Genomic analysis of aminotransferases in *Arabidopsis thaliana*. Crit. Rev. Plant Sci. *23*: 73-89.

Lorkovic, Z.J., Hilschera, J., and Barta, A. (2008). Co-localization studies of *Arabidopsis* SR splicing factors reveal different types of speckles in plant cell nuclei. Exp. Cell Res. *314*: 3175-3186.

Lorkovic, Z.J., Hilschera, J., and Barta, A. (2004). Use of fluorescent protein tags to study nuclear organization of the spliceosomal machinery in transiently transformed living plant cells. Mol. Biol. Cell *15*: 3233-3243.

Lu, Q., Tang, X., Tian, G., Wang, F., Liu, K., Nguyen, V., Kohalmi, S.E., Keller, W.A., Tsang, E.W.T., Harada, J.J., Rothstein, S.J., and Cui, Y. (2010). *Arabidopsis* homolog of the yeast TREX-2 mRNA export complex: components and anchoring nucleoporin. Plant J. *61*: 259-270.

Maeda, H., Yoo, H., and Dudareva, N. (2011). Prephenate aminotransferase directs plant phenylalanine biosynthesis via arogenate. Nat. Chem. Biol. *7*:19-21.

Maeda, H., Shasany, A.K., Schnepp, J., Orlova, I., Taguchi, G., Cooper, B.R., Rhodes, D., Pichersky, E., and Dudareva, N. (2010). RNAi suppression of Arogenate Dehydratase1 reveals that phenylalanine is synthesized predominantly via the arogenate pathway in Petunia petals. Plant Cell. *22*: 832-849.

Mano, S., Nakamori, C., Hayashi, M., Kato, A., Kondo, M., Nishimura, M. (2002). Distribution and characterization of peroxisomes in *Arabidopsis* by visualization with GFP: Dynamic morphology and actin-dependant movement. Plant Cell Physiol. *43*: 331-341.

Mas-Droux, C., Curien, G., Robert-Genthon, M., Laurencin, M., Ferrer, J-L., and Dumas, R. (2006). A novel organization of ACT domains in allosteric enzymes revealed by the crystal structure of *Arabidopsis* aspartate kinase. Plant Cell. *18*: 1681-1692.

Meier, J., and Brkljacic, J. (2010). The *Arabidopsis* nuclear pore and nuclear envelope. The *Arabidopsis* Book *8*: e0139. doi: 10.1199/tab.0139.

Miernyk, J.A. and Thellen, J.J. (2008). Biochemical approaches for discovering protein–protein interactions. Plant J. *53*: 597-609.

Moresco, J.J., Carvalhob,P.C., and Yates, J.R. III. (2010). Identifying components of protein complexes in *C. elegans* using co-immunoprecipitation and mass spectrometry. J. Proteomics. *73*: 2198-2204.

Natesan, S.K.A., Sullivan, J.A., and Gray, J.C. (2005). Stromules: A characteristic cell-specific feature of plastid morphology. J. Exp. Bot. *56*: 787-797.

Naumov, G., Turakainen, H., Naumova, E., Aho, S., and Korhola, M. (1990). A new family of polymorphic genes in *Saccharomyces cerevisiae*: alpha-galactosidase genes MEL1-MEL7. Mol. Gen. Genet. *224*: 119-128.

Piskacek, S., Gregor, M., Nemethova, M., Grabner, M., Kovarik, P., and Piskacek, M. (2007). Nine-amino-acid transactivation domain: Establishment and prediction utilities. Genomics *89*: 756-768.

Prade, L., Cowan-Jacob, S.W., Chemla, P., Potter, S., Ward, E., and Fonne-Pfister, R. (2000). Structures of adenylosuccinate synthetase from *Triticum aestivum* and *Arabidopsis thaliana*. J. Mol. Biol. *296*: 569-577.

Raikhel, N. (1992). Nuclear targeting in plants. Plant Physiol. *100*: 1627-1632.

Razal, R.A., Ellis, S., Singh, S., Lewis, N.G., and Towers, G.H.N. (1996). Nitrogen recycling in phenylpropanoid metabolism. Phytochem. *41*: 31–35.

Rippert, P., Puyaubert, J., Grisollet, D., Derrier, L., and Matringe, M. (2009). Tyrosine and phenylalanine are synthesized within the plastids in *Arabidopsis*. Plant Physiol. *149*: 1251-1260.

Rodríguez-Concepción, M., and Boronat, A. (2002). Elucidation of the methylerythritol phosphate pathway for isoprenoid biosynthesis in bacteria and plastids. A metabolic milestone achieved through genomics. Plant Physiol. *130*: 1079-1089.

Rose, M.D., Winston, F., and Hieter, P. (1990). Methods in yeast genetics. A laboratory manual. Cold Spring Harbor Laboratory Press, Cold Spring Harbor, New York.

Sattarzadeh, A., Krahmer, J., Germain, A.D., and Hanson, M.R. (2009). A myosin XI tail domain homologous to the yeast myosin vacuole-binding domain interacts with plastids and stromules in *Nicotiana benthamiana*. Mol. Plant *2*: 1351-1358.

Schattat, M., Barton, K., Baudisch, B., Klösgen, R.B., and Mathur, J. (2011). Plastid stromule branching coincides with contiguous endoplasmic reticulum dynamics. Plant Physiol. *155*: 1667-1677.

Schmid, J. and Amrhein, N. (1995). Molecular organization of the shikimate pathway in higher plants. Phytochem. *39*: 737-749.

Seo, M., Aoki, H., Koiwai, H., Kamiya, Y., Nambara, E., and Koshiba, T. (2000). Comparative studies on the *Arabidopsis* aldehyde oxidase (*AAO*) gene family revealed a major role of AAO3 in ABA biosynthesis in seeds. Plant Cell Physiol. *45*: 1694-1703.

Shaw, P.J., and Brown, J.W.S. (2004). Plant nuclear bodies. Curr. Opin. Plant. Biol. *7*: 614–620.

Shaw D.J., and Gray, J.C. (2001). Visualization of stromules in transgenic wheat expressing a plastid-targeted yellow fluorescent protein. Planta *233*: 961-970.

Silhavy, D., Molnár, A., Lucioli, A., Szittya, G., Hornyik, C., Tavazza, M., Burgyán, J. (2002). A viral protein suppresses RNA silencing and binds silencing-generated, 21- to 25-nucleotide double-stranded RNAs. EMBO J. *21*: 3070-3080.

Sprenger, G.A. (2007). Aromatic amino acids. *In*: Amino acid biosynthesis – pathways, regulation and metabolic engineering. Microbiology monographs (A. Steinbüchel, ed.). Springer, Berlin.

Sweetlove, L.J., Heazlewood, J.L., Herald, V., Holtzapffel, R., Day, D.A., Leaver, C.J., and Millar, A.H. (2002). The impact of oxidative stress on *Arabidopsis* mitochondria. Plant J. *32*: 891-904.

Tan K., Li, H., Zhang, R., Gu, M., Clancy, S.T., and Joachimiak, A. (2008). Structures of open (R) and close (T) states of prephenate dehydratase (PDT) - Implication of allosteric regulation by L-phenylalanine. J. Struct. Biol. *16*: 94-107.

Theg, S.M., and Scott, S.V. (1993). Protein import into chloroplasts. Trends Cell Biol. *3*: 186-190.

Traven, A., Jelicic, B., and Sopta, M. (2006). Yeast GAL4: A transcriptional paradigm revisited. EMBO Rep. *7*: 496-499.

Tsuchisaka, A., Yu, G., Jin, H., Alonso, J.M., Ecker, J.R., Zhang, X., Gao, S., and Theologis, A. (2009). A combinatorial interplay among the 1-aminocyclopropane-1-carboxylate isoforms regulates ethylene biosynthesis in *Arabidopsis thaliana*. Genetics *183*: 979-1003.

Tzin, V. and Galili, G. (2010a). New insights into the shikimate and aromatic amino Acids biosynthesis pathways in plants. Mol. Plant. *3*: 956-972.

Tzin, V. and Galili, G. (2010b). The biosynthetic pathways for shikimate and aromatic amino acids in *Arabidopsis thaliana*. The *Arabidopsis* Book *8*: e0132. doi: 10.1199/tab.0132.

van Aelst, L., Barr, M., Marcus, S., Polverino, A. and Wigler, M. (1993) Complex formation between RAS and RAF and other protein kinases. Proc. Natl. Acad. Sci. USA *90*:6213–6217.

Ververidis, F., Trantas, E., Doublas, C., Vollmer, G., Kretzschmar, G., and Panopoulos, N. (2007). Biotechnology of flavonoids and other phenylpropanoid-derived natural products. Part I: Chemical diversity, impacts on plant biology and human health Biotechnol.J. *2*: 1214-1234.

Vidal, M., and Legrain, P. (1999). Yeast forward and reverse 'n'-hybrid systems. Nuc. Acids Res. *27*: 919-929.

Vivan, A.L., Andrade, R.A., Abrego, J.R.B., Borges, J.C., Neto, J.R., Ramos, C.H.I., de Azevedo, W. F., Basso, L.A., and Santos, D.S. (2008). Structural studies of prephenate dehydratase from *Mycobacterium tuberculosis* H37Rv by SAXS, ultracentrifugation, and computational analysis. Proteins *42*: 1352-1362.

Voinnet, O., Rivas, S., Mestre, P., and Baulcombe, D. (2003). An enhanced transient expression system in plants based on suppression of gene silencing by the p19 protein of tomato bushy stunt virus. Plant J. *33*: 949–956.

Walter, M., Chaban, C., Schütze, K., Batistic, O., Weckermann, K., Näke, K., Blazevic, D., Grefen, C., Schumacher, K., Oecking, C., Harter, K., and Kudla, J. (2004). Visualization of protein interactions in living plant cells using bimolecular fluorescence complementation. Plant J. *40*: 428-438.

Warpeha, K.M., Gibbons, J., Carol, A., Slusser, J., Tree, R., Durham, W., and Kaufman, L.S. (2008). Adequate phenylalanine synthesis mediated by G protein is critical for protection from UV radiation damage in young etiolated *Arabidopsis thaliana* seedlings. Plant Cell Environ. *31*: 1756-1770.

Waters, M.T., Fray, R.G., and Pyke, K.A. (2004). Stromule formation is dependent upon plastid size, plastid differentiation status and the density of plastids within the cell. Plant J. *39*: 655-667.

Wildman, S. G., Hongladarom, T., and Honda, S.I. (1962). Chloroplasts and mitochondria in living plant cells: Cinephotomicrographic studies. Science *138*:434-436.

Wise, A.A., Liu, Z., and Binns, A.N. (2006). Three methods for the introduction of foreign DNA into *Agrobacterium*. *In*: Agrobacterium Protocols. Methods in Molecular Biology (J.M. Walker, ed). pp. 43-54.

Wroblewski, T., Tomczak, A., and Michelmore, R. (2005). Optimization of *Agrobacterium*-mediated transient assays of gene expression in lettuce, tomato and *Arabidopsis*. Plant Biotech. J. *3*: 259–273.

Wydro, M., Kozubek, E., and Lehmann, P. (2006). Optimization of transient *Agrobacterium*-mediated gene expression system in leaves of *Nicotiana benthamiana*. Acta Biochim. Pol. *53*: 289–298.

Yamada, T., Matsuda, F., Kasai, K., Fukuoka, S., Kitamura, K., Tozawa, Y., Miyagawa, H., and Wakasaa, K. (2008). Mutation of a rice gene encoding a phenylalanine biosynthetic enzyme results in accumulation of phenylalanine and tryptophan. Plant Cell. *20*: 1316-1329.

Yamagami, T., Tsuchisaka, A., Yamada, K., Haddon, W.F., Harden, L.A., and Theologis, A. (2003). Biochemical diversity among the 1-amino-cyclopropane-1-carboxylate synthase isozymes encoded by the *Arabidopsis* gene family. J. Biol. Chem. *278*: 49102-49112.

Yazaki, K., Sasaki, K., and Tsurumaru, Y. (2009). Prenylation of aromatic compounds, a key diversification of plant secondary metabolites. Phytochem. *70*: 1739-1745.

Youngman, E.M., and Green, R. (2007). Ribosomal translocation: LepA does It backwards. Curr. Biol. *17*: R136-R139.

Zhang, S., Pohnert, G., Kongsaeree, P., Wilson, D.B., Clardy, J., and Ganem, B. (1998). Chorismate mutase-prephenate dehydratase from *Escherichia coli*. Study of catalytic and regulatory domains using genetically engineered proteins. J. Biol. Chem. *273*: 6248-6253.

Zhao, G., Xia, T., Fischer, R.S., and Jensen, R.A. (1992). Cyclohexadienyl Dehydratase from *Pseudomonas aeruginosa*: Molecular cloning of the gene and characterization of the gene product. J. Biol. Chem. *267*: 2487-2493.

Appendix 1. List of Primers

Primer Name [a]	Primer Sequence (5' to 3') [b]	Direction	Restriction or Attenuation Site	Purpose [c]
Y2H-ADT1-F-FL	**GTCGAC**AGGCTCTGAGGTGTTTTCC	Forward	*SalI*	Y2H
Y2H-ADT1-F-I	**GTCGAC**TACCGCTAACTGCAAACAGTC	Forward	*SalI*	Y2H
Y2H-ADT1-F-M	**GTCGAC**AGCGAATTTCGTTTCAGG	Forward	*SalI*	Y2H
D-Y2H-ADT1-F-M	*GCA***GTCGAC**AGCGAATTTCGTTTCAGG	Forward	*SalI*	Y2H
Y2H-ADT1-R-FL	**GCGGCCGC**TTATCTGACTAGATCCATTGG	Reverse	*NotI*	Y2H
D-Y2H-ADT1-R-FL	*TG***GCGGCCGC**TTATCTGACTAGATCCATTGG	Reverse	*NotI*	Y2H
Y2H-ADT3-F-FL	**GTCGAC**TAAGAACTCTCTTACCTTCC	Forward	*SalI*	Y2H

Appendix 1. (continued)

Primer Name [a]	Primer Sequence (5' to 3') [b]	Direction	Restriction or Attenuation Site	Purpose [c]
D-Y2H-ADT3-F-FL	*CAT***GTCGAC**TAAGAACTCTCTTACCTTCC	Forward	*Sal*I	Y2H
Y2H-ADT3-F-I	**GTCGAC**AACCTTTAAGTATTTCAGATC	Forward	*Sal*I	Y2H
D-Y2H-ADT3-F-I	*CAC***GTCGAC**AACCTTTAAGTATTTCAGATC	Forward	*Sal*I	Y2H
Y2H-ADT3-F-M	**GTCGAC**GCCGTGTAGCTTATCAAGG	Forward	*Sal*I	Y2H
D-Y2H-ADT3-F-M	*ATA***GTCGAC**GCCGTGTAGCTTATCAAGG	Forward	*Sal*I	Y2H
Y2H-ADT3-R-FL-EcoRI	**GAATTC**TCACAATGAAAATGTTGATG	Reverse	*Eco*RI	Y2H
D-Y2H-ADT3-R-FL-EcoRI	*CG***GAATTC**TCACAATGAAAATGTTGATG	Reverse	*Eco*RI	Y2H

Appendix 1. (continued)

Primer Name [a]	Primer Sequence (5' to 3') [b]	Direction	Restriction or Attenuation Site	Purpose [c]
D-Y2H-ADT3-R-FL-XbaI	*A7***TCTAGA**TCACAATGAAAATGTTGATG	Reverse	*Xba*I	Y2H
attB1-ADT1-F-FL	*GGGG***ACAAGTTTGTACAAAAAAGCAGGCT**CTGC TCTGAGGTGTTTTCC	Forward	*attB1*	Y2H and BiFC
attB2-ADT1-R-FL	*GGGG***ACCACTTTGTACAAGAAAGCTGGGT**GTCT GACTAGATCCATTGG	Reverse	*attB2*	BiFC
attB2-ADT1-RY-FL	*GGGG***ACCACTTTGTACAAGAAAGCTGGGT**GTTA TCTGACTAGATCCATTGG	Reverse	*attB2*	Y2H
attB1-ADT2-F-FL	*GGGG***ACAAGTTTGTACAAAAAAGCAGGCT**CTGC AATGCACACTGTTCG	Forward	*attB1*	Y2H and BiFC
attB2-ADT2-R-FL	*GGGG***ACCACTTTGTACAAGAAAGCTGGGT**GGA GCATTGTAGTGTCCACTGG	Reverse	*attB2*	BiFC
attB2-ADT2-RY-FL	*GGGG***ACCACTTTGTACAAGAAAGCTGGGT**GTTA GAGCATTGTAGTGTCCACTGG	Reverse	*attB2*	Y2H

Appendix 1. (continued)

Primer Name [a]	Primer Sequence (5' to 3') [b]	Direction	Restriction or Attenuation Site	Purpose [c]
attB1-ADT3-F-FL	*GGGG***ACAAGTTTGTACAAAAAAGCAGGCT**GTAG AACTCTCTTACCTTCC	Forward	*attB1*	Y2H and BiFC
attB2-ADT3-R-FL	*GGGG***ACCACTTTGTACAAGAAAGCTGGGT**GCAA TGAAAATGTTGATG	Reverse	*attB2*	BiFC
attB2-ADT3-RY-FL	*GGGG***ACCACTTTGTACAAGAAAGCTGGGT**GTCA CAATGAAAATGTTGATG	Reverse	*attB2*	Y2H
attB1-ADT4-F-FL	*GGGG***ACAAGTTTGTACAAAAAAGCAGGCT**CTCA AGCCGCAACGTCGTG	Forward	*attB1*	Y2H and BiFC
attB2-ADT4-R-FL	*GGGG***ACCACTTTGTACAAGAAAGCTGGGT**GTGC TTCTTCTGTGGATGTC	Reverse	*attB2*	BiFC
attB2-ADT4-RY-FL	*GGGG***ACCACTTTGTACAAGAAAGCTGGGT**GTCA TGCTTCTTCTGTGGATGTC	Reverse	*attB2*	Y2H
attB1-ADT5-F-FL	*GGGG***ACAAGTTTGTACAAAAAAGCAGGCT**CTCA AACCATTTCGCCTGC	Forward	*attB1*	Y2H and BiFC

Appendix 1. (continued)

Primer Name [a]	Primer Sequence (5' to 3') [b]	Direction	Restriction or Attenuation Site	Purpose [c]
attB2-ADT5-R-FL	*GGGG***ACCACTTTGTACAAGAAAGCTGGGT**GTAC GTCTTCGCTAGGTAACG	Reverse	*attB2*	BiFC
attB2-ADT5-RY-FL	*GGGG***ACCACTTTGTACAAGAAAGCTGGGT**GTCA TACGTCTTCGCTAGGTAACG	Reverse	*attB2*	Y2H
attB1-ADT6-F-FL	*GGGG***ACAAGTTTGTACAAAAAAGCAGGCT**CTAA AGCTCTATCATCTTCTTCTCC	Forward	*attB1*	Y2H and BiFC
attB2-ADT6-R-FL	*GGGG***ACCACTTTGTACAAGAAAGCTGGGT**GCGA TGAAGTTGATGATGTTGG	Reverse	*attB2*	BiFC
attB2-ADT6-RY-FL	*GGGG***ACCACTTTGTACAAGAAAGCTGGGT**GTTA CGATGAAGTTGATGATGTTGG	Reverse	*attB2*	Y2H

[a] FL: full length, I: intermediate, M: short.

[b] Bold: induced restriction or attenuation site; Italics: nucleotides added to promote efficient recombination or provide a docking site for the restriction enzyme; Underlined: sequence complementary to template; Grey Box: stop codon; Regular Text: nucleotides added to adjust frame.

[c] Y2H: Yeast-2-Hybrid; BiFC: Bi-molecular Fluorescence Complementation.

Appendix 2. List of Completed Constructs.

Construct Name [a]	Cloning Technique	Primer Pair Used	Fusion [b]	Self-Activating
Constructs for Yeast-2-Hybrid System I				
pBI770-ADT1-FL	Ligation - Subcloned via pGEM	Y2H-ADT1-F-FL Y2H-ADT1-R-FL	Bait	No
pBI770-ADT1-I	Ligation - Subcloned via pGEM	Y2H-ADT1-F-I Y2H-ADT1-R-FL	Bait	No
pBI770-ADT1-S	Ligation - Direct digest of PCR	D-Y2H-ADT1-F-M D-Y2H-ADT1-R-FL	Bait	No
pBI770-ADT3-FL	Ligation - Direct digest of PCR	D-Y2H-ADT3-F-FL D-Y2H-ADT3-R-XbaI	Bait	Yes
pBI770-ADT3-I	Ligation - Subcloned via pGEM	Y2H-ADT3-F-I D-Y2H-ADT3-R-FL-XbaI	Bait	Yes
pBI770-ADT3-S	Ligation - Direct digest of PCR	Y2H-ADT3-F-M D-Y2H-ADT3-R-FL-XbaI	Bait	Yes
pBI771-ADT1-FL	Ligation - Subcloned via pGEM	Y2H-ADT1-F-FL Y2H-ADT1-R-FL	Prey	No

Appendix 2. (continued)

Construct Name [a]	Cloning Technique	Primer Pair Used	Fusion [b]	Self-Activating
pBI771-ADT1-I	Ligation - Subcloned via pGEM	Y2H-ADT1-F-I Y2H-ADT1-R-FL	Prey	No
pBI771-ADT1-S	Ligation - Direct digest of PCR	Y2H-ADT1-F-M Y2H-ADT1-R-FL	Prey	No
pBI771-ADT3-FL	Ligation - Direct digest of PCR	D-Y2H-ADT3-F-FL D-Y2H-ADT3-R-FL-EcoRI	Prey	No
pBI771-ADT3-I	Ligation - Subcloned via pGEM	D-Y2H-ADT3-F-I D-Y2H-ADT3-R-FL-EcoRI	Prey	No
pBI771-ADT3-S	Ligation - Subcloned via pGEM ne via	D-Y2H-ADT3-F-M D-Y2H-ADT3-R-FL-EcoRI	Prey	No
Constructs for Yeast-2-Hybrid System II				
pGBKT7-ADT1-FL	Gateway®	attB1-ADT1-F-FL attB2-ADT1-RY-FL	Bait	No
pGBKT7-ADT2-FL	Gateway®	attB1-ADT2-F-FL attB2-ADT2-RY-FL	Bait	No

Appendix 2. (continued)

Construct Name [a]	Cloning Technique	Primer Pair Used	Fusion [b]	Self-Activating
pGBKT7-ADT3-FL	Gateway®	attB1-ADT3-F-FL attB2-ADT3-RY-FL	Bait	(Yes) [c]
pGBKT7-ADT4-FL	Gateway®	attB1-ADT4-F-FL attB2-ADT4-RY-FL	Bait	(Yes)
pGBKT7-ADT5-FL	Gateway®	attB1-ADT5-F-FL attB2-ADT5-RY-FL	Bait	(Yes)
pGBKT7-ADT6-FL	Gateway®	attB1-ADT6-F-FL attB2-ADT6-RY-FL	Bait	(Yes)
pGBKT7-CRA1	Gateway®	attB1-CRA1-F attB2-CRA1-RY	Bait	No
pGADT7-ADT1-FL	Gateway®	attB1-ADT1-F-FL attB2-ADT1-RY-FL	Prey	No
pGADT7-ADT2-FL	Gateway®	attB1-ADT2-F-FL attB2-ADT2-RY-FL	Prey	No
pGADT7-ADT3-FL	Gateway®	attB1-ADT3-F-FL attB2-ADT3-RY-FL	Prey	No

Appendix 2. (continued)

Construct Name [a]	Cloning Technique	Primer Pair Used	Fusion [b]	Self-Activating
pGADT7-ADT4-FL	Gateway®	attB1-ADT4-F-FL attB2-ADT4-RY-FL	Prey	No
pGADT7-ADT5-FL	Gateway®	attB1-ADT5-F-FL attB2-ADT5-RY-FL	Prey	No
pGADT7-ADT6-FL	Gateway®	attB1-ADT6-F-FL attB2-ADT6-RY-FL	Prey	No
pGADT7-CRA1	Gateway®	attB1-CRA1-F attB2-CRA1-RY	Prey	No
Constructs for Bi-molecular Fluorescence Complementation				
pEarleyGate201-YN-ADT1-FL	Gateway®	attB1-ADT1-F-FL attB2-ADT1-R-FL	YFP-N	No
pEarleyGate201-YN-ADT2-FL	Gateway®	attB1-ADT2-F-FL attB2-ADT2-R-FL	YFP-N	No
pEarleyGate201-YN-ADT3-FL	Gateway®	attB1-ADT3-F-FL attB2-ADT3-R-FL	YFP-N	No

Appendix 2. (continued)

Construct Name [a]	Cloning Technique	Primer Pair Used	Fusion [b]	Self-Activation
pEarleyGate201-YN-ADT4-FL	Gateway®	attB1-ADT4-F-FL attB2-ADT4-R-FL	YFP-N	No
pEarleyGate201-YN-ADT5-FL	Gateway®	attB1-ADT5-F-FL attB2-ADT5-R-FL	YFP-N	No
pEarleyGate201-YN-ADT6-FL	Gateway®	attB1-ADT6-F-FL attB2-ADT6-R-FL	YFP-N	No
pEarleyGate201-YN-CRA1	Gateway®	attB1-CRA1-F attB2-CRA1-R	YFP-N	No
pEarleyGate201-YC-ADT1-FL	Gateway®	attB1-ADT1-F-FL attB2-ADT1-R-FL	YFP-C	No
pEarleyGate202-YC-ADT2-FL	Gateway®	attB1-ADT2-F-FL attB2-ADT2-R-FL	YFP-C	No
pEarleyGate202-YC-ADT3-FL	Gateway®	attB1-ADT3-F-FL attB2-ADT3-R-FL	YFP-C	No
pEarleyGate202-YC-ADT4-FL	Gateway®	attB1-ADT4-F-FL attB2-ADT4-R-FL	YFP-C	No

Appendix 2. (continued)

Construct Name [a]	Cloning Technique	Primer Pair Used	Fusion [b]	Self-Activation
pEarleyGate202-YC-ADT5-FL	Gateway®	attB1-ADT5-F-FL attB2-ADT5-R-FL	YFP-C	No
pEarleyGate202-YC-ADT6-FL	Gateway®	attB1-ADT6-F-FL attB2-ADT6-R-FL	YFP-C	No
pEarleyGate202-YC-CRA1	Gateway®	attB1-CRA1-F attB2-CRA1-R	YFP-C	No

[a] FL: full length, I: intermediate, S: short.

[b] Bait: GAL4-DB domain fusion; Prey: GAL4-TA domain fusion; YFP-C: C-terminal half-YFP fusion; YFP-N: N-terminal half-YFP fusion.

[c] (Yes): Activation only of the *MEL1* reporter

Appendix 3. Controls for pBI770 (DB) and pBI771 (TA) Constructs. Each control combination was assayed for growth, histidine prototrophy, and β-galactosidase activity. Growth of white colonies in the absence of histidine and production of a blue pigment in the presence of X-β-gal indicates the ability to activate reporter gene expression in the absence of an interaction. A summary of the assay results is shown to the right of each panel. **A.** DB-ADT1 constructs do not activate expression of the reporters in any control combination. **B.** DB-ADT3 constructs are able to activate expression of the reporters in all three control combinations. **C.** TA-ADT1 constructs do not activate expression of the reporters in any control combination. **D.** TA-ADT3 constructs do not activate expression of the reporters in any control combination.

+: interaction; –: no interaction; ADT: arogenate dehydratase; C: CRA1, CRUCIFERINA; DB: GAL4 DNA binding domain; FL: full length; G: growth; H: histidine prototrophy; I: intermediate length; L: *lacZ*, β-galactosidase; S: short length; TA: GAL4 transcription activation domain.

A.

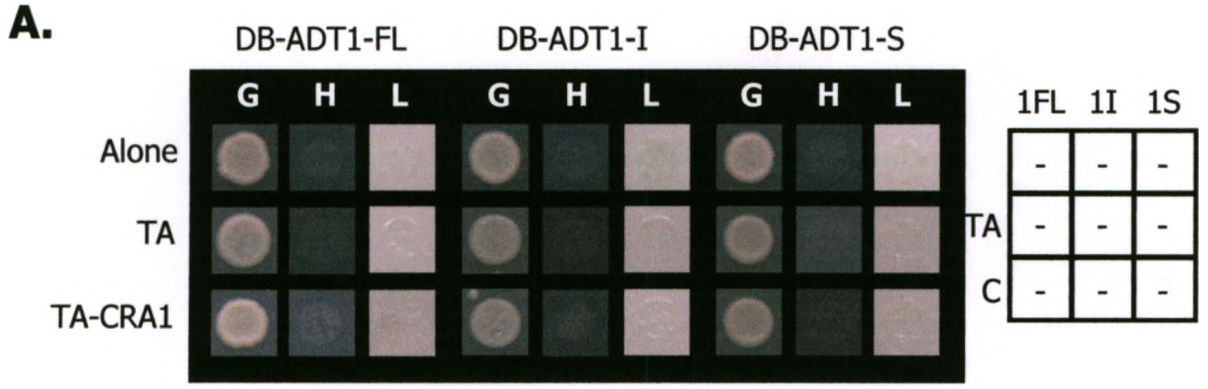
DB-ADT1-FL
DB-ADT1-I
DB-ADT1-S
G H L G H L G H L
Alone
TA
TA-CRA1
1FL 1I 1S
TA
C
- - -
- - -
- - -

B.

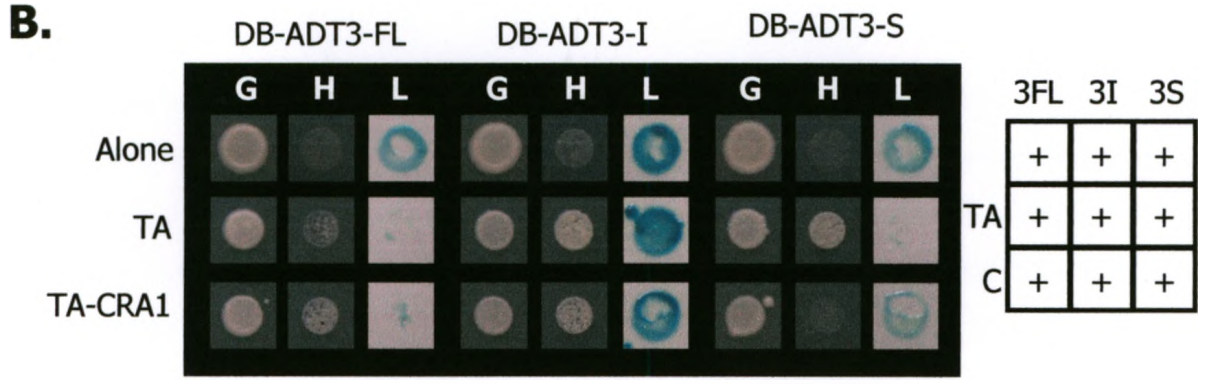
DB-ADT3-FL
DB-ADT3-I
DB-ADT3-S
G H L G H L G H L
Alone
TA
TA-CRA1
3FL 3I 3S
TA
C
+ + +
+ + +
+ + +

C.

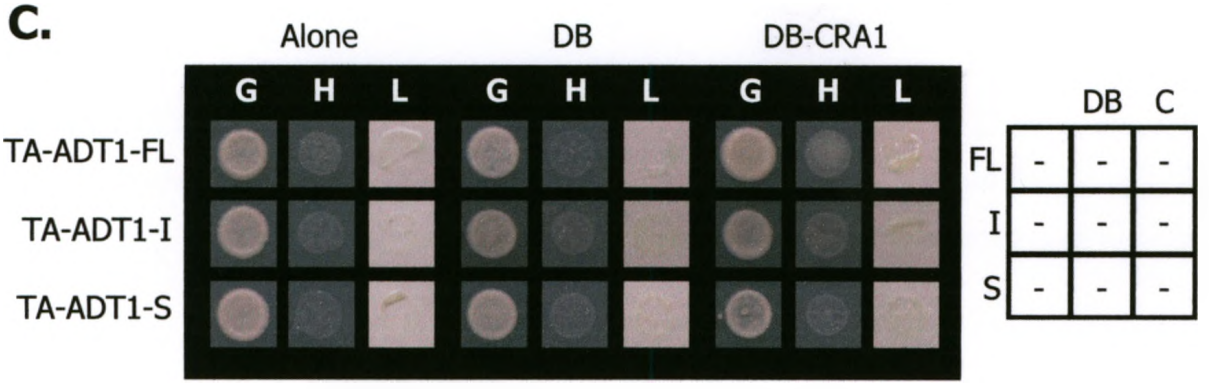
Alone
DB
DB-CRA1
G H L G H L G H L
TA-ADT1-FL
TA-ADT1-I
TA-ADT1-S
DB C
FL
I
S
- - -
- - -
- - -

D.

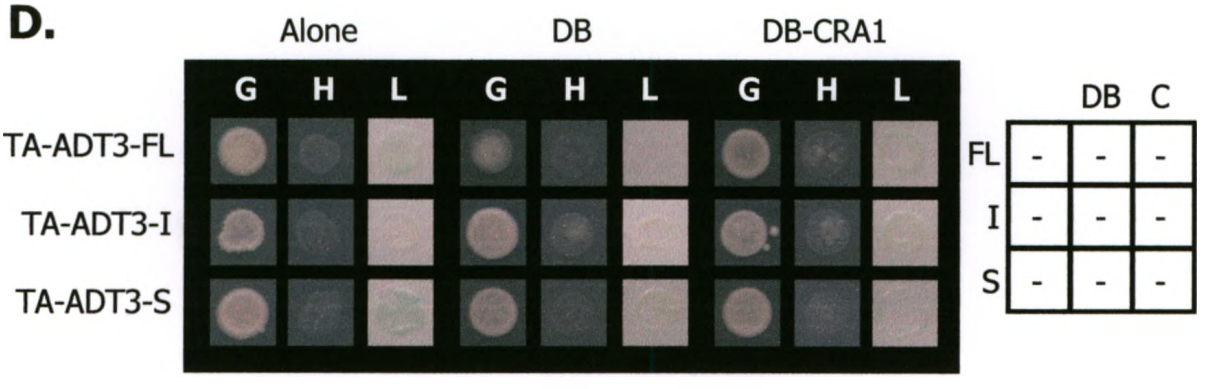
Alone
DB
DB-CRA1
G H L G H L G H L
TA-ADT3-FL
TA-ADT3-I
TA-ADT3-S
DB C
FL
I
S
- - -
- - -
- - -

Appendix 4. Controls for pGADT7 (TA) Constructs. Each control combination was assayed for growth, histidine prototrophy, adenine prototrophy, and α-galactosidase activity. Growth of white colonies in the absence of histidine, growth of white or red colonies in the absence of adenine, or production of a blue pigment in the presence of X-α-gal would indicate the ability to activate reporter gene expression in the absence of an interaction. None of the TA-ADT constructs are able to activate expression of the reporters in any control combination. A summary of the assay results is shown to the right of the panels.

+: interaction; –: no interaction; ADT: arogenate dehydratase; C: CRA1, CRUCIFERINA; DB: GAL4 DNA binding domain; FL: full length; G: growth; H: histidine prototrophy; M: *MEL1*, α-galactosidase; TA: GAL4 transcription activation domain.

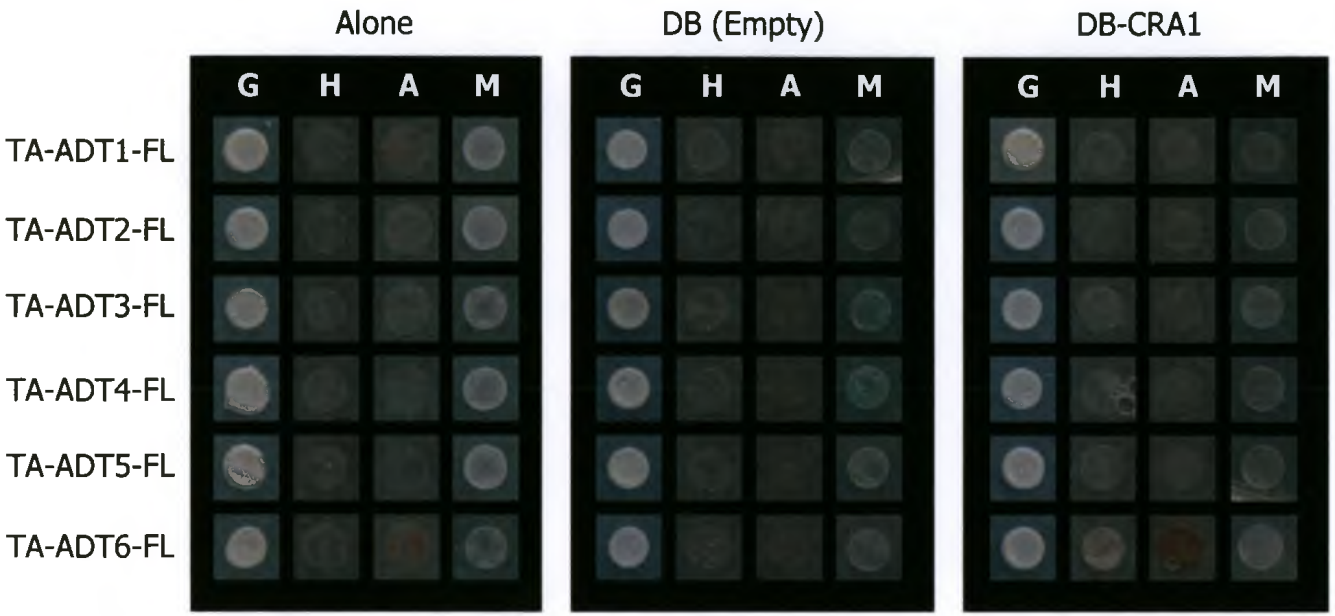

	Alone	DB	CRA1
1FL	-	-	-
2FL	-	-	-
3FL	-	-	-
4FL	-	-	-
5FL	-	-	-
6FL	-	-	-

Appendix 5. Controls for pGBKT7 (DB) Constructs. Each control combination was assayed for growth, histidine prototrophy, adenine prototrophy, and α-galactosidase activity. Growth of white colonies in the absence of histidine, growth of white or red colonies in the absence of adenine, or production of a blue pigment in the presence of X-α-gal would indicate the ability to activate reporter gene expression in the absence of an interaction. None of the DB-ADT constructs are able to activate expression of the *HIS3* or *ADE2* reporters in any control combination, however DB-ADT3-FL, DB-ADT4-FL, DB-ADT5-FL, and DB-ADT6-FL are able to activate expression of the *MEL1* reporter in all control combinations. A summary of the assay results is shown to the right of the panels.

+: interaction; (+): weaker activation; –: no interaction; ADT: arogenate dehydratase; C: CRA1, CRUCIFERINA; DB: GAL4 DNA binding domain; FL: full length; G: growth assay; H: histidine prototrophy assay; M: *MEL1*, α-galactosidase assay; TA: GAL4 transcription activation domain.

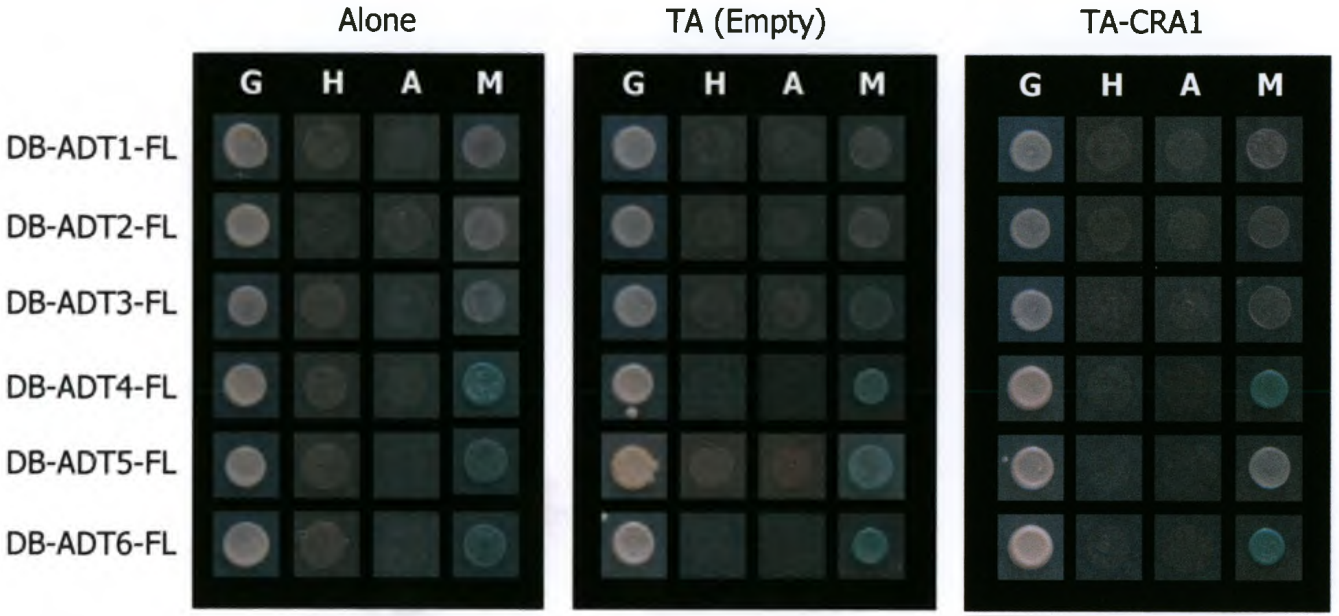

	Alone	TA	CRA1
1FL	-	-	-
2FL	-	-	-
3FL	(+)	(+)	(+)
4FL	+	+	+
5FL	+	+	+
6FL	+	+	+

Appendix 6. Putative Interactors Recovered from the Normalized Commercial cDNA Library Screen using DB-ADT1-FL. Panels A and G show the spotting patterns for each set of assays. Each putative interactor was assayed for growth (B and H), adenine prototrophy (C and I), histidine prototrophy (D and J), and α-galactosidase activity (E, F, K, and L). Note that the α-galactosidase assays were double-spaced to combat bleeding of the blue pigment into the medium. Bolded transformant numbers (E and K) were spotted on a separate plate from non-bolded numbers (F and L). **A-F.** Transformants 2-36. Note that the empty spaces in the pattern shown in panel A were skipped in panel C. **G-L.** Transformants 37-73.

A.

B.

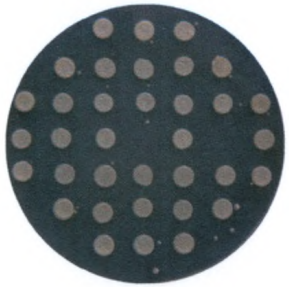

C.

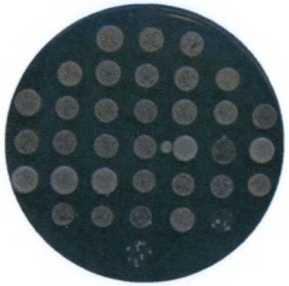

D.

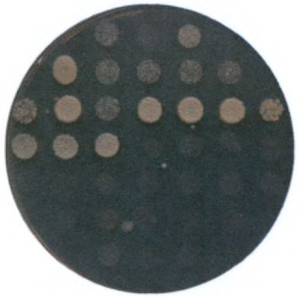

E.

F.

G.

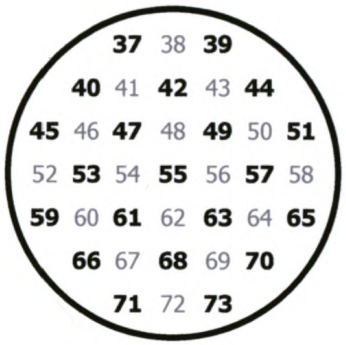

H.

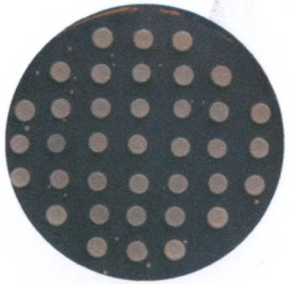

I.

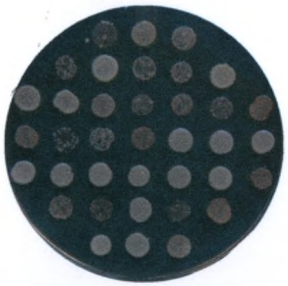

J.

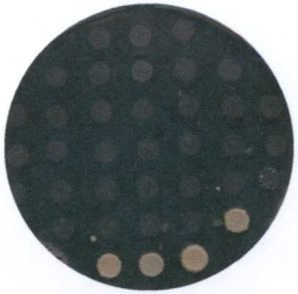

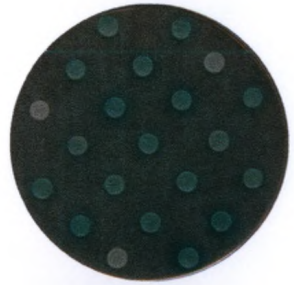

K.

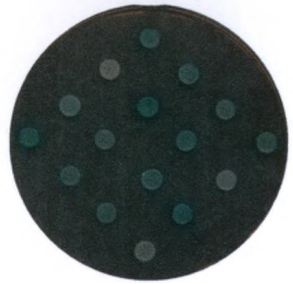

L.

Appendix 7. Controls for Interactors Recovered from the Normalized Commercial cDNA Library Screen using DB-ADT1-FL. Each control combination was assayed for growth, histidine prototrophy, adenine prototrophy, and α-galactosidase activity. Growth of white colonies in the absence of histidine, growth of white or red colonies in the absence of adenine, or production of a blue pigment in the presence of X-α-gal would indicate the ability to activate reporter gene expression in the absence of an interaction. Interactors are identified to the left of the panels, and only interactors which were in frame with the GAL4-TA domain in the fusion protein were tested. Note that the *MEL1* reporter was activated in all control combinations, and so is not informative in this study. Only ADT6, ADT4, BCAT3, a putative elongation factor, a putative protein kinase, and the Succinyl CoA Ligase alpha subunit did not activate expression of the reporters in any control combination. A summary of the assay results is shown to the right of the panel, and descriptions of each interactor can be found in Table 5.

+: interaction; –: no interaction; ADT: arogenate dehydratase; C: CRA1, CRUCIFERINA; DB: GAL4 DNA binding domain; FL: full length; G: growth assay; H: histidine prototrophy assay; M: *MEL1*, α-galactosidase assay.

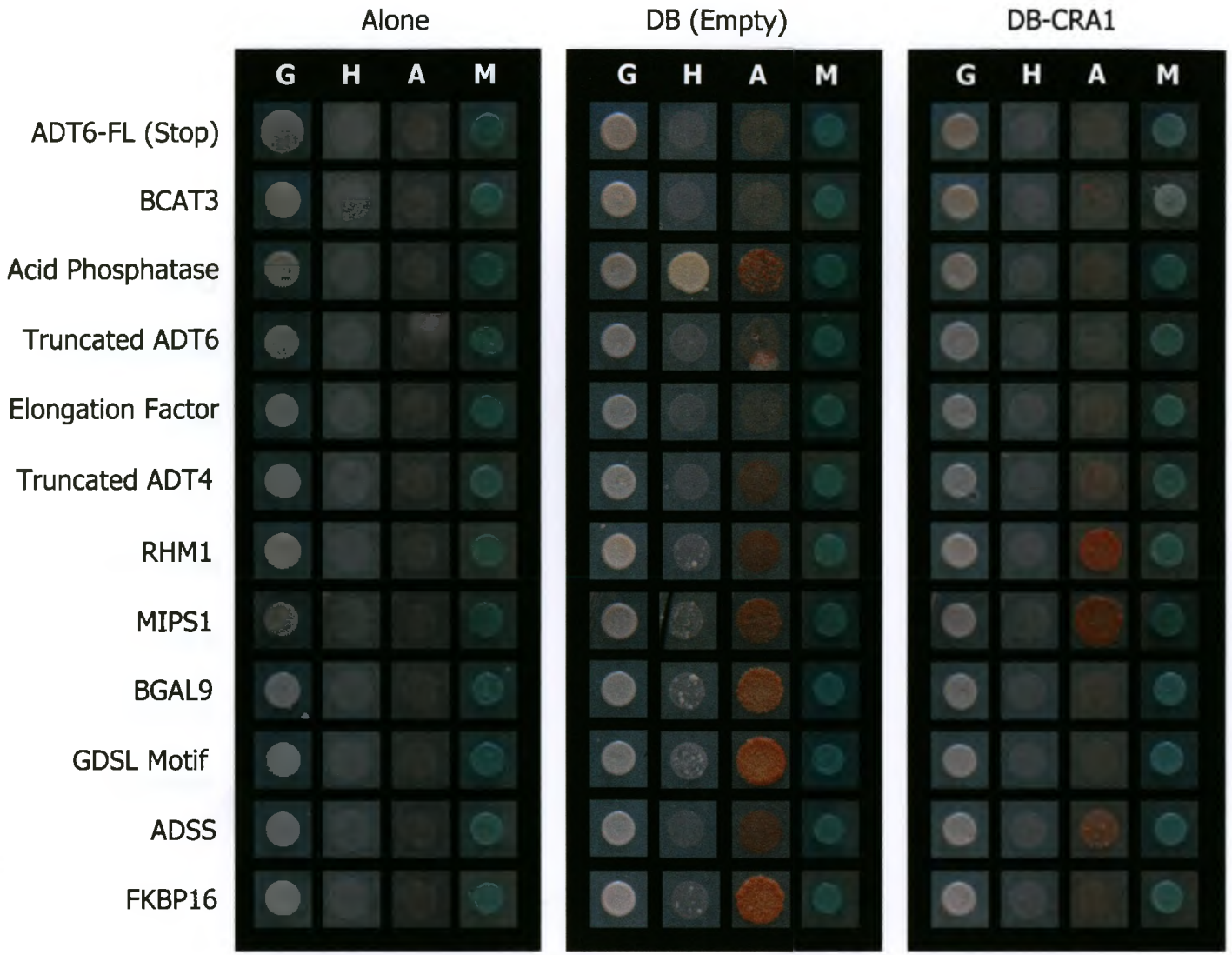

	Alone	DB	CRA1
ADT6-FL	-	-	-
BCAT3	-	-	-
AP	-	+	-
ADT6 (t)	-	-	-
EF	-	-	-
ADT4 (t)	-	-	-
RHM1	-	+	+
MIPS1	-	+	+
BGAL9	-	+	-
GDSL-like	-	+	-
ADSS	-	-	+
FKBP16	-	+	-

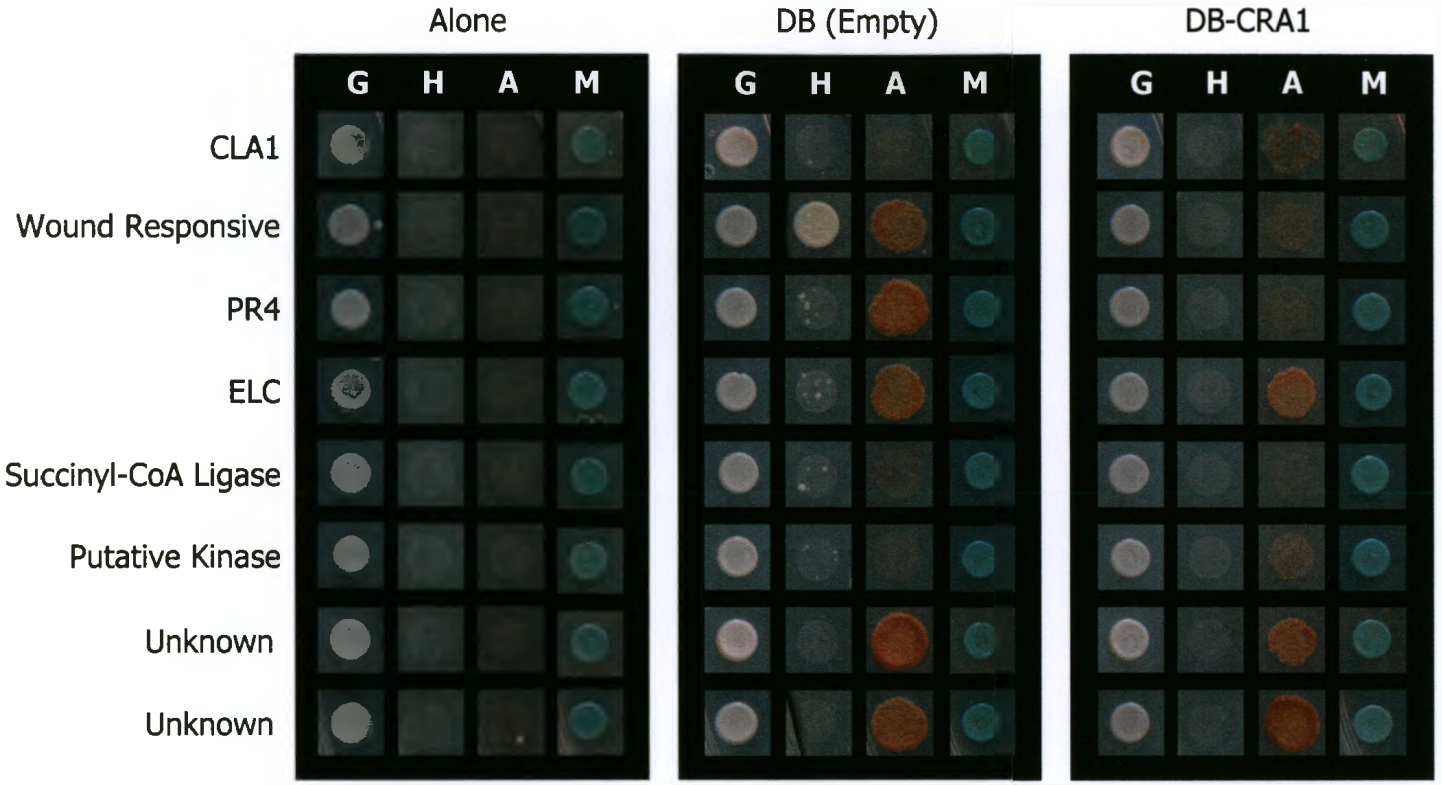

	Alone	DB	CRA1
CLA1	-	-	+
WR	-	+	-
PR4	-	+	-
ELC	-	+	+
S-CoA	-	-	-
Kinase	-	-	+
Unknown	-	+	+
Unknown	-	+	+

Appendix 8. Controls for YN-ADT and YC-ADT Constructs in *N. benthamiana* Leaves. Transient expression of YN- and YC-ADT constructs alone or with corresponding YC- and YN-CRA1 constructs in *N. benthamiana* leaves does not result in the accumulation of yellow fluorescence. Control combinations are identified to the left of each row, and columns represents the YFP channel, chloroplast autofluorescence, and overlay, respectively. **A.** Fluorescence in a wild type, un-infiltrated *N. benthamiana* leaf. **B.** Fluorescence in a leaf infiltrated only with p19. Note that all subsequent control infiltrations also include p19. **C-P.** Fluorescence in leaves infiltrated with either an YN or YC fusion construct alone. **Q-BB.** Fluorescence in leaves co-infiltrated with a YN-ADT or YC-ADT construct and a corresponding YN-CRA1 or YC-CRA1 construct. The scale bar in panel B is 10μm, and in panel V is 15μm. All other panels are 25μm.

ADT: arogenate dehydratase; CRA1: CRUCIFERINA; WT: wild type; YC: C-terminal half YFP; YN: N-terminal half YFP.

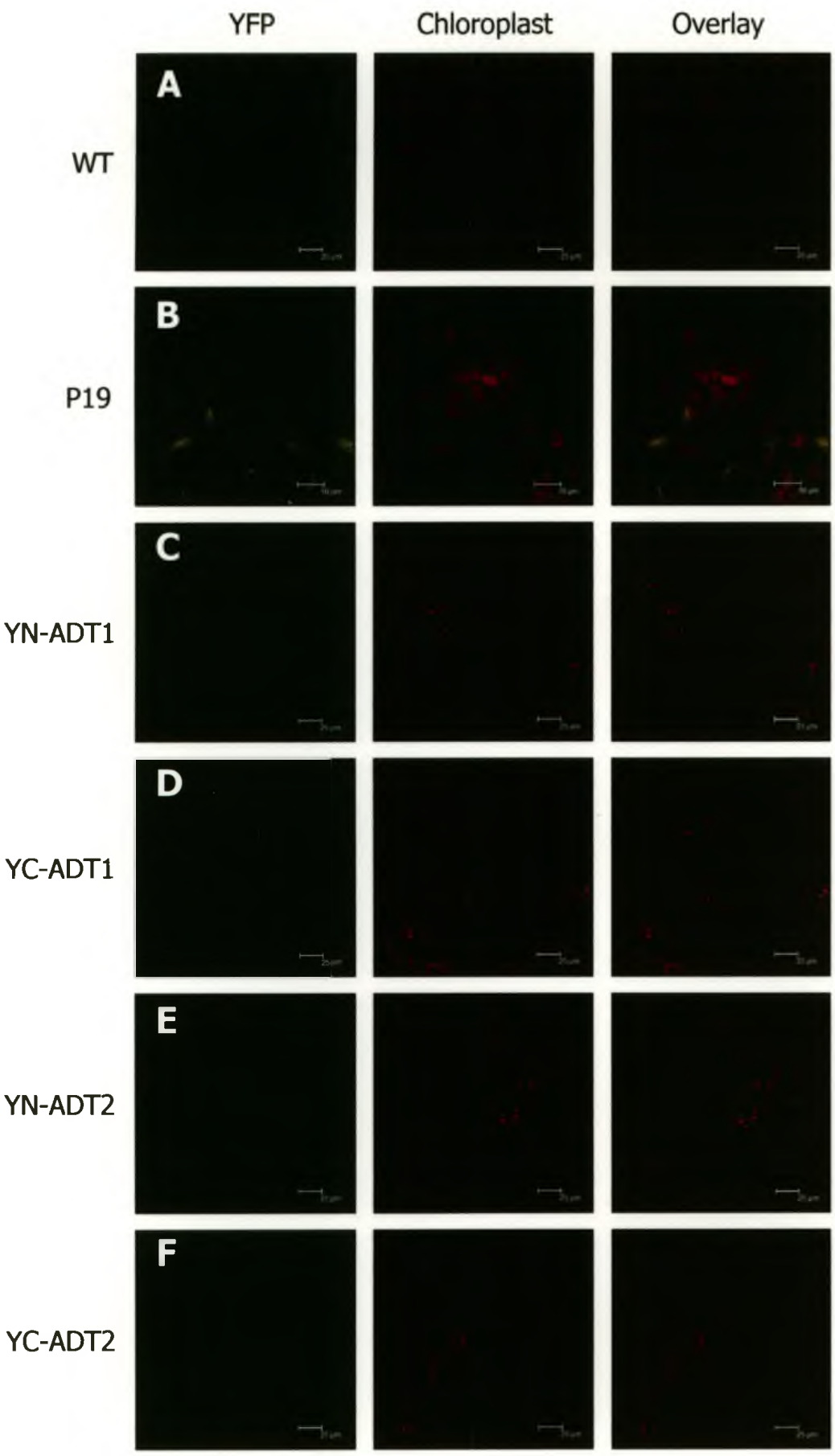
YFP
Chloroplast
Overlay
A
WT
B
P19
C
YN-ADT1
D
YC-ADT1
E
YN-ADT2
F
YC-ADT2

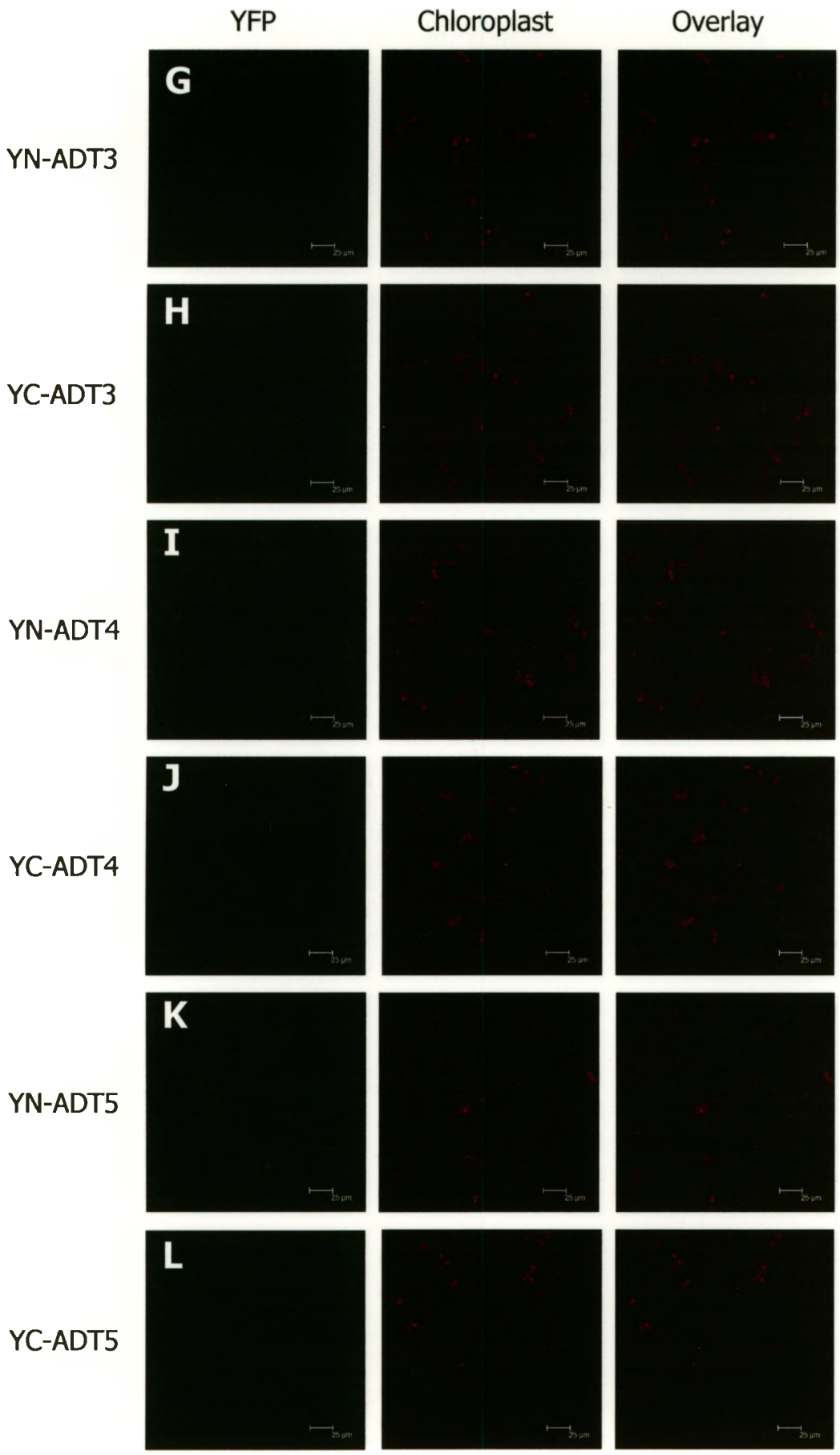
YFP
Chloroplast
Overlay
G
YN-ADT3
H
YC-ADT3
I
YN-ADT4
J
YC-ADT4
K
YN-ADT5
L
YC-ADT5

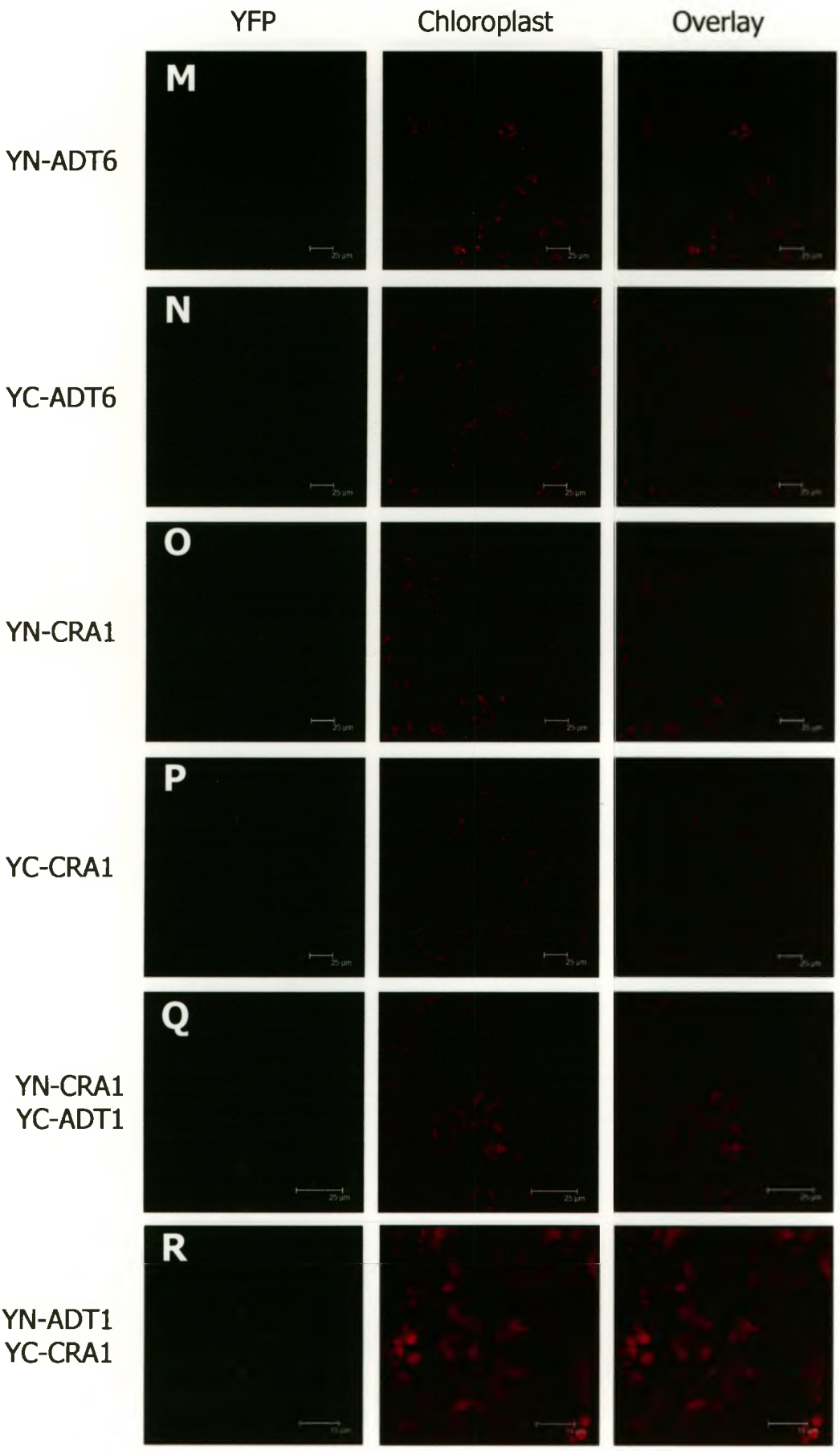
YFP
Chloroplast
Overlay
M
YN-ADT6
N
YC-ADT6
O
YN-CRA1
P
YC-CRA1
Q
YN-CRA1
YC-ADT1
R
YN-ADT1
YC-CRA1

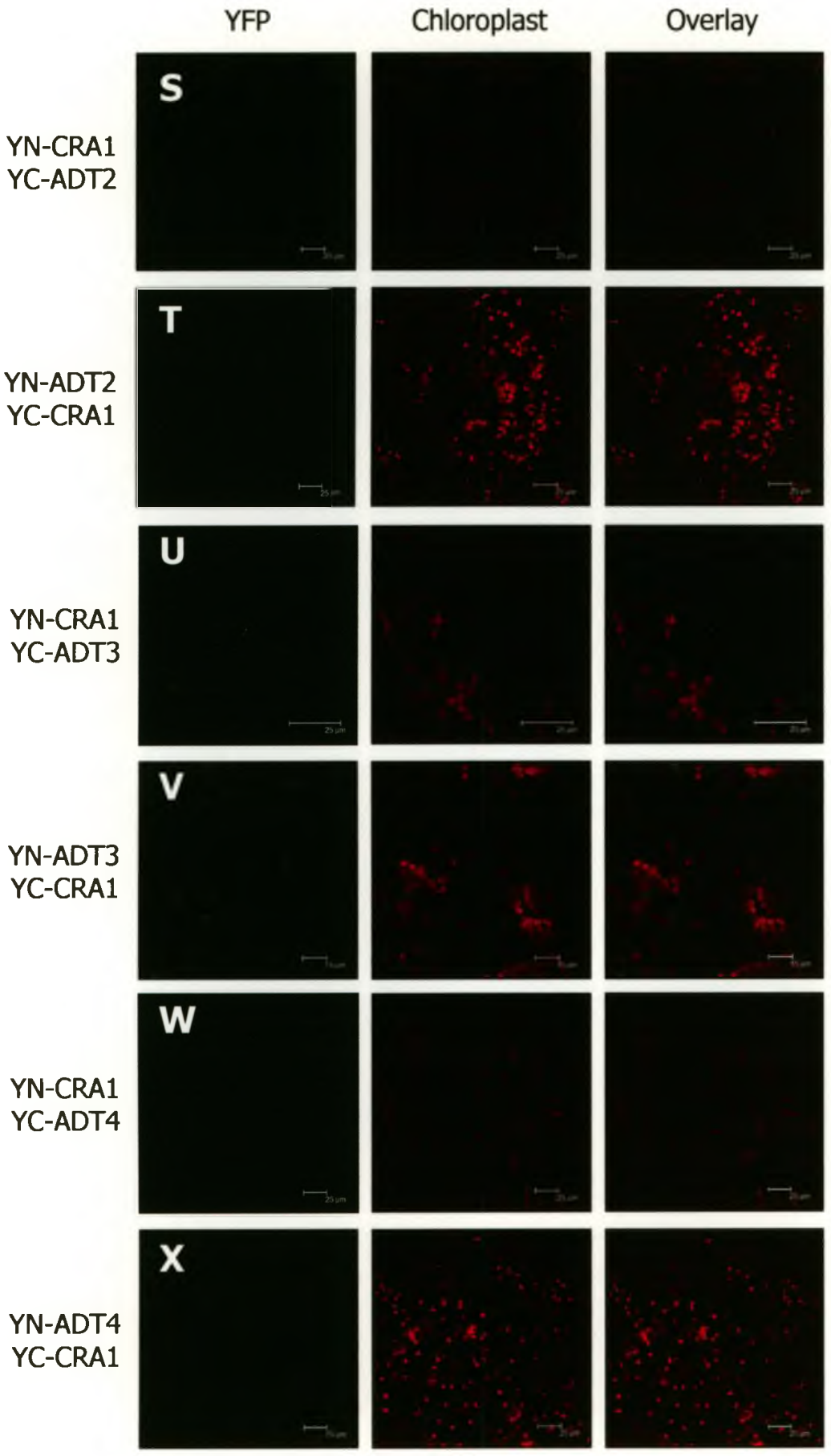
YFP
Chloroplast
Overlay
S
YN-CRA1
YC-ADT2
T
YN-ADT2
YC-CRA1
U
YN-CRA1
YC-ADT3
V
YN-ADT3
YC-CRA1
W
YN-CRA1
YC-ADT4
X
YN-ADT4
YC-CRA1

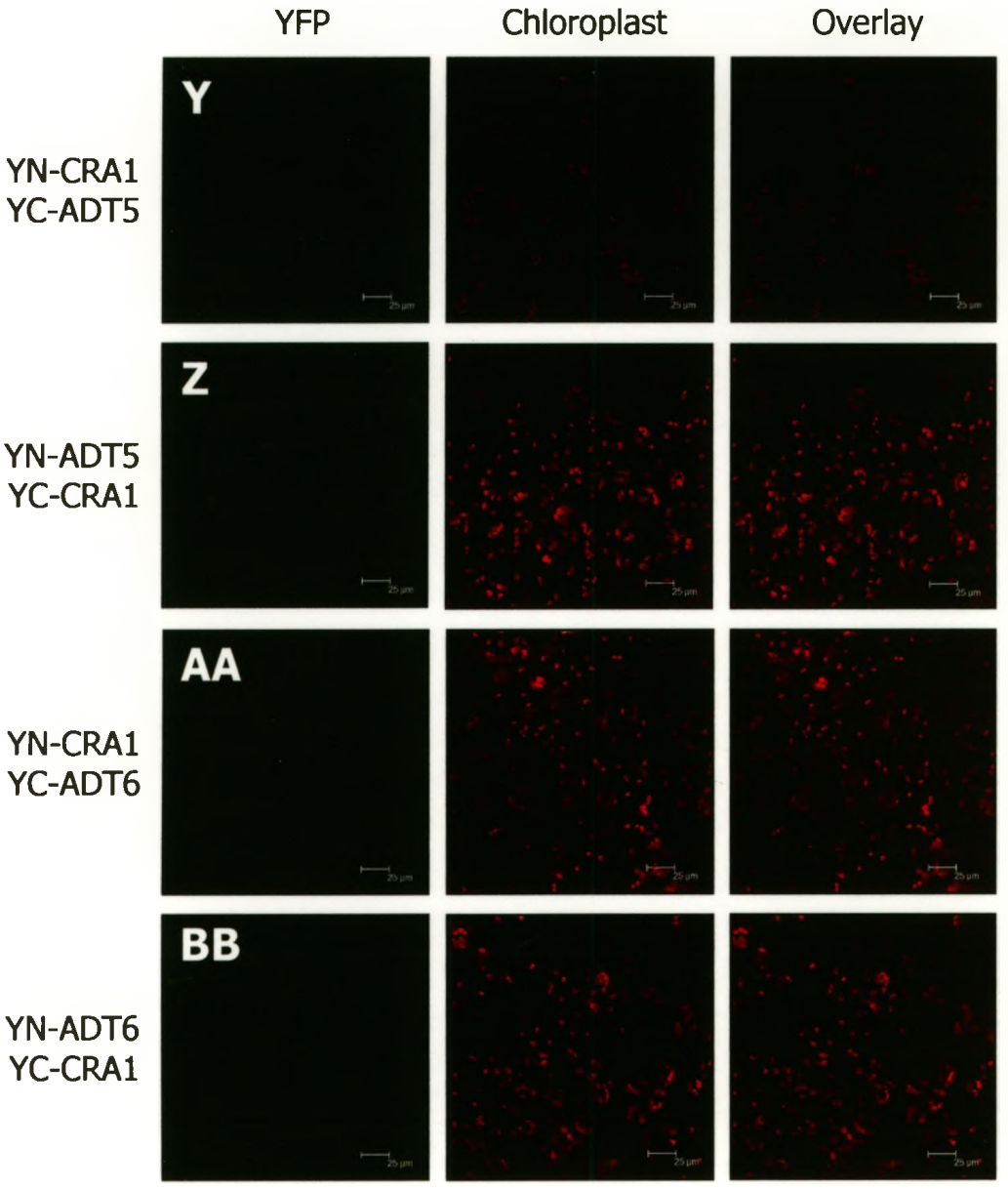
YFP
Chloroplast
Overlay
Y
YN-CRA1
YC-ADT5
Z
YN-ADT5
YC-CRA1
AA
YN-CRA1
YC-ADT6
BB
YN-ADT6
YC-CRA1

Appendix 9. Controls for YN-ADT and YC-ADT Constructs in *Arabidopsis* Leaves.
Transient expression of YN- and YC-ADT constructs alone or with corresponding YC- and YN-CRA1 constructs in *Arabidopsis* leaves does not result in the accumulation of yellow fluorescence. Control combinations are identified to the left of each row, and columns represents the YFP channel, chloroplast autofluorescence (red), and overlay, respectively. **A.** Fluorescence in a wild type, un-infiltrated *Arabidopsis* leaf. **B.** Fluorescence in a leaf infiltrated only with p19. Note that all subsequent control infiltrations also include p19. **C-F.** Fluorescence in leaves co-infiltrated with a YN-ADT or YC-ADT construct and a corresponding YC-CRA1 or YN-CRA1 construct. All scale bars are 10μm.

ADT: arogenate dehydratase; CRA1: CRUCIFERINA; WT: wild type; YC: C-terminal half YFP; YN: N-terminal half YFP.

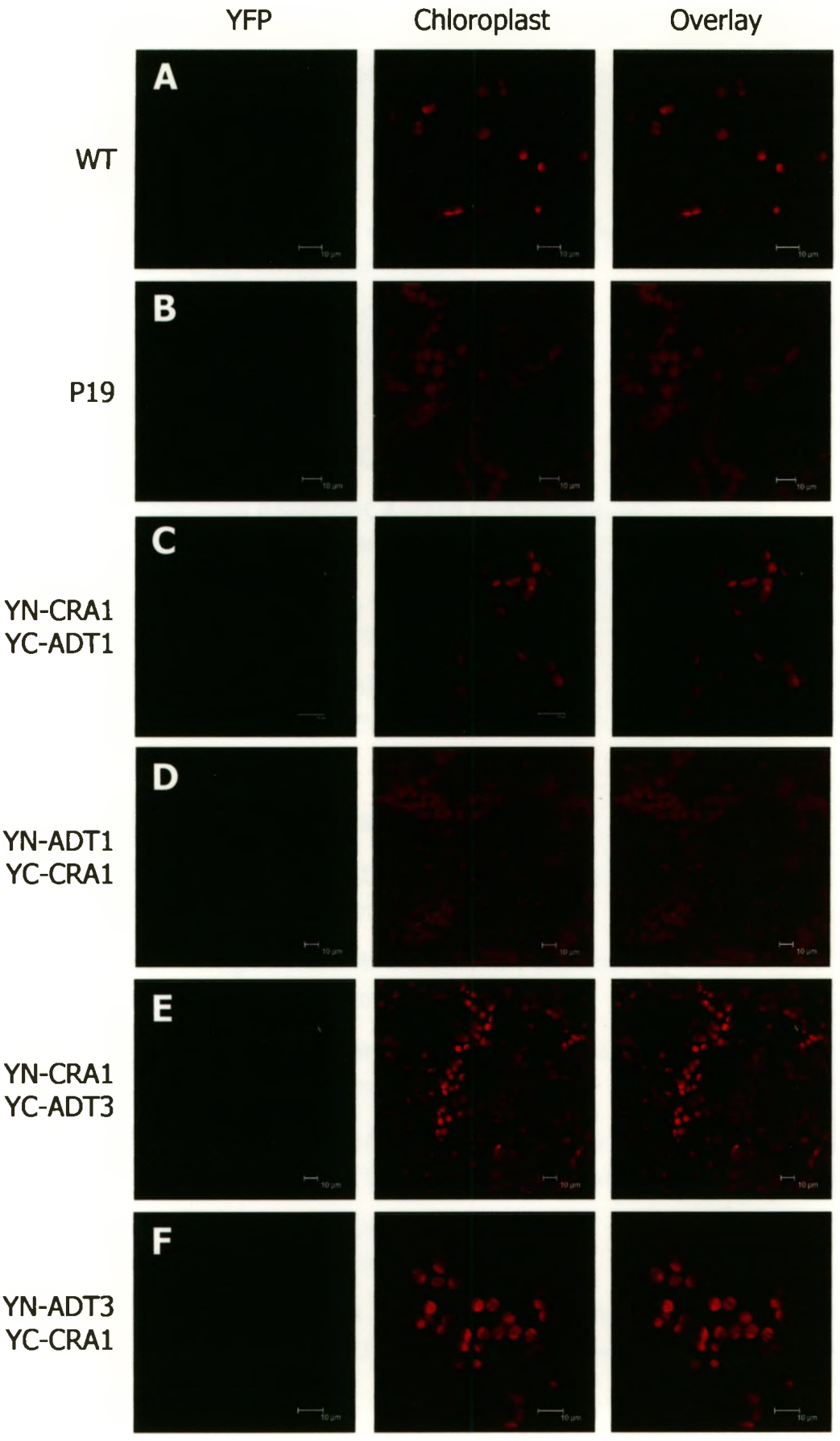
YFP
Chloroplast
Overlay
A
WT
B
P19
C
YN-CRA1
YC-ADT1
D
YN-ADT1
YC-CRA1
E
YN-CRA1
YC-ADT3
F
YN-ADT3
YC-CRA1